UNIVERSITÀ DEGLI STUDI DI NAPOLI

"FEDERICO II"

SCUOLA POLITECNICA DELLE SCIENZE DI BASE

DIPARTIMENTO DI INGEGNERIA CHIMICA, DEI MATERIALI E DELLA PRODUZIONE INDUSTRIALE

DICMAPI

PHD COURSE

IN

INDUSTRIAL PRODUCT AND PROCESS ENGINEERING

DESIGN OF A MICROFLUIDIC PLATFORM TO STUDY THE STABILITY OF BIOLOGICS

Supervisor

Professor Enza Torino

PhD Candidate

Osvaldo Bortone

XXXVI CYCLE

Table of contents

Thesis Abstract

BACKGROUND: Biologics, such as protein-based injectables, can improve clinical outcomes in treating challenging diseases. Despite their potential, the use of biologics in clinics is still facing some obstacles due to various aspects. Among these, the major concern is represented by their immunogenicity, *i.e.* the propensity of the biotherapeutics to induce the body to mount an immune response aimed at modifying or neutralizing the therapy efficacy, or triggering severe side effects. The immunogenic behavior of protein therapeutics lies in their natural propensity to destabilize in response to external physico-chemical stimuli and form protein aggregates that are recognized as dangerous from the body. With the aim to preserve their therapeutic effect, the stabilization of proteins in solution against external stressors is typically attempted through the addition of co-solutes, named *excipients*. The final solution including the latter and the protein active ingredient (API) is named *formulation.* The latter, also named *drug product* (DP), can be defined as a multicomponent solution having challenging chemical (high API concentration and complex protein-protein/excipient-protein network of interactions) and rheological (high viscosity) properties. In order to be safely administered to patients, the proper formulation composition intended to stabilize the API as best as possible is determined through a *formulation development study*, *i.e.*, the process where major factors threatening the API stability are identified and their impact mitigated through the modulation of excipients nature and combination. In general, in a formulation development process a set of candidate DPs, having same API but different combinations of excipients, are exposed to a number of physico-chemical stimulations (*e.g.,* high temperature or agitation). These stresses are intended to accelerate the API degradation, so as to rapidly generate data about therapeutic protein stability behavior. The different compositions of candidate formulations cause them to exhibit dissimilar resistance to the aforementioned stimulations. Consequently, it is possible to identify a formulation ranking where DPs performing the worst are discarded, while those having the best stability behaviors are eligible to further investigations, manufacturing, (pre)clinical trials and potential marketization.

AIM OF THE THESIS: While there is a pressing requirement for more robust formulations to precisely address patients' needs and enhance clinical outcomes, the stabilization of therapeutic proteins proves to be a challenging task due to the elevated number of instability sources and the complex physico-chemical nature of formulations. Current *in-batch* approach result to be low-throughput and expensive. Plus, they fall short of adequately simulating destabilizing conditions and do not provide the chance to combine stress sources - a common occurrence in real formulation lifecycles. Consequently, the protein stability behavior is only partially caught and a significant gap still exists in the scientific understanding of the intricate connections among therapeutic protein stability, physico-chemical destabilizing sources and potential mitigation strategies.
To clarify this correlation, unconventional technologies are needed to enable cost-effective and systematic formulation screening against unexplored instability sources, such as high intensity hydrodynamic forces typical of manufacturing process conditions and combination of stresses. The integration of this information to the knowledge from current formulation development approaches could lead to a comprehensive understanding of the therapeutic biomolecule behavior, aiming to set more appropriate formulation studies as well as suitable molecule-related manufacturing process parameters.
In light of the needs reported above, the present work aims to study the physical stability of therapeutic proteins in high concentration and viscous pharmaceutical formulations through the adoption of a miniaturized strategy based on the microfluidics. In fact, while the microfluidics has been successfully applied to the characterization of diverse aspects of therapeutic protein, its employment remains limited to diluted biomolecule solutions, with no clear focus on industrial context, where the main emphasis is on highly concentrated and viscous multicomponent formulations. In particular, we report the design and the development of an automated and programmable *modular microfluidic platform* able to apply *unconventional physical stimulations* to pharmaceutical formulations spanning a wide range of component concentration and viscosity. Specifically, it is intended to expose therapeutic formulations to unconventional thermal stress, mechanical stimulation (manufacturing-relevant shear rate levels) or a combination of them in an extremely controlled and reproducible manner. The platform is properly thought to automatically guide candidate formulations through predefined isolated or combined stress pathways, in order to induce API instability.

METHODS: The microfluidic platform was thought to present a modular logic, including a pumping (syringe pumps) and stress modules (thermal and mechanical (shear) stress). Each stress module consists of a (thermal or mechanical) stress station and a recirculation line, properly intended to control the exposure time of formulation to the stimulation. Particularly, for the stress station, suitable microfluidic chip geometries were designed, characterized through numerical simulations and fabricated by machining polymethyl methacrylate (PMMA) through a micromilling process. For the recirculation lines and other fluidic path connections, automatic and programmable parts (Peltier cell, valves and pumps) were selected from the market on the basis of the operation requirements and the nature of processed fluids. Microfluidic chip geometries and process parameters were studied through simulative and experimental approaches to offer platform flexibility in terms of viscosity operational range, temperature control and shear rate thresholds.
Highly concentrated (120 mg/ml) nanobody (nAb) - based formulations with different excipient combinations were thermally stimulated (at 49 and 52 °C) close to the protein melting temperature through the microfluidic platform over different stimulation time (2 and 5 min). Its ability to determine aggregation was characterized *via* size exclusion high performance liquid chromatography (SE-HPLC). Results were compared to a well established miniaturized batchwise approach, through which the same formulations were thermally stressed at the same conditions. Additionally, the formulation ranking returned by microfluidics and small volume

miniaturized stimulation was compared to those coming from long term standard pharmaceutical protocols, *i.e.*, storage (5°C) and accelerated (25 °C) stability studies.
Same formulations were subjected to isolated high shear levels (5500, 8000 and 20000 s^{-1}) for different stimulation time (single passage through microfluidic shear station, 2, 5 and 10 min). Also, the formulations were subjected to conventional agitation protocols (300 RPM, 3 days). The effects of such mechanical stimulations were characterized by conventional analytics (SE-HPLC) and a *quasi-real-time analysis* (soon after the stimulation) based on dynamic light scattering (DLS) and Fourier transform infrared spectroscopy (FTIR). Additionally, the ability of the platform to combine stresses was demonstrated by subjecting a nAb-based formulation to thermal-mechanical and mechanical-thermal serial stimulation. Destabilization induced by the combination of solicitations were characterized through the same *quasi-real-time analysis* approach set up for the microfluidic mechanical stress investigation.

RESULTS: The microfluidic platform exhibits high flexibility, as enables the possibility to process fluids spanning a wide viscosity range ([1;20] mPaxs) in a vast isothermal window ([25; 80]°C) and in a broad mechanical shear rate interval ([5500; 20000] s^{-1}).
The investigation conducted on the thermal stress led to demonstrate the microfluidic platform to express precise isothermal control with irrelevant temperature fluctuations. The comparison with well-established small-volume batch-wise thermal stress approaches showed the microfluidic platform to determine similar destabilization on nAb-based formulations. Additionally, the same formulation ranking obtained upon microfluidic thermal stress is comparable with the ones obtained through conventional storage and accelerated stability protocols.
The experimentation of mechanical (shear) stress demonstrated the ability of the platform to induce dynamic/transient structural and colloidal instabilities. While conventional SE-HPLC was not able to detect any aggregation trend, the *quasi-real-time* analytical approach pointed out variations of biomolecule physical properties with different impact, depending on the stimulation intensity and formulation composition. Surprisingly, for some formulation compositions, more impactful destabilization might occur at lower shear rate thresholds, indicating how the excipient-protein interaction can be sensitive to specific hydrodynamic conditions.
Additionally, the coupling of conventional agitation protocols to *quasi-real-time* analysis did not return any relevant trend. This confirmed the inadequacy of the agitation test to probe formulation robustness with respect to high hydrodynamic forces typical of manufacturing processes.
Lastly, the versatility of the platform was shown by conducting serial thermal-mechanical and mechanical-thermal solicitations. Interestingly, the *quasi-real-time* analytical strategy highlighted unobvious formulation behaviors. In fact, it came out that the commutability of the stresses (thermal prior to mechanical and vice versa) was not verified. In other words, the order in which the stresses are applied might completely change the magnitude of structural and colloidal destabilizations.

DISCUSSIONS: Although the microfluidics is often related to process scaling-down intended for cost reduction, in this application the microfluidic platform has proven to be much more than that. In fact, the predictability of transport phenomena in a microfluidic context enables a better correlation of stress sources and biomolecule instability behavior. Additionally, thanks to the possibility to subject DPs to unexplored stressors, the collection of novel and alternative instability information, that cannot be caught by conventional stress (*e.g.*, agitation) and analytical protocols, can be achieved. Thus, the integration of such an approach to the current practice might broaden the knowledge of protein stability behavior at early development stages, gathering meaningful indications for later phases of a drug product lifecycle (*e.g.*, manufacturing). This technology has the potential to shift the paradigm from a *downstream corrective mode* to an *upstream testing approach* and steer the development of biologics towards a more *quality-oriented* perspective, with the possibility to influence clinical outcomes.

1. Biologics: clinical, scientific and industrial background

ABSTRACT

Biological therapeutics, also referred to as biologics, are a class of medicines that consist of complex molecules, cells, tissues for transplantation or a combination of these substances. In particular, protein-based liquid injectables are a group of biologics that have shown exceptional quality for a broad range of clinical applications. In fact, they are superior to synthetic drug molecules for a number of reasons. Mainly, their complex physico-chemical structure and target specificity enable biological functions that are not possible to achieve with synthetic drug molecules. Of particular importance, monoclonal antibodies (mAbs) and nanobodies (nAbs) have proven to be highly effective in different clinical fields ranging from oncology, dermatology, hematology to autoimmune diseases. Despite their potential, the use of biologics in clinics is still facing some obstacles due to various aspects. Among these, the major concern is represented by their immunogenicity, *i.e.* the propensity of the biotherapeutics to induce the body to mount an immune response aimed at modifying or neutralizing the therapy efficacy, or triggering severe side effects. The immunogenic behavior of protein therapeutics lies in their natural propensity to lose conformational or colloidal stability and form protein aggregates that are recognized as dangerous from the body. Indeed, the protein stability in solution is jeopardized by intrinsic, such as solution pH or ionic strength, or external factors, such as temperature, agitation, air/solid-liquid interface and hydrodynamic forces (*e.g.,* high shear) encountered during the manufacturing process, transportation and delivery to the patients. The stabilization of therapeutic proteins in solutions is typically attempted through the addition of co-solutes, named *excipients*, that may interact either with the bulk water or the biomolecules in order to stabilize their structure, thus preserving their therapeutic effect. The final solution including excipients and the protein active ingredient (API) is named *formulation.* The latter, also named *drug product* (DP), can be defined as a multicomponent solution having challenging chemical (high API concentration and complex protein-protein/excipient-protein network of interactions) and rheological (high viscosity) properties. The proper formulation composition intended to stabilize the API as best as possible is determined through a *formulation development study*, that is the process where major factors threatening the API stability are identified and their impact mitigated through the addition of excipients. In general, in a formulation development process a set of candidate DPs, having same API but different combinations of excipients, are exposed to a number of physico-chemical stimulations (e.g., high temperature or agitation). The stimulations are intended to accelerate the API degradation, so as to rapidly generate data about therapeutic protein stability behavior. The different compositions of candidate formulations cause them to exhibit dissimilar resistance to the aforementioned stimulations. Consequently , it is possible to identify a formulation ranking where DPs performing the worst are discarded, while those having the best stability behaviors are eligible to further investigations, manufacturing, (pre)clinical trials and potential marketization.

1.1 The importance of biologics and their advantages over synthetic drug molecules

Biological therapeutics, also referred to as Biologicals or Biologics, are those class of medicines which, instead of being chemically synthetized, are grown and then purified from large-scale cell cultures of bacteria or yeast, or plant or animal cells [1]. They consist in complex molecules (proteins, nucleic acids, carbohydrates), cells, tissues for transplantation or a combination of these substances [2]. Unquestionably, the recent COVID-19 pandemic has heightened the global awareness regarding the importance of biologics in healthcare. In fact, biological-based vaccines as well as monoclonal and polyclonal antibodies have resulted beneficial in the prevention and treatment of the infection [3, 4].

Whilst the definition of biologicals embraces a wide spectrum of biomolecules, the main focus in this work will be on protein therapeutics that have gained a growing attention and application since the advent, in the early 20th century, of the serum therapy and the purification of insulin from bovine pancreas [5, 6]. Both events represented a breakthrough in this field, opening the possibilities to treat infectious diseases such as diphtheria or scarlet fever [7, 8], or provide glucose control for diabetes patients [9]. Subsequently, protein therapeutics encountered an even larger diffusion thanks to the introduction of the DNA recombinant technology in the 1970s [5, 7]. In fact, with the introduction of this technology, proteins, previously of animal origin, were produced through a controlled expansion by cloning a gene into prokaryotic (bacterial) or eukaryotic (human) cells [6]. This technology really improved the quality of the products by providing higher controllability of the production process, enhanced purity and homogeneity, improved stability and increased yield [6]. Moreover, the DNA recombinant technology brought into the field the possibility to exactly transcript a human gene, enhancing the protein specificity and reducing the exposure to diseases of which the original animal source might have been affected [10]. Since the establishment of the DNA recombinant technology, the number and the type of proteins used for therapeutic scopes have incredibly grown, and currently, different classes of protein therapeutics can be identified based on their pharmacology [10, 11].

The reason why biological therapeutics are tremendously attractive in clinical applications lies in the advantages they offer when compared to other drug classes, such as the synthetized molecules [6, 10, 12]. To better work out the benefits coming from biologics, it might be helpful briefly comparing their physical, chemical and pharmacokinetic features to those of synthetic drugs. From a physical point of view, the two classes of molecules show different *molecular size*. Typically, it ranges from 0,5 to 1 kDa for a small drug molecule, while biologics have molecular weights around 1-30 kDa for peptides and proteins, and >100 kDa for monoclonal antibodies [6]. Chemically speaking, synthetized drug molecules exhibit a *non-specific* structure, causing them to distribute to off-target body districts with increased potential toxicity. Conversely, biologics express *high specificity* in binding pharmacological target [6]. From a pharmacokinetic point of view, the *routes of administration* can be of multiple types for small drug molecules, including oral, parenteral, dermal and nasal, while they are mainly intravenous, subcutaneous and intramuscular for biologics [6, 11, 12]. Despite the scientific community has been committed to make the oral administration of biological molecules feasible, the acidic environment encountered by the macromolecules in the gastro-intestinal tract still represents a big challenge [13, 14]. Intuitively, the difference in routes of administration of synthetic molecules and biologics hugely impacts their *bioavailability*, that is typically <40% for the former and either ≈80% for the latter when injected subcutaneously or 100% when administered intravenously [6, 12]. In addition, remarkable differences can be individualized in the *drug half-life*, that is a few hours for synthetized drugs, while it spans a highly variable time period for biologics. Particularly, it can be comparable to that of synthetized molecules for peptides and small proteins, while it can reach up to 30 days in the case of mAbs [6, 11, 12, 15-17]. Plus, unlike synthetic molecules, the *metabolization* of biologics do not produce potential toxic byproducts, as they are cleaved into amino acids as for endogenous proteins [11].

These differences together determine the biologicals to express some evident advantages over synthetized drug molecules. In fact, thanks to their complex chemical structure, peptides and protein therapeutics can accomplish biological actions by far more complicated than those performed by synthetic molecules. This is mainly due to their higher *specificity*, that enhances the targeting of specific body districts and reduces the

protein drug interference with other biological processes. Plus, due to their metabolization into amino acids, biologics are more likely to have a reduced or null toxicity than small molecules. Finally, it should be noticed that, in case the body suffers from depletion or total absence of an essential protein biomolecule, biological therapeutics might provide an efficient replacement [10].

Among the therapeutic proteins, mAbs are the fastest growing sector of pharmaceutical industry. To witness this rapid growth, just consider that 153 therapeutic mAbs have been approved in 2022 by the food and drug administration (FDA), while in 2017 only 17 obtained the authorization by the same agency [18]. mAbs are big molecules (≈150 kDa) exhibiting an intricate chemical organization. *Figure 1* (reproduced by [19]) depicts the structure of an Immunoglobulin G (IgG) (one of the antibodies produced by the immune system in response to foreign molecules). It consists in four polypeptide chains, two identical *heavy chains* (including V_H, C_{H1}, C_{H2}, and C_{H3} domains) and two identical *light chains* (V_L and C_L). They are held together by disulfide linkages and fold to form a "Y" shaped tetramer. The region connecting C_{H1} and C_{H2} is called hinge region, while the complementarity-determining region (CDR), crucial in defining the antibody specificity, is a variable domain reported in green on top of the Fab region [19, 20].

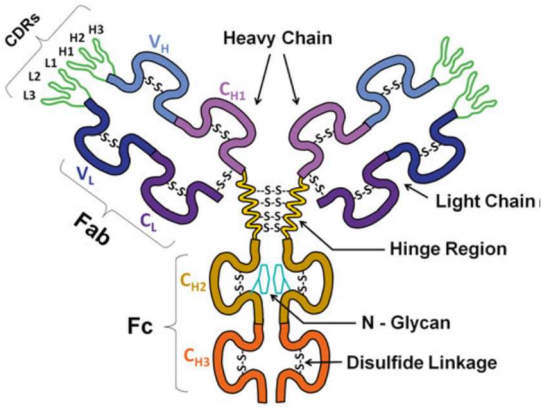

Figure 1 – Structural scheme of typical IgG

The mAb CDR specificity is an exquisite attribute enabling highly effective targeted therapies. As matter of fact, mAbs have proven to be highly useful in a wide spectrum of clinical fields, including oncology, dermatology, cardiology, ophthalmology and hematology [16, 21, 22]. Other examples where mAbs can be particularly promising and efficient comprise kidney [16] and autoimmune diseases, such as rheumatoid arthritis and Alzheimer's diseases [21].

In addition, thanks to ameliorations in the control of development technologies and due to clinical need for improved drug safety and efficacy, the scientific community and pharmaceutical industries have begun exploring bi-specific or tri-specific antibodies, where a single compact molecule expresses two ore three target antigen specificities [23, 24].

Besides mAbs (mono-, bi- and tri-specific), another relevant class of therapeutic proteins is represented by nanobodies (nAbs). A nAb is a single domain antibody derived from heavy-chain antibodies typical of camelids, or immunoglobulin new antigen receptors in sharks [25, 26]. nAbs are small-sized biomolecules (≈15 kDa), roughly ten times smaller than antibodies. In fact, they are the smallest antigen-binding domain of antibodies and preserve the full antigen binding capacity with high specificity and affinity. As for mAbs, nAbs have proven to be excellent solutions in many clinical applications [27, 28]. This is mainly because of their small size that make them better penetrate tissues, more engineerable for enhanced clinical applications and more structurally stable (a crucial point for therapy safety and efficacy) [29]. *Figure 2,* reproduced by Yang and Shah's work [30], reports a schematic representation of a nAb.

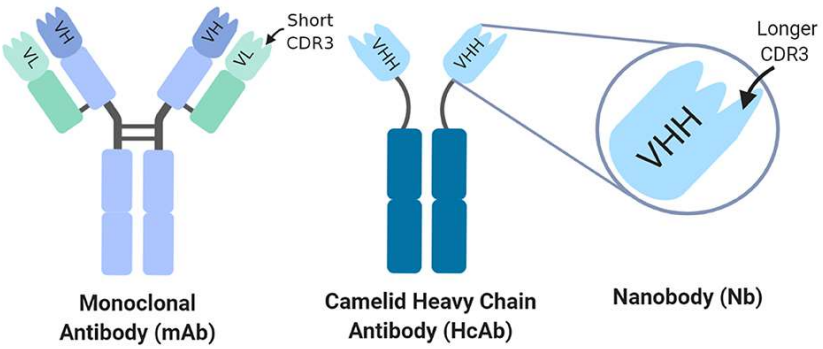

Figure 2 – schematic representation of a nanobody as smallest part of antigen binding domain of an antibody

1.2 The clinical challenges of biologics and the major concern of protein immunogenicity

Despite of the several advantages they express when compared to other classes of drugs, biological therapeutics are still facing a series of challenges that are hardly limiting their use in the clinics [31]. The nature of the obstacles is heterogeneous and embraces different fields. First, the challenges can be related to the design of a proper protein therapeutic for an optimized pharmacokinetic and pharmacodynamic profile [32]. This might include the selection of a precise molecule structure, the identification of chemical modifications for prolonged half-life or tissue specificity [32, 33], individualization of a proper route of administration and definition of appropriate physicochemical properties of injectable solutions [34] that might impact the stability of protein therapeutics [35]. Certainly, pharmacological challenges are not the sole factors jeopardizing the widespread adoption of biologics in clinics. Indeed, the cost of biologics is one of the hardest challenges when compared to synthetic drug molecules [36]. It has been estimated that, on average, a daily dose of a biological therapeutics costs 22 times more than that of a small drug molecule [37]. Intuitively, the most impacting factor justifying the higher cost of biologics compared to other synthetic drugs is the intrinsic complexity of the production process [36]. Besides this, it must be noticed that synthetic drugs have been around for longer time, and this translates in a larger number of competitors that are currently present on the market that produce generic versions of the same molecule. Due to their complex structures, science and scarce availability of insights into biological process, producing less expensive generic versions of biologics (*i.e.,* biosimilars) is hugely complicated [38]. As matter of fact, developing a biosimilar means getting a new product having same therapeutic function of the brand biologics, but with a different active ingredient. In other words, producing generic versions of biological therapeutics is not as easy as making generic versions of other synthetic drug molecules [36]. In addition to these aspects, it is important to note that the proper handling and administration of biologics entail additional costs for skilled medical personnel to oversee patient treatments [36, 39].

Moreover, an outmost relevant issue related to the administration of biologics is their *immunogenicity*, that is the propensity of a protein biotherapeutics to elicit an immune response in the human body [40]. The immune response is typically seen after the biologics injection and it is characterized by the formation of anti drug antibodies (ADAs) and the manifestations of some hypersensitivity reactions [41, 42]. The latter can be of different types, meaning that they can involve diverse biological mechanisms and exhibit different severity of side effects [43-45]. The ADAs formation is mediated by the so-called antigen presenting cells (APCs) (macrophages and dendritic cells). They engulf, process and present therapeutic proteins to T-cells, that are signaled to mount an immune response by activating B-cells differentiation in Memory B-cells and plasma cells, which have the capability of producing ADAs [40]. The immune response can be also triggered through independent T-cell mechanisms, where protein therapeutics directly activate B-cells, leading to the their differentiation in plasma cells with consequent formation of ADAs [46]. The latter have a strong influence on the protein therapeutic efficacy. In particular, they can act against the drugs by binding the protein therapeutics without interfering with its interaction with target. These ADAs, referred to as non-neutralizing ADAs, indirectly determine an alteration in biologics efficacy by modifying their pharmacokinetic behavior. On the other side, neutralizing ADAs, have the ability to bind the drug at its active sites, thus directly impacting its efficacy [40].

Protein therapeutics immunogenicity has been ascribed to several factors. Different routes of administration and injection frequencies have been proven to be responsible of a different intensities of immune response [47-49]. In particular, subcutaneous injection (the one becoming more popular for a better patient compliance) seems to be more immunogenic than intravenous as it is likely to establish a migratory potential of dendritic cells [47, 48]. Also, therapies with higher administration frequency have been shown to be more prone to induce immune response [49]. Besides route of administration and injection frequency, other factors proven to influence immune response are patient-related aspects [40].
Furthermore, the immunogenic behavior of proteins can be linked to their physical and chemical properties. Indeed, alteration of their structure as well as post translational modifications may cause the body to mount a severe immune response [50]. Particularly, an intense attention is devoted to the presence of protein aggregates in biologics. While deeper focus on the physical status of aggregation will be provided in next paragraph, here it suffices to know that aggregation status is an agglomeration of protein monomers. As matter of fact, aggregates have been shown to elicit immune response [35, 51, 52], even though the exact correlation of their characteristics and immunogenicity is still under investigation. Probably, the immune response is triggered because protein aggregates, which are clusters of multiple monomers, contain repetitive patterns of amino acids. These patterns mimic the ligands of scavengers and other receptors, enhancing their uptake by APCs, that detect microbial antigens in a similar manner [53-55].
Since therapeutic proteins have an inherent tendency to destabilize and come together to form larger, varied-size complexes [56], studying their stability behavior related to solution and environmental conditions is of crucial importance while developing a biological therapeutic. Actually, finding reliable strategies and processes to induce and detect specific protein aggregation pathways is a major challenge for the pharmaceutical companies.
The mechanisms and factors able to influence the natural propensity of proteins to aggregate can be adequately understood if a proper discussion is outlined. To this purpose, the following paragraphs offer a concise overview of protein stability, accompanied by a brief excursus of the methodologies employed for its examination in both simple (*i.e.,* diluted) solutions and intricate pharmaceutical formulations (highly concentrated and viscous injectables).

1.3 Protein stability and aggregation

As previously outlined, protein aggregation can be defined as a biomolecule *physical state* coming from protein-protein interactions that leads to the formation of higher molecular weight species [57]. The occurrence of protein aggregation is mostly related to the loss of molecule *stability,* that can be mainly divided into conformational and colloidal stability.

The *conformational stability* is the ability of the protein to retain its native folded state. A more rigorous definition requires a thermodynamic point of view, according to which the protein stability can be given as the difference in free energy between folded and unfolded states in equilibrium $\Delta G_{unf} = G^U(T) - G^F(T) = -RTln\frac{\langle U\rangle}{\langle F\rangle}$, where U and F denotes the unfolded and folded state, respectively; R is the gas constant and $\langle U\rangle$ and $\langle F\rangle$ are the population of unfolded and folded protein at a given temperature (T) [58-60]. The most conventional approach to extrapolate information about the protein stability is the thermodynamic calorimetry (*e.g.,* differential scanning calorimetry or isothermal titration calorimetry), through which heat changes induced by protein denaturation (*i.e.*, unfolding) can be detected [61]. The main thermodynamic quantities providing biophysical insights of the protein conformational stability are the protein heat capacity (Cp), enthalpy (H), entropy (S) and Gibbs free energy (G). H is a direct measure of the adsorbed or generated heat, S is an indication of the number of the configurations available to the protein and G a relation between the enthalpic and entropic contributions. Instead, Cp may have different interpretation. Generally, it can be considered as a measure of the form of entropy/enthalpy compensation related to the temperature change [61]. Under the assumption of constant Cp (typically holding for T<100°C) [62], change in enthalpy, entropy and Gibbs free energy describing protein unfolding at a specific temperature can be extracted by Gibbs-Helmholtz

equation [61]. In particular, under this assumption the relation between ΔG_{unf} and temperature T can be expressed as reported in equation (1) [63]:

$$\Delta G_{unf}(T) = \Delta H_m \frac{(T_m - T)}{T_m} - \Delta C_p[T_m - T\left(1 - \ln\frac{T}{T_m}\right)]. \quad (1)$$

In this relation the *Tm* is the *melting temperature*, that represents a largely used parameter to indicate the thermal stability of a protein. It expresses the temperature at which the 50% of the protein molecule in a *pure and homogeneous solution* loses its native structure [64]. In other words, it is the condition where $G^U(T) = G^F(T)$, thus resulting in $\Delta G_{unf} = 0$. Intuitively, ΔH_m represents the denaturation enthalpy at *Tm*.
The melting temperature is a highly relevant parameter evaluated in an industrial context. It is worth precising that the *Tm* determination is not straightforward and is dependent on several factors, including the structural complexity of the protein under investigation. As an example, multidomain proteins like IgGs show multiple melting temperatures which correspond to independent denaturation of Fc and Fab. Particularly, the former may have *Tm* ranging from 63-71°C (typically indicated as first thermal transition Tm_1), while the latter can degrade at even higher temperatures falling in a range of 73-82 °C (indicated as second thermal transition Tm_2) [65, 66].
Plotting equation (1) returns the so-called "protein stability curve", of which a qualitative representation is reported in *figure 3* [64].

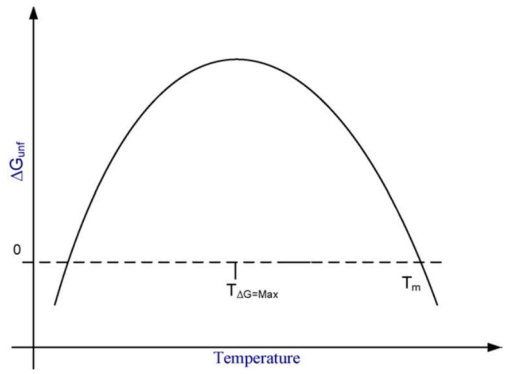

Figure 3 – relationship between temperature and protein thermodynamic stability (picture reproduced by [64])

Historically, scientists used to look at proteins as an *"all-or-none"* system *(fully folded or fully unfolded)*, where protein unfolding is a global event. This behavior can be described through a two-state mathematical model. This results in $\Delta G_{unf}(T)$ having a typical parabolic profile (*figure 3*) with the null point ($\Delta G_{unf} = 0$) being the thermodynamic condition for half conversion of protein to unfolded state [59, 60]. More recently, sophisticated models have been developed to interpret DSC results, pointing out that the protein denaturation is rather a multistep process that achieves many short-lived intermediates configurations [67, 68].
Besides calorimetric thermodynamics, other approaches are used to study protein conformational changes. These might include the use of Fourier Transform Infrared (FTIR) spectroscopy to detect changes in the secondary structure, or Circular Dichroism (CD) for variations of the protein tertiary structure [57].

The other aspect of protein stability in solution is linked to the propensity of molecules to interact with each other. This type of stability can be referred to as *colloidal stability* [69, 70] and is typically described by some physical parameters such as the "second virial coefficient" (B_{22}) or the "diffusion based interaction parameter" (K_D) [69]. These parameters are extrapolated by light scattering experiments in diluted systems [71] and are of huge relevance to the industrial practice to explore the protein-protein interactions (PPIs) in different solution

conditions [72-74]. More in details, B_{22} is derived from the slope of linear regression of light scattering intensity at different protein concentrations (typically < 1 mg/ml). A negative value of B_{22} designates net attractive PPIs, while positive B_{22} indicates the opposite [75].
Despite conformational and colloidal stability refer to two different aspects, the forces (chemical interactions) taking place for both of them are essentially the same. They include electrostatic interactions (*e.g.,* ionic forces), hydrogen bonds, van der Waals forces and hydrophobic interactions [56, 76]. Identifying the dominance of one type over the others can be challenging, as its prevalence is closely tied to the solution conditions, such as pH and ionic strength. Rather, it can be said that the protein stability is the result of all these forces acting together (*network of interactions*) [62] contributing to the energetical condition of the system.

When conformational or colloidal stability is somehow threatened, the thermodynamic of the system may favor the formation of lower energy proteinaceous entities, which result from specific *degradation pathways*. The most common are fragmentation, deamidation, oxidation and aggregation. In particular, the latter is worth being discussed deeper as it covers a key role in this thesis work.
As previously reported, the aggregation is nothing but a process leading to the formation of bigger species named *protein aggregates*. It may take place in different ways, including *self association of native monomers* [77], *association of (partially) unfolded monomers* [77] and *association to contaminants,* which might occur even when the biomolecule exhibits affinity to non-protein species in solution, ending up forming bigger clusters [78].
The occurrence of a specific aggregation pathway does not mutually exclude the others. In fact, it is rather difficult identifying a single pathway being the only responsible for protein aggregation. They are very likely to act concomitantly [77]. However, regardless of the type, all aggregation pathways share an *initial nucleation* phase and a subsequent *aggregate growth* step [79]. In the former, monomeric (partially) (un)folded native species interact with other protein or non-protein entities, leading to the formation of non-native oligomers, that can be referred to as *nuclei* [79]. The nucleation is characterized by a certain lag time, which is the time needed for the nuclei to form. It may take from a few minutes to several days depending on the solution conditions and external factors [77]. In the aggregation growth step, monomer addition and aggregate-aggregate interactions lead to the formation of higher molecular weight species [79, 80]. As for the nucleation phase, *aggregation growth* is affected by both protein conformational and colloidal instability. In fact, the former could provide additional binding spots for further aggregation, while the latter influences interaction among oligomeric species or bigger particles. From a kinetic point of view, aggregation growth phase follows a non-linear trend with time, and different kinetic models have been proposed to fit experimental data of different protein aggregation behaviors [81, 82]. A very famous mathematical kinetic model is the one by Finke and Watzky [83] that looks at protein aggregation kinetics as a two-step model described by two different kinetic constants, one for the nucleation and the other for the aggregation growth phase. The Finke and Watzky's expression is reported hereafter:

$$-\frac{dC}{dt} = k_1 C + k_2(C_0 - C). \qquad (2)$$

In the equation (2) C is the monomer concentration at time t, C_0 is the initial monomer concentration, k_1 and k_2 are the nucleation and growth kinetic constants, where the former is described as a slow and continuous process and the latter as a typical faster one.
The oligomeric species forming during nucleation and aggregate growth steps can be *reversible* or *irreversible* [84, 85] and this usually depends on the kind of interactions as well as the amount of monomers involved. As matter of fact, monomers and dimers can be in a dynamic equilibrium according to a dissociation constant. Typically, *n-mers* (with n up to ≈100) can be dissociated and reversed through dilution or by changing solution pH [56]. In general, reversible aggregation occurs in early stages (nucleation phase) and it is

thermodynamically driven. On the contrary, irreversible aggregates are late-stage products appearing in the aggregation growth step and are characterized by a specific formation kinetics [86].

1.4 Protein-based therapeutic solutions and aggregation-inducing factors

The approaches described in the previous paragraph to investigate conformational and colloidal stability are conducted on protein solutions that are characterized by high homogeneity and purity (as for calorimetric thermodynamic analysis), or by low concentrations (as for light scattering-based PPI analysis). Chemical and rheological properties of such fluids are profoundly different from the actual injectable solutions (properly referred to as *formulations)*. As a consequence, protein behavior in these *ideal solutions* might hardly divert from the one expressed in real formulations.

Since the subcutaneous delivery of protein therapeutic has become more common and preferred to the intravenous injection for patient convenience and compliance to biological therapies, development of *high concentration formulations* has been required [87]. Defining thresholds to identify the meaning of "high concentration" is not easy, specially considering that with the advancement of formulation technologies, what is highly concentrated today might not be considered such in few years. According to the categorization proposed by Rodrigues and colleagues [88], low concentration formulations present < 50 mg/ml of active protein ingredient (API), high concentration injectables are those falling in the range of 50-150 mg/ml of API and ultra-high concentration formulations are solutions characterized by an even higher concentration (> 150 mg/ml). Leaving aside the debatable identification of thresholds, what is crucial to be understood is the effect of a very populated solution on the liquid physico-chemical properties. It could be noted that in a very crowded system, the intermolecular space becomes smaller, resulting in more intense PPIs [89, 90]. This has a direct impact on the solution viscosity, which increases exponentially with protein concentration and can even reach values >50 cP [91-94]. Eventually, this poses challenges in the development of therapeutics at different levels, including manufacturing process (solution transfer, filtration or filling) [95] and administration [96].

Although conformational and colloidal protein stability keep their meaning and validity, in a formulation context they are more difficult to be defined due to the system chemical and rheological complexity. However, as discussed in the section 1.2, their preservation in protein-based therapeutics is pivotal for an effective and trouble-free therapy. The conformational and colloidal stability of proteins in a formulation can be susceptible to several internal or external factors [79, 97]. Among the formers, *primary*, *secondary* and *tertiary protein structure* are primarily involved in the determination of the propensity degree of a biomolecule to destabilize due to scarce conformational or colloidal stability. For example, hydrophobic amino acidic components of the protein chain impact the aggregation rate and the stability of aggregated species [98, 99]. Similarly, tertiary structure can be characterized by some aggregation prone regions (*e.g.,* hydrophobic patches) determining poor colloidal stability. Other internal factors include the *solution conditions*, that is an expression mainly used to indicate the pH and the ionic strength of a formulation. Different works in the literature show the pH to be highly influent on the conformational and colloidal stability of proteins impacting on the degree of PPIs and the protein solubility [85, 100, 101]. Equally, the ionic strength (concentration of ions in solution) strongly influences both conformational and colloidal stability, as salt cations and anions can specifically bind or screen protein molecules, thus modulating their aggregation propensity [102-104].

Besides the aforementioned factors, other external (environmental) variables might have an impact on formulation stability. The most important and largely characterized factor is the *temperature.* As seen in the previous paragraph, high temperature impacts on the conformational stability of a protein by controlling the population of (partially) unfolded species. Along with this, high temperature is expected to modify the solubility of protein monomers/aggregate and increases the rate of protein diffusion, thus altering the nature of PPIs and elevating the probability of molecule collision [79]. This has a direct impact on the propensity of the protein to form larger aggregates. Equally detrimental, lowering the temperature may induce oligomerization in pharmaceutical formulations, resulting in opalescence or liquid-liquid phase separation [105].

In addition to the temperature, protein stability in formulation can be endangered by some processes occurring during the manufacturing or the transportation of therapeutics [106-108]. For example, different kind of pumps are used in the pharmaceutical manufacturing to accomplish formulation container filling, or transfer therapeutics to different manufacturing plant districts [109]. During the *pumping*, fluids can experience very high shear [110] or cavitation, which have a negative impact on the formation of aggregated species [111]. Furthermore, formulation may encounter *agitation* during transportation. While agitating, protein formulations are exposed to different stressing sources, including container wall shearing and exposure to air/liquid interface that have been shown determining factors in the formation of protein aggregates [112, 113]. Specifically, the air-liquid interface represents a hydrophobic trap for protein molecules. They tend to adsorb to the interface, serving as nuclei to trigger the aggregation process. The presence of agitation can exasperate this phenomenon by renewing the film of adsorbed protein and releasing conformational destabilized biomolecules into the bulk solution [112].

Discussing about air-liquid interface may suggest that, in general, interfaces have a role in exasperating the protein aggregation tendency. As matter of fact, during manufacturing process (pumping or filtration) protein formulations get in contact to various solid or liquid surfaces [106]. Such interactions may lead to loss of protein or might contribute to induce biomolecule instability and aggregate formation. Among the solid surfaces one could mention glass, stainless steel, aluminum and different types of plastics or polymers [114-118]. Also, silicone oil, typically adopted in formulation containers to facilitate operations (vials or prefilled syringes) may negatively interact with protein therapeutics determining adsorption/desorption phenomena that promote biomolecule aggregation [115, 119].

The external stress sources discussed so far (temperature and mechanical stress encountered during manufacturing process and transportation) are particularly relevant to the present work, as they will be directly involved in the research activity conducted and described in following chapters. However, to complete the discussion on the spectrum of environmental factors impacting therapeutic formulation stability, some hints on other destabilizing sources are provided hereafter.

In addition to temperature and mechanical stress, protein stability in formulation can be harmfully altered by other pharmaceutical processes. This is the case of *freeze-thawing* and *freeze-drying* that have been proven to determine chemical degradation of protein structures, thus influencing aggregation propensity [79, 97].

An important destabilization factor is represented by the presence of any potential *contaminant* that may trigger aggregation even in case the therapeutic protein in solution expresses an optimal colloidal or conformational stability. For example, metal coming from process equipment, leachables introduced by pharmaceutical containers or any other nanoparticulate from raw materials or excipient can have a negative impact on the protein aggregation trend [79].

The presence of the overmentioned impurities, along with the contact with air, may determine the protein *chemical degradation* (oxidation, deamidation). Intuitively, this strongly influences the protein conformational and colloidal stability, yielding the formation of bigger aggregated species [77].

Another major destabilizing source that is worth mentioning is the *light*. In fact, when exposed to light, protein formulations may undergo degradation reactions by different pathways, such as photodimerization, photoinduced hydrolysis, photooxidation, photoreduction, etc. [120]. These reactions proceed through the formation of free radicals, whose presence eventually enhances the generation of oligomeric species [121, 122].

Since the retainment of protein stability in therapeutic formulation is of huge importance to have effective drugs with absent or irrelevant side effects, different strategies need to be applied in order to render an injectable biologic as stable as possible. In the next paragraph, it is discussed that the API is not the only component in a pharmaceutical formulation. In facts, the addition of other co-solutes to the final solution can help achieve the protein stabilization and protection against various stress sources.

1.5 Therapeutic protein stabilization through the addition of excipients

Co-solutes intended to improve protein stability in therapeutic formulations are named *excipients*. There are different classes of protein stabilizers, comprising buffers, salts, sugars, polyols, polymers, amino acids, other proteins and surfactants. The excipients, with some exceptions, stabilize the proteins in solution *without binding* them [123]. This is extremely functional to the cell biology in terms of optimal preservation of osmotic pressure levels [124, 125]. Ohtake and colleagues [123] report that excipients can stabilize proteins in solutions through different inter-related mechanisms, including *excluded volume effect or preferential hydration.* In simple words, the presence of excipients in the bulk water, creates entropically unfavorable conditions that force the proteins to retain the conformational stability (*i.e.,* higher ΔG_{unf}). This means that excipients occupy space that could be otherwise used by the protein to explore different altered structural conformations [123, 126].

While the effects and the purpose of the different classes of excipients on the mitigation of protein aggregation against destabilizing sources have been reviewed by various authors [79, 97, 127-130], hereafter, just a little information about the most important categories of stabilizers will be reported.

Firstly, as the protein in solution are particularly susceptible to pH changes, *buffering agents* (*e.g.,* acetate, citrate, tris, histidine, etc.) are extensively included into the formulations to maintain the pH of the solution [129]. Also, *salts* (NaCl, KCl, $CaCl_2$, etc.) are typically used in liquid formulations as tonicity-adjusting agents. They are strongly influent on the protein conformational and colloidal stability as they can modify protein-solvent system interactions and screen electrostatic charges. The Hofmeister series categorizes salts in chaotropes*,* promoting the protein unfolding, and kosmotropes, instead intended to prevent it [127]. Moreover, *sugars* (trehalose, sucrose, etc.) and *polyols* (mannitol, sorbitol, etc.) are largely used to stabilize proteins in solution (specially against thermal induced destabilizations). They are also referred to as osmolytes and mainly act through preferential hydration mechanism [127]. The H-bonds between sugars and water molecules are tighter than water-water ones. This determines an important reduction in the reorganization rate in bulk water, thus indirectly improving the conformational stability of proteins [97]. Furthermore, a rather important class of excipients is represented by *amino acids*. Due to their nature they promote protein stabilization by directly binding the proteins in solution (*e.g.,* arginine). Also, they can express buffering capacity (*e.g.,* histidine) or antioxidant properties (*e.g.,* methionine) [130]. In particular, their ability to bind proteins resides in the fact that amino acids are hydrogen bond donors or acceptors, thus they can form multiple H-bonds with the biomolecules in solution influencing their conformational stability and mitigating the aggregation [97]. Besides the classes of excipients discussed above, also *surfactants* (e.g., Poloxamer, Tween, etc.) are largely used in pharmaceutical formulations. Their employment is manly intended to compete with biomolecules adsorption to interfaces (air-liquid and solid-liquid) in order to mitigate their detrimental effects [128].

1.6 Development of protein-based liquid formulation

At this point, it is rather clear that a formulation is a highly intricate system with peculiar physical and chemical properties. As reported in previous paragraphs, a pharmaceutical formulation, also named *Drug Product* (DP), is an extremely crowded multicomponent system that includes the therapeutic protein ingredient and a number of excipients (typically 5 or 6) intended to stabilize the API by directly interacting with either the biomolecules or the surrounding water. In addition, the pharmaceutical formulations are typically characterized by elevated API concentration, which makes them very challenging fluids from a rheological and chemical point of view (high viscosity and complex network of intermolecular interactions).

In such a complicated context, determining the conditions for the therapeutic protein to exhibit optimal stability in order to bring low immunogenic and effective therapeutic product to the clinics is definitely a hard task. The process leading to the evaluation of the major-influencing factors and the definition of appropriate formulation composition for protein maximal stability goes by the name of *formulation development* [131]. In practical and general terms, this is a process in which many solution conditions (pH, ionic strength) and different excipients are dissolved in varying amounts and combinations with the API. The set of DPs are exposed to an array of physico-chemical stress conditions (high temperature, mechanical stress, light exposure, chemical degradants)

aiming to exacerbate protein degradation pathways and rapidly collect data about their stability [97]. Different formulations are expected to exhibit dissimilar stability behaviors in response to destabilizing stress factors because of a modified protein-solvent and protein-protein network of interactions mediated by stabilizers. This is crucially significant to pharmaceutical companies, as it enables the possibility to identify a formulation ranking pointing out which DPs perform the best in terms of stability and deserve to be further investigated.
More in detail, stability tests of formulations are regulated by the International Council for Harmonization of Technical Requirements for Pharmaceuticals for Human Use (ICH) guidelines, that provide general indications depending on the type of biologics and its form (*e.g.,* whether liquid or solid) [132]. An example that is functional to the activities reported later in this thesis is that of a liquid DP whose long-term storage condition is 2-8 °C. For such a formulation, the typical stability tests can be divided in:

(i) Stability in *storage conditions*: this test is regulated by the ICH document Q1A [133]. It consists in keeping the different formulations at temperature and relative humidity (RH) proper of the storage conditions (5 ± 3 °C and 60 ± 5 %, respectively) for a typical time period of 12 months. This test is aimed to identify the real stability of formulations at actual storage conditions.

(ii) Stability in *accelerated conditions*: this test is conducted at quiescent conditions at 25 ± 3 °C and 60 ± 5 % RH, for a time period in the range of 6-12 months (however, shorter than stability at storage conditions). This test is aimed to gather information about protein stability faster than storage condition test thanks to the exposure to higher temperatures. This stability study is regulated by ICH documents Q1A and Q5C [133].

(iii) Stability in *forced degradation conditions*: this study is also referred to as *stress testing.* It identifies a class of physico-chemical stimulation tests (thermal, mechanical, light, chemical stresses, etc.) conducted at conditions that exceed the ones used for storage and accelerated stability [134]. Intuitively, this is aimed to gather information about protein stability (in particular, protein aggregation level) in short time periods, such as a week [134, 135]. Further details about the application and the nature of forced degradation conditions are discussed below.

To start with, it must be precised that, in contrast to stability testing at storage and accelerated conditions, forced degradation procedures are not regulated by any documentation coming from ICH or other regulatory body such as FDA or European Medicine Agency (EMA) [134]. The only regulated forced degradation condition is the *light stress*, that is detailed in ICH Q1B document [136].
In this case, some scientific reviews [134, 135, 137] come to help as they summarize the most typical conditions applied in the forced degradation conditions both based on authors' experience and other works reported in the literature.
The aim of forced degradation studies covers a wide range of purposes. Among them, we can mention the individualization of *degradation pathways,* identification of formulation *critical quality attributes*, development of a proper *quality control analytical method*, or *comparability among different DP lots* [135].
Highly relevant to the present thesis is the application of forced degradation for the evaluation of DP *manufacturability* (tolerability of process parameters) and for a *formulation pre-screening*. In particular, the latter consists in the application of rather extreme stress conditions to different DPs, inducing an appropriate level of formulation degradation (typically around 5-20% of aggregate species based on chromatographic analysis [137]), aimed to gather meaningful information for further formulation development studies [135].
In their review, Nowak and colleagues [135] discuss the typical pre-screening stress conditions for a mAb liquid formulation intended to be stored at 2-8 °C. They include high temperature, agitation, freeze-thaw cycles, pH change, light stress and exposure to degradants.
Specifically, reaffirming that it depends on the intensity of the conditions, a typical thermal stress on such a formulation can be, but it is not limited to, conducted at 40 or 50°C (in general, 10-20°C below the *Tm* [134])

for a time period that covers a few days (up to a week). During the stimulation, different time points are set in order to check the aggregation level of the DPs under stimulation and come up with aggregation rate [135]. A very famous mathematical expression used to relate aggregation kinetics to the temperature is the Arrhenius relationship, here reported in the form proposed by Eyring:

$$k = \frac{k_B T}{h} \exp\left(-\frac{\Delta G_a}{RT}\right). \quad (3)$$

In equation 3, k is the rate of chemical reaction (in this case the protein aggregation), T is the absolute temperature, $k_B$is the Boltzmann's constant, h is the Plank's constant, R is the ideal gas constant and ΔG_a is the Gibbs free energy of activation. This relation has a practical meaning for pharmaceutical companies, as it enables the possibility to predict the shelf life of formulations based on these short-term forced degradation studies [138, 139]. However, it is well known that Arrhenius relationship might not hold for all the proteins, or could be only valid in a narrow temperature range. This non-Arrhenius aggregation behavior may lead to wrong estimations of the aggregation rate based on short-term studies [140]. As reported by Hawe and co-workers in their review [134], predicting the aggregation through the Arrhenius relation might be possible just in case the degradation pathways experienced by the biomolecule in solution are exactly the same of those taking place in storage and accelerated stability studies. In fact, while the high temperature can accelerate the degradation pathways, it could potentially trigger the formation of intermediate species that in actual storage/accelerated conditions might not be present (*e.g.,* chemical modifications of protein structures). Besides the practice reported above, some works in the literature describe the application of thermal forced degradation studies by using high-throughput screening approaches [141, 142]. These degradation studies are performed at miniaturized scale (*i.e.,* multiwell plates), at temperatures close to *Tm* and over time periods in the order of minutes.

Another important forced degradation stress is applied by exposing the different DPs to the agitation. It consists in shaking or stirring the formulations (200-300 rpm) at room temperature. Also in this case, different time points are typically fixed at 0, 3 and 5 days to check the aggregation level of each candidate formulation [135]. This test is intended to challenge the formulation sensitivity with stressing conditions that are encountered during manufacturing process and transportation (as reported in paragraph 1.4, solid-liquid and air-liquid interface).

Both high temperature and agitation have been better detailed above as they are of direct interest of this work. Conversely, other typical forced degradation tests are not directly involved in the research activity reported in next chapters, hence just a brief summary of them is provided in the *table 1.*

Forced degradation source	Tested conditions
Freeze-thaw [135]	Freeze to -80 °C Thaw to predefined temperature (e.g., 25°C) 3-8 cycles
pH change [135]	Low pH (3, 4, 5) at 25, 30, 37 °C High pH (9, 10) at 25, 30, 37 °C Time points: Day 0, 1, 2, 3, 4
Light [136]	Minimum dose of *visible light*: 1.2 mln Lux hour Minimum energy dose of *near UV light* (UVA): 200 $\frac{\mathrm{W}}{\mathrm{m}^2}$ hour Exposure time: from 7 to 21 hours depending on the lamp type and irradiance
Chemical degradants [135]	Oxidation: exposure to hydrogen peroxide [0.02; 1] % for 1 to 4 hours; Glycation: addition of glucose to the sample at different molar ratios to protein; incubation at 37°C for different days

Table 1 – typical forced degradation conditions (other than high temperature and agitation) for a liquid therapeutic formulation whose storage condition is 2-8 °C

After being exposed to physico-chemical stimulations, the stability of biologics is returned by different analytical techniques including spectrometric, spectroscopic, optical and fractionation-based methods, aiming

to characterize aggregated species in terms of size, concentration, shape and optical properties [143-146]. Currently, the gold standard technique for the detection of soluble aggregates is the Size Exclusion High Performance Liquid Chromatography (SE-HPLC) that returns a quantitative analysis of monomers and aggregated species in a formulation. Although it is widely used in pharmaceutical formulation development, this analytical technique presents some limitations. First, in order for the sample to be analyzed through the SE-HPLC, a significant dilution is required. As it can be deducted from previous paragraphs, the dilution can drastically change the protein stability behavior, determining the dissociation of some aggregations. Furthermore, generating high pressures to pump the sample through the SE-HPLC fluidic system may potentially lead to aggregation within the separation column. Lastly, this technique shows a limited resolution, typically restricted to aggregate whose molecular weight is less than MDa [143, 147]. Besides the SE-HPLC gold standard technique, other orthogonal techniques can be adopted to have a clearer picture of the physical state of the therapeutic protein in DPs. These techniques may include spectroscopic (Infrared, Ultraviolet, Raman) or light scattering (LS) based approaches (Dynamic or static LS, turbidimetry or nephelometry).
All this information together helps describe the instability level of therapeutic proteins in solution in order to return a ranking of formulations, where the ones performing the best are good candidates for additional investigations, manufacturing, (pre)clinical trials and potential marketization.

2. Unmet needs in the study of formulation stability and aim of the work

ABSTRACT

While there is a pressing requirement for more robust formulations to precisely address patients' needs and enhance clinical outcomes, the stabilization of therapeutic proteins proves to be a challenging task due to the elevated number of instability sources and the complex physico-chemical nature of formulations. Current *in-batch* approach result to be low-throughput and expensive. Plus, they fall short of adequately simulate destabilizing conditions and do not provide the chance to combine stress sources - a common occurrence in real formulation lifecycles. Consequently, the protein stability behavior is only partially caught and a significant gap still exists in the scientific understanding of the intricate connections among therapeutic protein stability, physico-chemical destabilizing sources and potential mitigation strategies.

To clarify this correlation, unconventional technologies are needed to enable cost-effective and systematic formulation screening against unexplored instability sources, such as high intensity hydrodynamic forces typical of manufacturing process conditions and combination of stresses. The integration of this information to the knowledge from current formulation development approaches could lead to a comprehensive understanding of the therapeutic biomolecule behavior, aiming to set more appropriate formulation studies as well as suitable molecule-related manufacturing process parameters.

In light of the needs reported above, the present work aims to study the physical stability of therapeutic proteins in high concentration and viscous pharmaceutical formulations through the adoption of a miniaturized strategy based on the microfluidics. In fact, while the microfluidics has been successfully applied to the characterization of diverse aspects of therapeutic protein, its employment remains limited to diluted biomolecule solutions, with no clear focus on industrial context, where the main emphasis is on highly concentrated and viscous multicomponent formulations. In particular, we report the design and the development of an automated and programmable *modular microfluidic platform* able to apply *unconventional physical stimulations* to pharmaceutical formulations spanning a wide range of component concentration and viscosity. Specifically, it is intended to expose therapeutic formulations to unconventional thermal stress, mechanical stimulation (manufacturing-relevant shear rate levels) or a combination of them in an extremely controlled and reproducible manner. The platform is properly thought to automatically guide candidate formulations through predefined isolated or combined stress pathways, in order to induce API instability.

2.1 The clinical, technological and scientific unmet needs

Biological therapeutics, such as protein-based injectable formulations, belong to a class of medicines that exhibit exceptional properties compared to other classes of drugs (*e.g.,* synthetic drug molecules). Their strength lies in their specificity and capability to accomplish complex biological tasks that no other kind of synthetic molecule could perform. Although their advantages and the improvements in the development technologies, the clinical use of biologics is significantly limited by diverse drawbacks. Among these, their immunogenic behavior is definitely the most concerning clinical challenge. As reported in detail in the previous chapter, along with the side effects in patients, the body immune response impacts the therapy efficacy of the biological therapeutics, neutralizing the API or modifying its pharmacokinetics. In the era of *patient centricity* [148], the patient satisfaction related to the use of biologics becomes of outmost attention. In light of this, the problem of biologics immunogenicity sounds inadequate, and the need for more effective and less immunogenic biological therapeutics remains, from a clinical point of view, to be met.

Although it is well known that the immunogenic behavior is strictly linked to the poor stability of the biomolecules (*e.g.,* natural propensity to aggregation), trying to stabilize an API in a pharmaceutical formulation is by far from being elementary. As previously reported, the number of instability sources is rather large and their occurrence cannot be easily predicted or, in some cases, properly tested at laboratory scale. Traditional formulation development is based on an *in-batch* stimulation approach, that is characterized by a series of drawbacks. First, it is **low-throughput**. This means that it makes use of large volumes of reagents (*i.e.* high amounts of protein therapeutics and co-solutes) that drastically increases the **expensiveness** of a formulation development study and, eventually, **limits the number of explored stressing conditions and stabilizer combinations**. Additionally, *in-batch* protocols **do not enable a precise control** of the environment process parameters. Practically, this might translate in a non-uniform distribution of thermal energy or in turbulent uncontrolled flow regime during the agitation stress. Importantly, the use of *in-batch* approach **do not allow the combination of different stresses**, which is something that is very likely to happen in the reality. The combination of stresses (*e.g.*, thermal plus mechanical) may trigger specific degradation pathways that might remain unrevealed with isolated solicitations. This is a significant limitation of the current approach that does not examine the stability of formulations against real-world destabilizing sources. In addition, the challenging fluid properties of the pharmaceutical injectables (high concentration and viscosity) worsen the applicability of stress and analytical processes. Their thermodynamic, chemical and physical complexity is so high, that certain levels of soluble aggregates in the solution (between 5-10 %) are considered impractical to be eliminated [149].

Such an approach to the study of pharmaceutical formulations has led to a limited scientific understanding about stability of protein therapeutics. At the current knowledge, each biomolecule behaves differently depending on internal and external environmental factors and there are no global guidelines suggesting the best cocktail of excipients able to stabilize the formulations against stresses occurring throughout their lifecycle (from the manufacturing, to transportation and patient injection). In other words, because of the limitations related to present technologies, we cannot clearly correlate and predict the biomolecule thermodynamic/physical stability in response to physico-chemical solicitations and other influencing factors.

To address the need of more performing approaches able to provide a deeper knowledge of therapeutic protein stability behavior, pharmaceutical companies are paying immense toils to find new ways based on *high-throughput and miniaturized formulation screening* and analysis to exponentially increase the amount and the quality of data about their candidate products [142, 150-154]. While using reduced amount of reagents, a high-throughput approach enables the possibility to explore a larger set of conditions (stress sources and excipient combinations), resulting in an enhanced knowledge of the biomolecule stability behavior. High-throughput screening can be applied at early stages of a formulation development study (pre-formulation phase – paragraph 1.6), to obtain valuable information for a more exhaustive set of conditions, including only highly promising formulations. As reported in Wang and Ohtake's review [97], a miniaturized high-throughput approach represents a paradigm shift with respect to the ongoing practice. It is characterized by some

cornerstones, such as *choice of speedy stress conditions* to accelerate protein degradations, *combination of stresses*, application of high-throughput *multiple analytical methods* and use of *automated and integrated systems*.

To sum up, there is a pressing requirement for more robust formulations to precisely address patients' needs and enhance clinical outcomes. Moreover, the stabilization of therapeutic proteins proves to be a challenging task due to the elevated number of instability sources and the complex physico-chemical nature of formulations. Current technologies fall short of adequately simulating stress conditions, often failing to capture the full spectrum of stress sources or allowing for their combination - a common occurrence in real formulation lifecycles. Consequently, the protein stability behavior is only partially caught and a significant gap still exists in the scientific understanding of the intricate connections among therapeutic protein stability, physico-chemical destabilizing sources and potential mitigation strategies.
To clarify this correlation, unconventional miniaturized technologies are needed to enable cost-effective and systematic pre-formulation screening against unexplored instability sources, such as actual manufacturing process conditions and combination of stresses. The integration of this information at early stages, along with the knowledge from current pre-formulation approaches could lead to a comprehensive understanding of the therapeutic biomolecule behavior, aiming to set more appropriate formulation studies as well as suitable molecule-related manufacturing process parameters.

2.2 Aim of the work

In light of the needs reported above, the present work aims to study the physical stability of therapeutic proteins in high concentration and viscous pharmaceutical formulations through the adoption of the microfluidics. Thanks to its highly predictable flow properties, superior control of the microenvironment and possibility to integrate multiple technologies for a broader range of applications with enhanced performances [155, 156], the microfluidics has been investigated for the characterization of therapeutic biomolecules for different purposes, including viscosity [157-160], solubility [161, 162], study of protein-protein interactions [163, 164], separation/purification [165, 166] and thermal stability [167, 168]. However, the application of the microfluidics has only been limited to simple protein solutions, while a closer look to its employment with multicomponent complex formulations typical of an industrial setting, is still missing. In these regards, we report the design and the development of an automated and programmable *modular microfluidic platform* able to apply physical stimulations to highly concentrated and viscous pharmaceutical formulations spanning a wide range of concentration of components and viscosity. Specifically, the platform is intended to exert thermal, mechanical and combined stresses to formulations in an extremely controlled and reproducible manner. Candidate formulations are automatically guided through predefined isolated or combined stress pathways, in order to induce API instability.
Chapter three reports the design and the implementation of the microfluidic thermal stress platform. It is validated by comparing microfluidic forced degradation of different therapeutic nanobody-based (nAb) formulations with conventional *in-batch* forced degradation and standard pharmaceutical stability study protocols.
Chapter four details the design and the implementation of a microfluidic mechanical stress platform. In the introduction of the chapter, the importance of testing formulation stability against high intensity hydrodynamic forces typical of manufacturing steps will be pointed out. Also, it will be discussed that conventional agitation methods are insufficient to probe the sensitivity of pharmaceutical formulations to overmentioned challenging fluid dynamic conditions, and a microfluidic automated platform will be proposed as a tool to screen candidate formulation stability under high shear conditions. The stability of processed formulations will not only be investigated through conventional gold-standard techniques (SE-HPLC), but also through orthogonal methods to catch peculiar instability protein behaviors. Also, at the end of this chapter, the microfluidic mechanical

stress is shown to be translatable to cell-based biologics, proving the concept that such an approach might help control the biogenesis of extracellular vesicles.
Finally, chapter five provides a proof of the concept that the combination of stresses might be meaningful to highlight unrevealed protein formulation behaviors thanks to a more reality-related stress context.

3. Design of a thermal stress microfluidic platform to screen stability of therapeutic proteins in pharmaceutical formulations

ABSTRACT

Therapeutic proteins have great potentialities for the care of a wide spectrum of diseases, for which other small synthetic drugs result ineffective. Due to challenges related to their immunogenicity, the journey of biologics into clinics still faces obstacles. Among the causes of protein immunogenicity, their natural propensity to aggregation is crucial, and the exposure of biomolecules to diverse environmental physicochemical conditions is highly relevant to study their stability in pharmaceutical formulations. Traditional approaches to explore protein behavior are effort-demanding, lengthy and expensive, resulting in a limited knowledge of the biomolecule stability. Faster and cost-effective miniaturized technologies urge to be developed. In this chapter, the conceptualization, design, characterization and implementation of a modular and automated microfluidic platform to provide thermal stress to highly concentrated and viscous pharmaceutical formulations is presented. The microfluidic platform validity in terms of reliability and comparability to a forced degradation batch-wise stimulation is demonstrated by thermally stimulating and analyzing through SE-HPLC different high concentration (> 100 mg/ml) therapeutic nanobody-based formulations. Furthermore, as it is a crucial step in a formulation development process, the ranking of formulations returned by the microfluidic thermal stress platform is compared to those given by standard pharmaceutical protocols, *i.e.*, storage (5°C) and accelerated (25°C) stability studies.

GRAPHICAL ABSTRACT

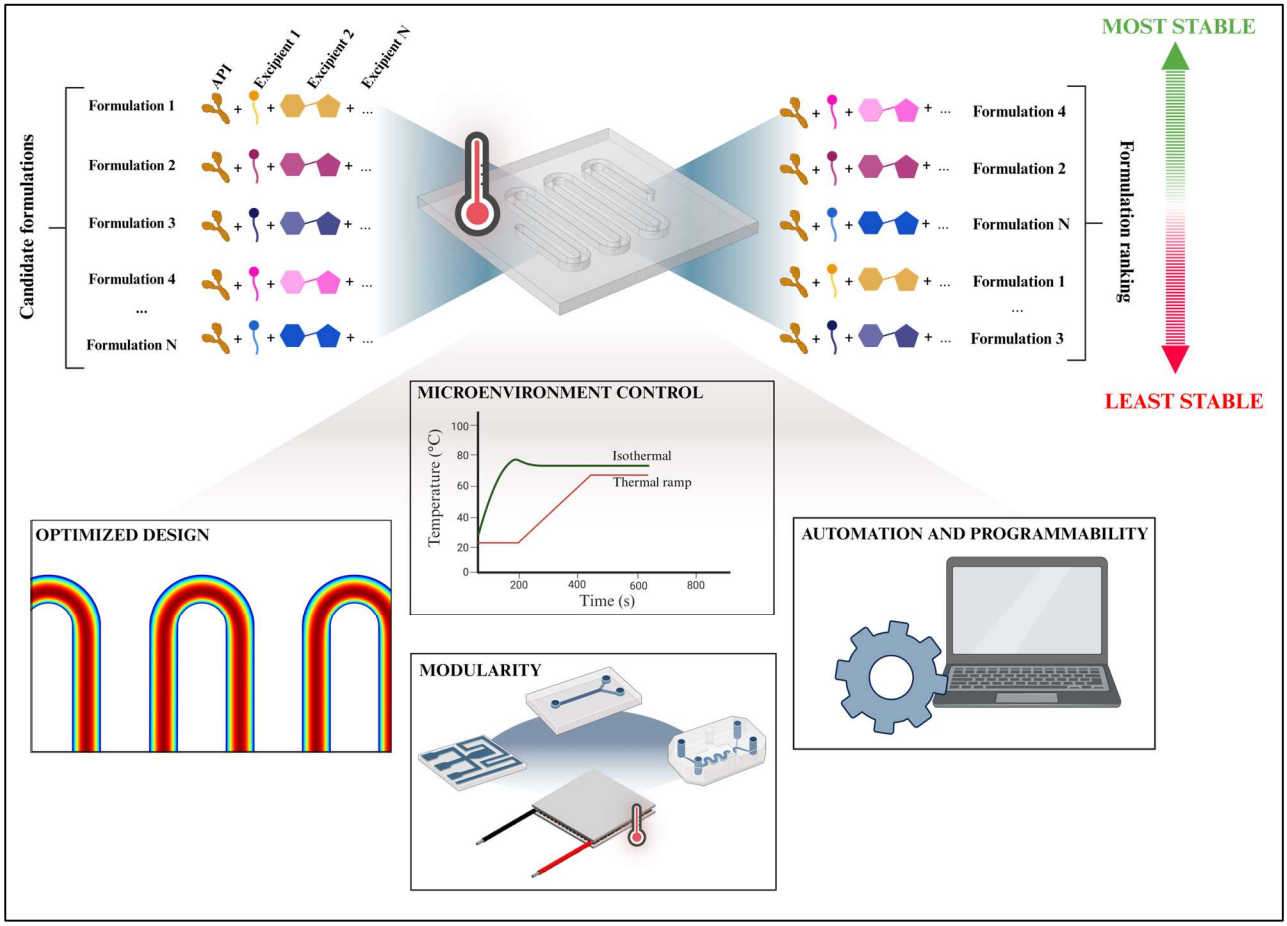

Image created with BioRender.com

3.1 Introduction

In previous chapters it is highlighted that biologics have gained great attention because of their incomparable properties. Numerous advantages are related to their high specificity and complexity that enable functions that cannot be mimicked by other synthetic drugs [6, 10, 12]. Nevertheless, scientists and pharmaceutical industries are still facing the problem of protein stability and are struggling to bring more robust and reliable products to the market. This task is far from being easy because of protein biomolecule natural propensity to get destabilized (*e.g.*, formation of aggregates) throughout their lifecycle, including manufacturing, drug transportation and patient injection [56, 77, 79, 106]. Aiming to obtain stable biological therapeutics, a study of the major destabilizing factors and solution conditions mitigating their effect is conducted during the development of protein-based injectable formulations [97, 135]. Typically, many solution conditions (pH, ionic strength) and different protein stabilizers (buffering agents, sugars, amino acids, surfactants and polymers) [97, 123, 128, 129, 134] are dissolved in varying amounts and combinations with the API. The DPs are then exposed to an array of stress conditions (high temperature, mechanical stress, light exposure, chemical degradation) with the purpose of exacerbating protein degradation pathways and rapidly collect data about their stability [134, 135]. Different formulations are expected to exhibit dissimilar stability behaviors in response to destabilizing stress conditions because of a modified protein-solvent and protein-protein network of interactions mediated by stabilizers. Hence, after exposure to the mentioned physico-chemical stresses and evaluation through various analytical techniques, a formulation ranking is determined. Specifically, DPs expressing worst performances are discarded, while formulations exhibiting the best stability behavior are further investigated. In particular, high temperature is one of the most employed environmental conditions to explore biomolecule instability [134, 135]. Conventional protocols can be classified, according to the used temperature, as storage (2-8°C), accelerated (25°C) and forced degradation, or thermal stress, (≥ 35°C) conditions [135]. The temporal range within these protocols are conducted are typically 6-12 months for storage and accelerated conditions [169], and a few days for the thermal stress [135].

These studies mainly rely on batch-wise and off-line analysis procedures, thus presenting some drawbacks that can be summarized in expensiveness, poor controllability of environmental conditions, scarce versatility in terms of stress combination, stress testing and analytical low-throughput.

With the aim to address the overmentioned issues, some authors have reported examples of temperature-based miniaturized formulation screening [141, 142, 150]. These forced degradation studies are performed at miniaturized scale (*i.e.,* multiwell plates), at temperatures close to *Tm* and over time periods in the order of minutes. Among the miniaturized approaches, a microfluidic-based strategy could be promising due to its highly predictable flow properties, superior microenvironment control, and integration of technologies for a broadened range of stresses [155, 156]. Indeed, the microfluidics has been investigated for the study of thermal stability of therapeutic proteins [167, 168]. In particular, in 2014 Yang and co-workers have presented a microfluidic setup for the generation of a linear thermal gradient, enabling the possibility to catch changes in UV absorption upon thermal denaturation or aggregation of proteins, deducing the melting temperature of the biomolecule under observation [167]. Moreover, in the same year, Alexander and colleagues have implemented a microfluidic approach to measure the chemical denaturant titrations by intrinsic fluorescence and microscale thermophoresis, preserving measurement quality, enhancing the process throughput and drastically reducing the protein consumption of conventional cuvette-based approaches [168]. Although these examples are clear indications of how the microfluidics can be successfully applied to the study of therapeutic biomolecules, the use of the microfluidics has been restricted to simple protein solution conditions, exhibiting few components, solubilized at relatively low concentrations. On the contrary, the main focus of an industrial context is on high concentration and viscous formulations, and the application of the microfluidics suited to this circumstances is still lacking.

In this chapter, the design, characterization and implementation of a novel microfluidic-based approach to apply thermal stress to therapeutic proteins in highly concentrated and viscous formulations is presented.

An experimental campaign was conducted by exposing nAb-based formulations to thermal stress through the microfluidic platform. Moreover, same formulations were processed (at same conditions) through an industrial thermal stress miniaturized *in-batch* approach. The ability of the microfluidic platform to induce similar aggregation of the well-established small volume batchwise process is assessed through a gold standard analytics (SE-HPLC). In addition, the formulation ranking returned by microfluidic and in-batch miniaturized approaches were compared to those obtained by standard pharmaceutical tests required for the approval of injectables, such as storage (5°C) and accelerated stability (25°C) [134, 135, 169].

3.2 Materials and Methods

3.2.1 Materials

Trehalose dihydrate (product number T-104-4) was supplied by Ferro/Pfanstiehl in solid form; Poloxamer-188 (product number X0003307) was provided by Merck Serono S.p.A., Rome, Italy (an affiliate of Merck KGaA, Darmstadt, Germany), L-Arginine (product number 1.01544) and Tris (product number 1.08386) were supplied by Sigma-Aldrich. The nAb (Mw 45 kDa) was provided by Merck Serono S.p.A., Rome, Italy (an affiliate of Merck KGaA, Darmstadt, Germany). The nAb was given in liquid form at a concentration of 150 mg/ml in 10 mM Tris buffer, pH 7,5. NaOH (product number 1.58793) and HCl (product number 1.00317.1000) were provided by Sigma-Aldrich and used to adjust the pH of the solutions. MilliQ water was used to prepare all the solutions. Polymethyl methacrylate (PMMA) sheets (product number ME30-SH-000110) were obtained from GoodFellow Cambridge Ltd.

3.2.2 *Preparation of buffer and formulations*

A 10 mM of Buffer solution was obtained by solubilizing 1,21 g of Tris in 1 liter of MilliQ water. HCl was used to bring the pH from ≈10 to 7,5.

Three formulations were prepared in 10 mM tris buffer so as to have a final volume of 15 ml for each solution, a final nAb concentration of 120 mg/ml and excipients at different concentrations. In particular, Trehalose concentration ranges from 53 to 106 mg/mL, L-Arginine spans from 0 to 14,7 mg/mL while Poloxamer-188 concentration is kept constant at 0,1 mg/mL. NaOH was used to adjust the final pH to 7,5. The composition of each formulation is detailed in *table 2*.

Formulation	Trehalose (mg/mL)	L-Arginine (mg/mL)	Poloxamer-188 (mg/mL)	nAb (mg/mL)
A	106	0	0,1	120
B	79,4	7,4	0,1	120
C	53	14,7	0,1	120

Table 2 - Composition of formulations

Solutions were gently stirred at 250 rpm and room temperature until complete and homogeneous mixing was obtained. The final solutions were filtered through 0,22 µm PES syringe filters.

3.*2.3 Design of the Microfluidic Platform*

The thermal stress platform is composed by two main sections: pumping and thermal stress modules. The former comprises two syringe pumps (Model 11 Elite, Harvard Apparatus USA) and two two-position/three-port automated valves (part number AV201-T116, LabSmith, USA). The latter was designed to account for a mainline (where the thermal stimulation takes place – *figure 4*a, from elements 7 to 9) and a recirculation one (intended to control the stimulation time – *figure 4*a, elements 11 and 12). In particular, the thermal stress module is composed by a set of two-position/three-port automated valves (part number AV201-T116, LabSmith, USA), a thermal station and a peristaltic micropump (part number 3200243, Dolomite Microfluidics, UK). Mainly, the thermal station includes a Peltier cell (part number uTE02-132020; max T 130°C; ΔT between faces 67°C; 13 W, LabSmith, USA), an aluminum heat sink (part number HS-2020,

LabSmith, USA), a custom-made microfluidic chip fabricated by using micromilling technology (Minitech CNC mini-mill/GX) and a temperature micro-sensor (K-type thermocouple - uTS01-STD-20, LabSmith, USA). Automated valves, Peltier cell, aluminum heat sink and thermocouple were bought from LabSmith, USA. All the microfluidic parts are interconnected through FEP tubes (ID 0,8 mm, OD 1,6 mm, Dolomite Microfluidics).

3.2.4 Setup and programming of the microfluidic platform for thermal stress

The setup of the microfluidic platform is outlined in *figure 4*. The two syringe pumps (*figure 4*a, elements 1 and 2) are connected in parallel by means of two automated valves (*figure 4*a, elements 5 and 6) that are used as switchers to enable selective injection of both buffer and formulation into the thermal stress module. In the latter, the main line consists of a serial connection between two automated valves (*figure 4*a, elements 7 and 9) and the thermal station (*figure 4*a, element 8). Specifically, the thermal station is assembled by sandwiching the Peltier cell between the heat sink (upper face) and the custom-made microfluidic chip (lower face). Finally, the latter is in touch with the thermocouple (*figure 4*d). The components are held together through a thermal tape (silicone, thickness 0,25 mm). The recirculation line starts from element 9 of *figure 4*a and ends up in the thermal station's inlet (*figure 4*a, element 8). It includes a serial connection between the peristaltic micropump (*figure 4*a, element 11) and an automated valve (*figure 4*a, element 12). In addition, both pumping and thermal stress modules have some outlet lines (*figure 4*a, elements 3, 4, 10, 13) realized through the FEP tubes. The thermal stress module (*figure 4*c) exhibits a dead volume of ≈300 µl. All the presented parts were mounted on a single breadboard, as reported in *figure 4*b. LabSmith proprietary software was used to program the platform in terms of fluid pathways and thermal control.

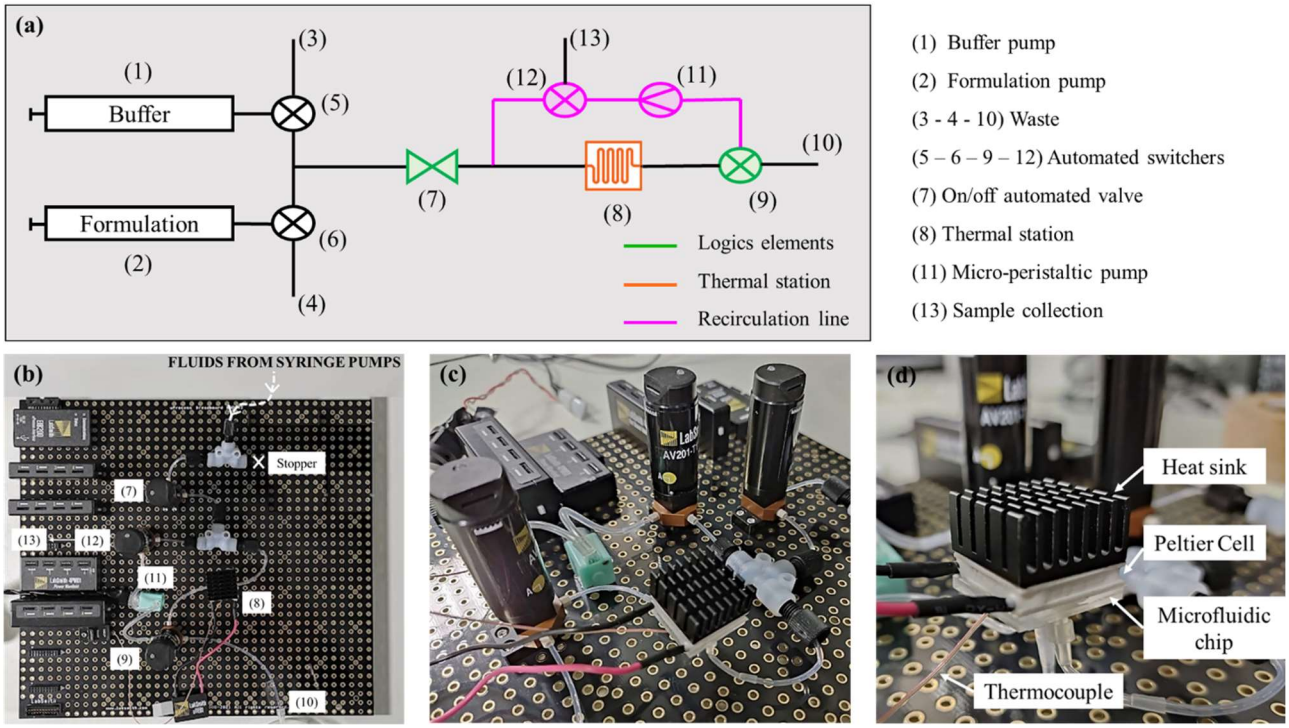

Figure 4 – (a) Microfluidic platform scheme including the pumping module and the thermal station. The elements for the fluid logic management are in green, the thermal station in orange and the recirculation line in magenta. 1-2 syringe pumps, 3-4-10 waste; 5-6-9-12 switchers; 7 on/off valve; 8 thermal station; 13 outlet for sample collection. (b) Microfluidic platform with same elements listed for the figure 4a. (c) close-up of thermal line including elements for the fluid logic, the thermal station and the recirculation line. (d) thermal station close-up.

3.2.5 Microfluidic Chip design and Device Fabrication by Micromilling technique

AutoCAD 2023 (didactic version T.72.0.0 AutoCAD 2023.0.1) was utilized to design different microfluidic chip geometries consisting of one-inlet-one-outlet spiral and serpentine channels with different cross-sectional dimensions (500x500 µm; 750x750 µm) and constant dead volume of 50 µl. The overall dimension of the custom-made microfluidic devices is 2x2 cm. DESKAM 2000 (version 5.1.5.11) was employed to realize computer-aided manufacturing (CAM) files for the fabrication.

The microfluidic chip is made out of polymethyl methacrylate (PMMA) and obtained through a micromilling process. The polymer was processed through a Minitech CNC mini-mill/GX (Minitech Machinery Corporation, USA) to build up the customized microfluidic chip. Prior to the chip realization, different milling operational parameters were systematically investigated (Appendix A – table A1), aiming to optimize the machining in terms of product roughness and fidelity to the CAD project. Different tips (100, 500, 1000 µm), diverse X-Y steps (default value returned by CAM software and its half) and various Z-steps (1/5 and 1/10 of the total channel height) were explored and the best parameters selected after Scanning Electron Microscopy (SEM) observation (Appendix A – *figure A2* b-g). For all the tips and listed operational parameters, the spindle rate was fixed at 10000 rpm and a varying feed rate was employed: 10%, 32.4% and 64.8% were set for 100, 500 and 1000 µm tip, respectively.

3.2.6 Ability of the microfluidic platform to process highly concentrated and viscous fluids

The ability of the platform to manage highly concentrated and viscous fluids was assessed by processing different Bovine Serum Albumin (BSA) and sucrose solutions at various concentrations. A *low* viscosity fluid (2 mPa*s) was achieved by solubilizing 50 mg/ml of BSA and 50 mg/ml of sucrose; a *moderate* viscosity level (7 mPa*s) was obtained by dissolving 175 mg/ml of BSA and 175 mg/ml of sucrose; finally, a *high* viscosity threshold (18 mPa*s) was reached by combining BSA and sucrose at 250 mg/ml each.

3.2.7 Fluid dynamic and energy transfer analysis

COMSOL Multiphysics® v. 5.6 was used to study the transport phenomena of designed chips in terms of fluid velocity profile, pressure drop at varying fluid viscosity, presence of inertial effects, shear rate intensity and rate of energy transfer.

3.2.8 Optimization of temperature control of the thermal stress module

A feasibility study (Appendix A - table A2) was executed to evaluate the best parameter settings for a fluctuation-free isothermal environment both with and without flowing buffer. Specifically, under no flow conditions, different target temperatures (37, 40, 50 °C) and voltage heating ramps (10; 1; 0,2 mV/s) with a tolerance interval around the target temperature equal to ±1,5°C were tested. Moreover, different target temperatures (40, 50; 55°C), heating voltage ramps (1; 5mV/s) and tolerance intervals (±0,5; ±1,5 °C) were experimented under flow recirculation.

3.2.9 Thermal stimulation through microfluidics

Fluids were processed at 800 µl/min in all the thermal stimulations through microfluidics. Formulations were thermally stimulated at unfolding (49°C) and melting (52°C) temperatures for different time periods (2 and 5 min). In addition, formulations treated at room temperature for 2 and 5 minutes were used as controls. *Table 3* reports the experimental points. The conditions were tested in triplicate.

The stimulation through the microfluidic platform was carried out following platform programming. First, the thermal station was programmed to reach the target temperature under buffer flow. After the stabilization of the temperature profile, the formulation is injected into the microfluidic plant to start the stimulation in an isothermal environment. Particularly, the automated valves were activated to switch to the syringe pump containing the formulation for the time needed to fill the thermal stress module (including main and recirculation lines). Then, automated valves were programmed to allow fluid recirculation by means of the

peristaltic micropump for the whole thermal stimulation time. Finally, the stressed samples were collected in 0,5 ml safe lock tubes (Eppendorf S.r.l., Italy). Further details on the specific thermal stress module configuration are reported in Appendix A - *figure A1*.

3.2.10 Thermal stimulation in-batch

In-batch protocols are routinely used in pharmaceutical industries. Here, in-batch forced degradation consisted in stressing 300 µl of each formulation with a mixing block instrument at the target temperature under no shaking conditions. In *table* 3 the stress conditions are reported (RT conditions were not run for miniaturized forced degradation in-batch protocol). Soon after the stimulation, the samples were quenched in ice to stop the solicitation instantly. The reported conditions were tested in triplicate.

Candidate formulations	Temperature (°C)	Stimulation time (min)
A, B, C	RT	2
		5
	49	2
		5
	52	2

Table 3 - Forced degradation conditions tested with both the in-batch and microfluidic approaches

In-batch storage and accelerated stability consisted in storing 1 ml of each formulation in glass vials at 5 ± 2 °C and 25 ± 2 °C, respectively, with a relative humidity equal to 60 ± 5 % for 13 weeks. The aggregate amount was checked at 4, 8 and 13 weeks. These conditions were tested in triplicate.
All the solicited and unsolicited samples were stored at 5°C before being analyzed through SE-HPLC technique.

3.3 Results And Discussion

3.3.1 Microfluidic chip design and fabrication parameters

The microfluidic platform scheme is reported in *figure 4*a and described in material and methods (section 3.2.4). Briefly, the microfluidic plant is divided into three parts reported in different colors. In particular, the elements for the fluid logics are highlighted in green, the thermal station in orange and the recirculation line reported in magenta. Also, a direct comparison with the real microfluidic plant assembly is reported in *figure 4*b.
Particular attention must be paid to the thermal station, of which a close-up is reported in *figure 4*d.
The microfluidic chip underneath the Peltier cell (*figure 5*a) has a ≈50 µl dead volume with a serpentine, 750x750 µm squared cross-section channel optimized to minimize shear rate and hydraulic resistance. These two aspects are essential in order to ensure the nAb formulations being destabilized just by thermal stress. In addition, considering the formulations being challenging fluids spanning a broad viscosity range (up to 20 mPa*s), minimization of hydraulic resistance (i.e., small pressure drop across the channel) guarantees no setbacks in the process. According to numerical simulations run for a 20 mPa*s fluid, the proposed geometry exhibits pressure drop and shear rate at the wall as low as 22 mbar and 380 s^{-1}, respectively.
In addition, the heat transfer rate was evaluated through a numerical simulation run for a fluid flowing at 800 µl/min being heated up to 49°C and 52°C (*figure 5*b). According to that, the fluid reached the 92% of the target temperature after 0,25 s, 97% after 0,5 s and 100% after 0,75 s, thus showing a quick heat exchange. Further details about numerical simulation for momentum transfer are reported in Appendix A (*figure A3*a,b).
It is well recognized that micro manufacturing has been a key enabling technology in industry for the development of micro products and processes. However, fine product quality should always be checked to avoid introduction of artifacts. Moreover, PMMA could also show propensity to protein interaction [170] and specially chip roughness may boost nAb deposition on the walls. For this reason, minimal roughness should be assured to avoid (or at least minimize) additional and unpredictable destabilizing sources other than the

thermal one. The feasibility study executed on the micromilling machine allowed to relate the machining parameters (tip, feed rate, X-Y and Z-step) to the final device quality. Insights are reported in Appendix A (table A1 and *figure A2*). Notably, despite the aforementioned characteristics, PMMA is highly preferable and cost-effective for use in prototyping purposes [171, 172], enabling the drawing of conclusions and making definitive advancements in material choices (such as glass or quartz), geometries, and fabrication techniques [173, 174].

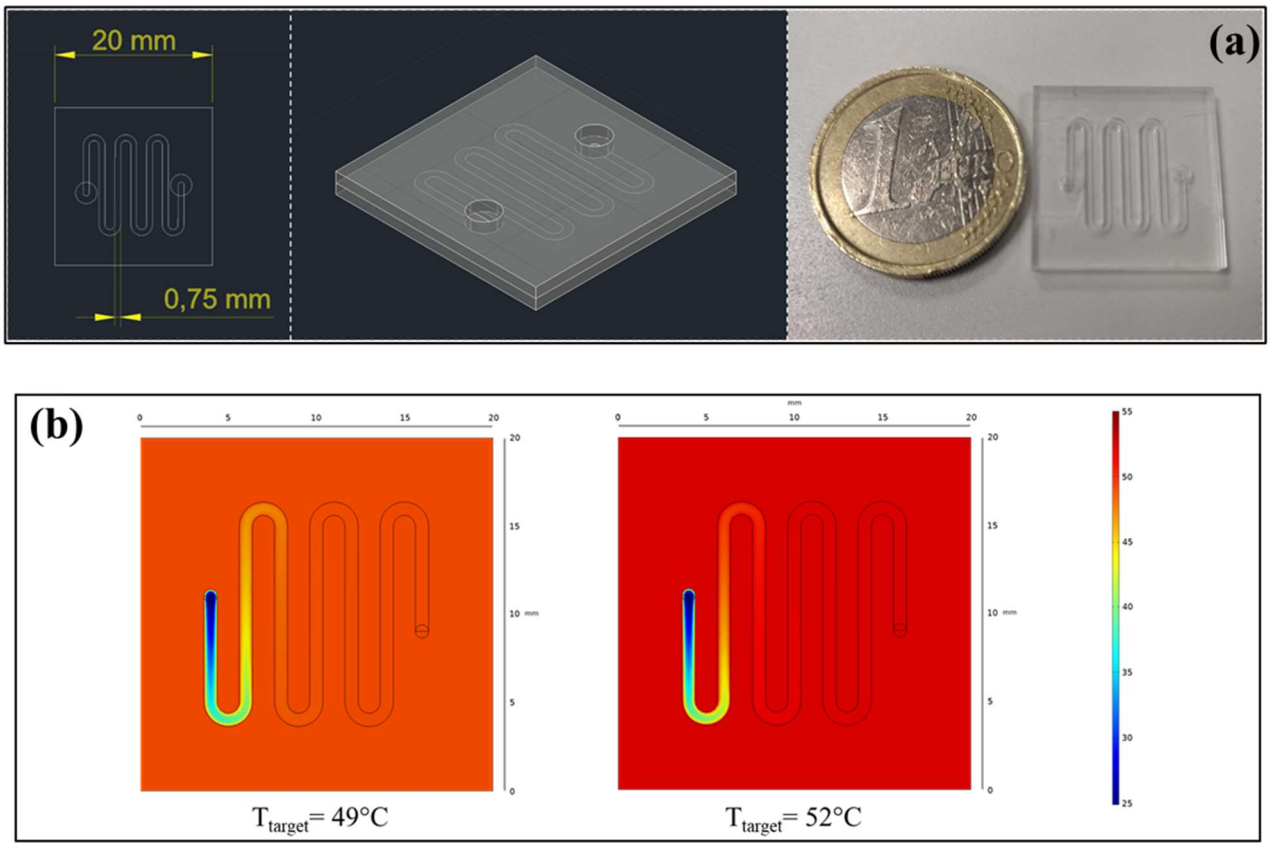

Figure 5 - (a) Thermal chip; (b) flowing fluid heating at stimulation temperatures

3.3.2 Optimal process parameters for fine temperature control

The feasibility study conducted under no flow condition (Appendix A table A2) was functional to understand the impact of the main parameters (tolerance and heating voltage ramp) on the temperature control. Under no fluid flow conditions, the best heating voltage ramp and tolerance for a temperature fluctuation-free environment resulted to be 0,2 mV/s and ±1,5 °C, respectively. In *figure 6* the trends returning from 37°C, 40°C and 50°C with a 0,2 mV/s and 1 mV/s, both with ±1,5°C tolerance interval, are reported. Generally, the higher the heating voltage, the faster the device reaches the target temperature. However, an excessively high voltage ramp (i.e., 37°C – 10 mV/s in *figure 6*a) causes the thermal station to overheat, with no hope to control the temperature. In addition, a lower ramp offers a minimized standard deviation to the target temperature, with 0,2 mV/s returning an average temperature ± standard deviation equal to 37,3 ± 1,0 °C, 40,4 ± 1,0 °C and 50,6 ± 1,6 °C for target temperature of 37°C, 40°C and 50°C, respectively (*figure*s 3a-c). As the thermal station was intended to be used under flow conditions, additional studies were conducted with the buffer being injected throughout the plant. The feasibility study (Appendix A table A2) carried out under flow conditions returned the optimal combination of parameters for a fine control and fast responsivity of the system to counteract temperature oscillations introduced by the fluid flow. At 800 µl/min, the best combination of heating voltage ramp and tolerance are 1 mV/s and ±1,5 °C, respectively.

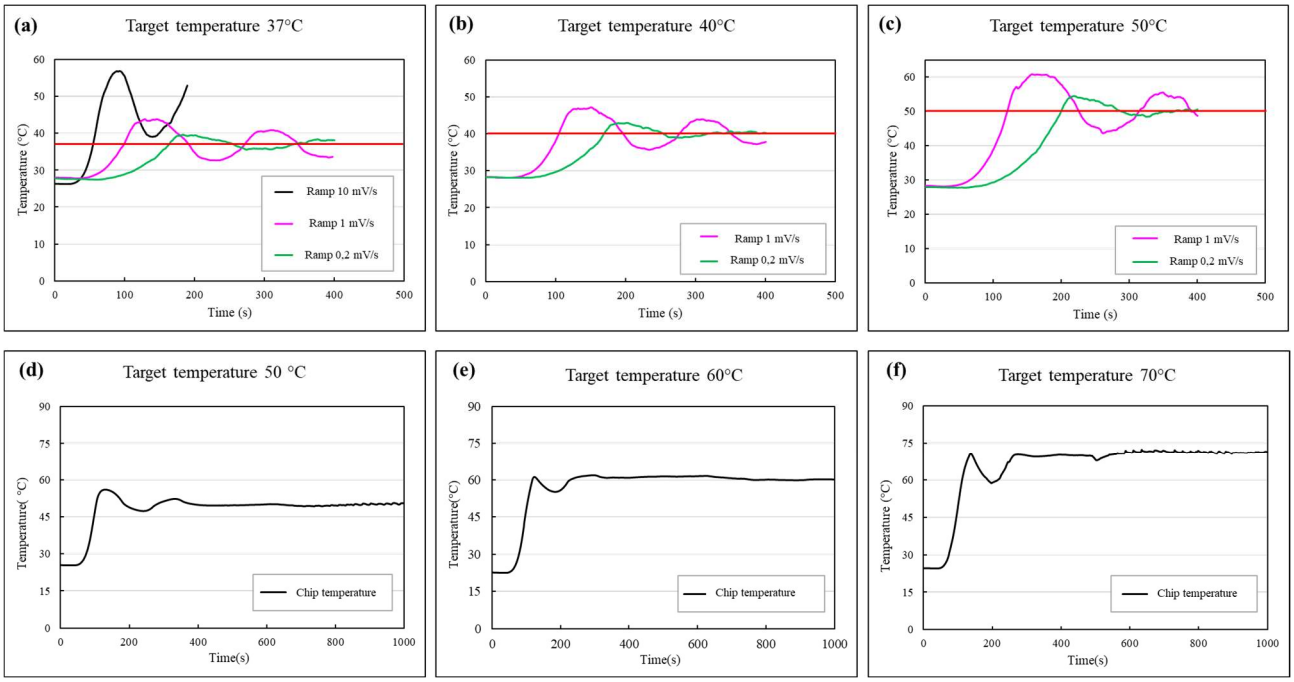

Figure 6 - (a, b, c) Temperature trend of the thermal station under no flow conditions at different heating voltage ramp and ±0,1°C tolerance interval. (a) Target temperature 37 °C; (b) Target temperature 40°C; (c) Target temperature 50°C. (d, e, f) Temperature trend of the thermal station under flow conditions at different target temperature. (d) Target temperature 50 °C; (e) Target temperature 60 °C; (f) Target temperature 70 °C.

After the feasibility study connected to the fluctuation of the thermal station at flow and no flow condition, we moved to evaluate the temperature stability around the setpoint. As reported in material and methods (section 3.2.8), the microfluidic plant was properly programmed to perform the stimulation process in three main phases. All of them are characterized by the parameter settings described above, except for the first phase, which is intended to make the thermal station reach the target temperature as fast as possible. For this reason, the voltage ramp was set to 5 mV/s instead of 1 mV/s. The second phase aims to dampen the system oscillations and prepare the system to the third phase, which is the actual thermal stimulation. The duration of the first and second phases depends on the target temperature: intuitively, the higher the latter, the longer the time required for the system to be stabilized. The only exception that exhibits the longest stabilization time can be detected for 70°C. In *table 4* the exact values of the equilibration time are reported. Also, in the same table the average temperature (± the standard deviation) is reported at different stimulation time (2, 5 and 10 min).

Target Temperature (°C)	Equilibration time (s)	Tavg - 2 min	Tavg - 5 min	Tavg - 10 min
50	140	49,0 ± 2,2	48,6 ± 1,6	48,5 ± 1,6
60	180	61,2 ± 0,1	61,4 ± 0,2	60,6 ± 0,9
70	320	70,4 ± 1,1	70,5 ± 1,2	70,6 ± 1,3
80	190	79,5 ± 0,9	78,2 ± 0,9	80,2 ± 1,9

Table 4 - Equilibration time at different target temperatures (second column) and average temperature over 2, 5 and 10 min

In addition, in *figure*s 3d-f, the temperature trends at three different target temperatures (50, 60 and 70 °C) are depicted. Specifically, after the stabilization time, the curves show minimal fluctuations around the target temperature, proving the establishment of a stable isothermal environment. The average temperatures obtained during the stimulation through the microfluidic thermal module are indicated in *table 5*.

Temperature (°C)	Stimulation time (min)	Tavg ± SD (°C)
49	2	49,0 ± 2,4

49	5	48,2 ± 1,1
52	2	52,0 ± 1,5

Table 5 - Average temperatures during the thermal stimulations of formulations.

3.3.3 Evaluation of nAb stability under thermal stress through SE-HPLC

In order to validate that the microfluidic platform itself does not induce nAb destabilization by sources other than the high temperature (*i.e.,* pumping, wall shear), each formulation (*i.e.,* control samples) was recirculated at room temperature for 2 and 5 minutes throughout the microfluidic platform.

From *figures 7a-c* it can be concluded that no aggregations are triggered by circuit elements or by simple shearing. This has to be considered as a remarkable result as the miniaturization may have introduced unexpected phenomena able to induce nAb instability. For all the experimental points shown in *figure 7a-c*, the standard deviations are within 5% of the reported values.

Moreover, for the specific thermal stimulation at 49°C and 52°C, results were also compared with in-batch protocols still conducted at the same temperatures.

As it can be deduced by *figures 7d-i*, the aggregation trend for both microfluidic and in-batch protocols are, as a point of fact, identical, thus making the microfluidic platform a valid alternative to batch-wise approach with the further advantage of process continuity and automation. Also for the experimental points reported in *figures 7d-i*, the standard deviations fall in a 5% range of the reported values.

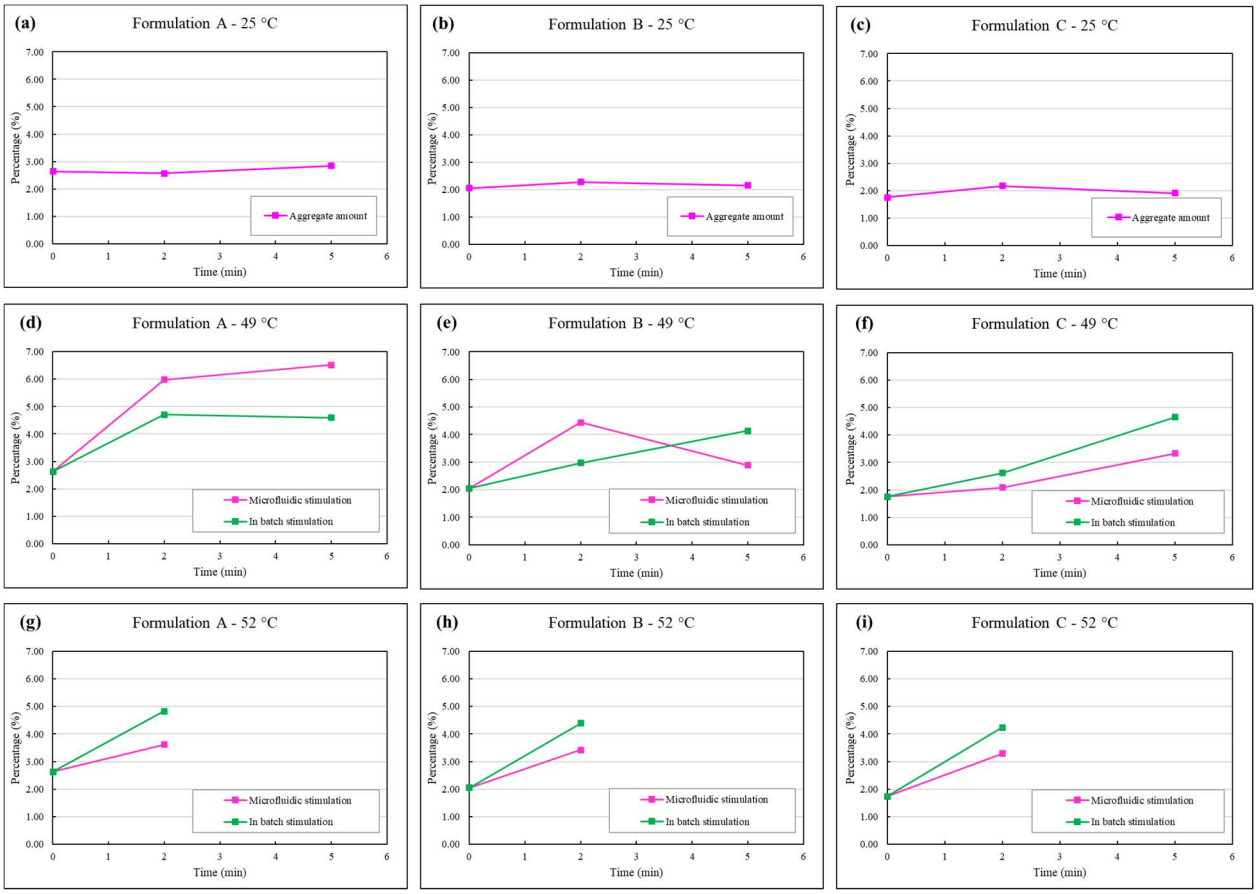

Figure 7 - SEC analysis of candidate formulations. (a-b-c) samples processed at room temperature throughout the microfluidic platform to ascertain the only destabilization source is the thermal heating. (d-e-f-g-h-i) samples treated at 49 and 52°C – comparison between in-batch and microfluidic stimulation.

3.3.4 Ability of the microfluidic platform to generate a formulation ranking in agreement to standard regulatory protocols

To further validate the platform, stimulations by microfluidics were also compared with typical in-batch storage and accelerated stability tests, as approved by the ICH Q1 A (R2) to certificate pharmaceutical formulations [169]. As reported in material and methods (section 3.2.10), stability tests are conducted at 5°C and 25°C for 13 weeks and obtained results are compared with in-batch and microfluidic forced degradations at 49°C and 52°C.

This is a relevant step not to evaluate the aggregation state, but rather to come up with a ranking among different formulations developed during pre-formulation screening (i.e., an important preliminary phase of pharmaceutical formulation development). In fact, it is incredibly relevant to pharmaceutical companies to select the most stable formulation and discard the one expressing the worst performance. In these regards, the data from the microfluidic thermal stress module agree with conventional stability tests (*figure 8a-b*). Indeed, as reported in *figure 8*, the stimulation through microfluidics (*figure 8e-f*) is able to point out, among the candidate formulations, which is the most and the least stable in accordance with the in-batch approaches (*figure 8*a-d). In other words, the platform is able to return information about the role of the excipients: it is rather clear that an increased level of arginine, if combined with a proper amount of trehalose, provides a better nAb thermal stability than the sugar alone. For all the experimental points reported in *figure 8*, the standard deviations are in a 5% range of the reported values.

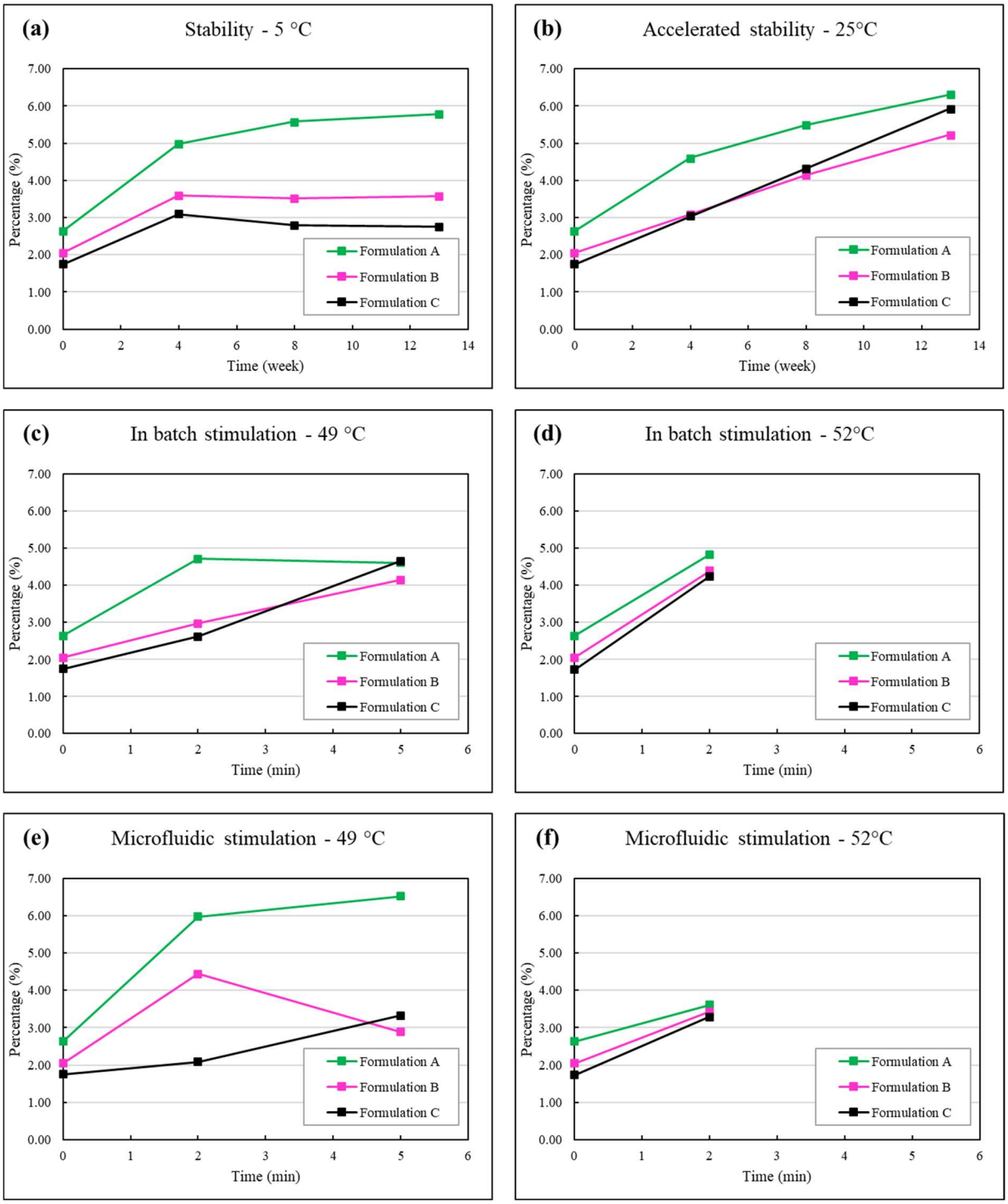

Figure 8 - Data ranking comparison among stability at 5°C (a), accelerated stability (25°C) (b), in-batch stimulation (c,d) and microfluidic stimulation (e,f).

3.4 Conclusions

Provided the great potential of the therapeutic proteins, their spreading in the clinics is still hindered due to challenges related to their stability, a main priority to guarantee drug efficacy and safety. Indeed, there is an urgent need to control and predict the protein behavior when exposed to typical physicochemical stimulations encountered during their lifecycle. This would open the possibility to have more robust and affordable products, impacting on the industrial world by reducing production and retail costs as well as enhancing the clinical outcomes. Since current protocols are time-consuming, expensive, poorly reliable and effort-demanding, there is still a prominent need for new approaches to address these limitations.

In this chapter, a novel miniaturized and automated platform was designed and validated to be an alternative to the current thermal stress analysis in use during pharmaceutical formulation development. Considering the rheological challenges posed by therapeutic fluids (high concentration and viscosity), the platform was properly designed and sized to exhibit minimized pressure drop and absent tendency to clogging.
While it may seem trivial, such a step was the most critical as, at small scales, pressure drop control becomes tedious. The capability to manage high viscosity guarantees the process continuity and prevents the latter from coming across setbacks. This achievement resulted from matching data acquired from the industrial repertoire (chemical, physical and rheological properties of typical solutions), sound scientific knowledge, and advanced engineering solutions. The plant presents a thermal stressing module able to offer an isothermal environment with negligible temperature fluctuations, expressing stimulation reliability validated by the comparison to well-established pharmaceutical protocols. In fact, the microfluidic platform returns the same aggregation trends and formulation ranking of traditional strategies, potentially resulting in a valid alternative to the current practice. Plus, the plant does not add any unpredictable stress due to the miniaturization (*i.e.,* tubing dimensions, valves, microfluidic chip). A concise experimental campaign was carried out to demonstrate that the platform enables to acquire knowledge on the role of the excipients added to the formulations, hence showing to be an applicable tool to study the protein behavior in formulation under different environmental conditions. To the current status, the proposed miniaturized thermal stress approach is already an excellent option to address the expensiveness limitation posed by conventional technological approaches while preserving their resolution. In fact, small volumes are required, thus providing a solid cost reduction compared to the large volumes typical of formulation screening. In addition, the automation of the process can facilitate the conduction of the stimulation, assuring its repeatability, reliability, absence of operator-dependent mistakes and easy exploration of broad solicitation ranges and types (*e.g.,* application of temperature ramps to the same formulation in a one-step process) while paying minimum effort.

4. Design and implementation of an automated mechanical stress microfluidic platform to screen therapeutic formulation stability under high intensity hydrodynamic forces (HIHFs)

ABSTRACT

Therapeutic proteins cover a pivotal role in the care of challenging diseases, however the translation to clinics is plenty of obstacles threatening their stability, a primary requirement to be maintained for their therapeutic effect. Among the destabilizing factors, mechanical stress sources are largely present during a formulation lifecycle. Particularly, while being manufactured, the formualation are exposed to high intensity hydrodynamic forces (HIHFs) that can have a negative impact on the therapeutic protein stability. The gold standard mechanical stress test conducted during a pre-formulation study consists in the agitation of formulations for a time period ranging from 3 to 5 days. Based on the scientific literature, it emerges that, while they remain efficient to test the robustness of formulations against air-liquid interface, agitation methods have scarce ability to replicate HIHFs established during the formulation manufacture. Moreover, they are batchwise approaches requiring large formulation volumes and offering poor control of process parameters. Various authors have investigated the impact of HIHFs (such as shear and elongational stress), and current research acknowledges that the combined influence of the solid-liquid interface and HIHFs may lead to protein destabilization, affecting processes like adsorption and desorption. While this might hold true, it should be pointed out that the tendency to aggregation is molecule- and formulation component-dependent. Thus, generalization of the effect of HIHFs on protein stability are very difficult to be drawn. Nevertheless, testing formulations with respect to more realistic stress conditions (such as high shear) typical of manufacturing step, remains an industrial problem to be addressed. Overcoming this issue would permit formulation scientists to have a full picture of formulation behavior that remains incomplete through the application of conventional tests, thus bringing more robust products to post-formulation development phases.

In this chapter, the microfluidics is explored as a tool to overcome expensiveness of batchwise agitation protocols and to recreate, in a more reliable manner, stress sources proper of a manufacturing step. An automated microfluidic platform is designed and set up in order to generate HIHFs in a wide range of shear rate (up to 20000 s^{-1}). Some nAb-based formulations are tested through the microfluidic mechanical stress platform and their physical status is characterized through conventional analytical methods (SE-HPLC) and orthogonal *quasi-real-time analysis* techniques (DLS and FTIR). The application of the microfluidic stress in combination to a proper analytical strategy (*quasi-real-time*) returns undisclosed behaviors of formulation colloidal and structural configuration in relation to stress intensity and type of excipients. Results presented in this chapter highlight the importance of testing formulations with respect to HIHFs in an early development phase and underline the limitations of conventional analytical approaches.

GRAPHICAL ABSTRACT

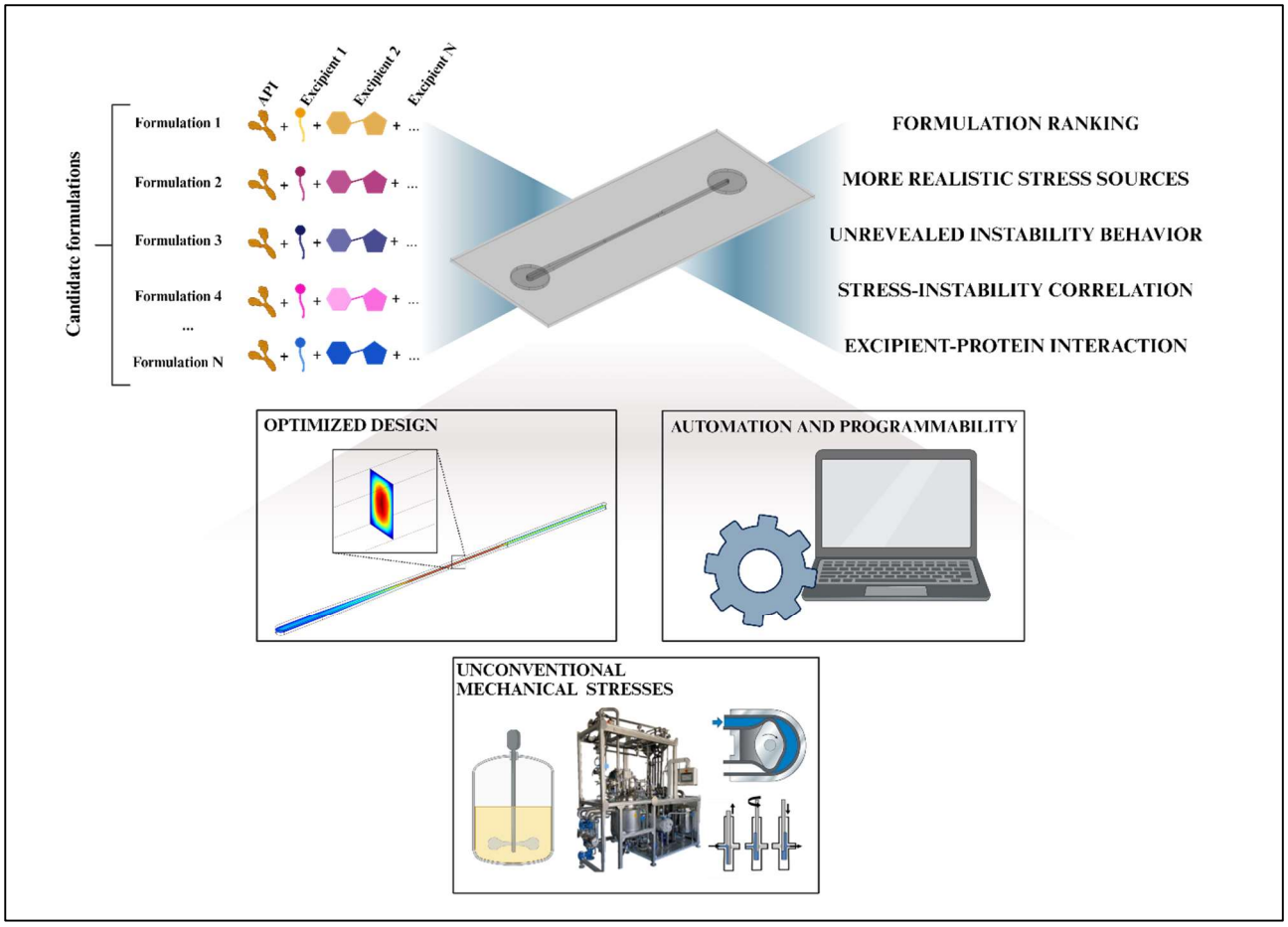

Image created with BioRender.com

4.1 Introduction

The lifecycle of a biologic, from its development to the patient injection, is full of obstacles threatening its stability. In previous chapters, the formulation development has been identified as the process where the main mitigation strategies against instability sources are identified. To this purpose, formulations are exposed to different challenging environments (*i.e.,* physical and chemical stimulations) to exasperate protein degradation pathways. Previously in this work, high temperature has already been mentioned as a largely adopted agent to force therapeutic protein degradation and, from a practical point of view, it has been shown to be highly impacting on the aggregation status of a therapeutic nAb.

In addition, while being developed, manufactured, transported and injected into patients, biologics eventually come across different interfaces (solid-liquid or air-liquid) [106] or challenging hydrodynamic conditions (*e.g.,* high shear or elongational strain) [175, 176]. In other words, formulations are exposed to different mechanical stress sources, and their robustness with respect to them is needed to be investigated during the formulation development through mechanical stress tests.

As previously detailed (chapter 1, paragraph 1.6), in a traditional formulation development approach [97], the mechanical stress testing is mainly performed through agitation, that includes shaking or stirring studies [134, 177]. These tests are typically conducted at room temperature on tens of DPs that are exposed to different intensities of shaking or stirring (100-300 rpm). Usually, during the agitation tests, the amount of aggregates are monitored at specific time points: 0, 3, 5 days [135].

In the agitation-induced protein aggregation, stability of formulated proteins is tested against different stress factors including shearing, exposure to air-liquid, liquid-container interfaces, cavitation and local warming effect [178]. Particularly, the presence of air-liquid interface incredibly impacts on the outcome of mechanical stress studies. In fact, proteins adsorption to this interface influences the rearrangement of the H-bonds, inducing protein unfolding [129]. Moreover, the agitation intensifies this phenomenon by renewing the air-liquid interface and exposing new liquid solution to it [179].

Although agitation tests might seem a comprehensive and versatile approach to investigate the robustness of formulations against a number of mechanical stress sources, it can be noticed that they are poorly representative of other typical solid-liquid interfaces (*e.g.,* stainless steel or polymers) and more intense hydrodynamic forces (*e.g.,* high shear rate) that are usually encountered by biologics during manufacturing (filtration, mixing, pumping and filling) [77, 79, 106, 109]. Shear rate intensities in these processes span a wide range, going from ≈50 s^{-1} during mixing to tens of thousands s^{-1} during filling (*e.g.,* 20000 s^{-1}) [180]. Furthermore, these values can reach far higher peaks during high-pressure homogenization (>10^6 s^{-1}) or patient injection (≈10^5 s^{-1}) [180-182]. According to a computational model of typical conditions of different agitation methods (rotation at 35 rpm, orbital shaking at 300 rpm, vortex mixing at 1000 rpm and magnetic stirring at 1000 rpm conducted in a 3 ml glass container filled with 1 ml of water-like fluid at 25°C), maximum shear rate intensities taking place at the walls range from ≈1000 s^{-1} for the rotation method to ≈3000 s^{-1} for a vortex mixing process [179]. Based on these indications, it can be concluded that agitation is an efficient approach to test the stability of formulations against air-liquid interfaces, while it might be poorly relevant for the examination of stability under high intensity hydrodynamic forces (HIHFs) typical of manufacturing process. In addition, it can be pointed out that all agitation methods make use of rather large volumes, thus resulting to be expensive and low-throughput approaches. While new miniaturized strategies based on well-plates are being developed to address expensiveness and enhance test throughput [183], the performance of formulations against HIHFs (*e.g.*, shearing >10^4 s^{-1}) and solid-liquid interfaces remains mostly unexplored during early DP development stages.

Many works in the literature investigate the impact of HIHFs (shearing and extensional strain) in a wide intensity range, on diverse proteins and different solution conditions, leading to a non-unanimous consensus on their role. In fact, some authors [110, 113, 181, 184] do not identify high shear rates as determining cause of protein unfolding or aggregation even at high shear rate intensity (≈10^8 s^{-1}) [113], while others report protein unfolding [185] and particle formation due to exposure to shearing [180, 186, 187]. Also, some authors have

explored the impact of the extensional flow on protein stability, identifying unfolding or aggregation for strain rates $>10^4$ s^{-1} on a number of protein molecules and solution conditions [187, 188]. Conversely, other works have found similar strain rates not to have same detrimental effects on mAb solutions [189].
The literature also highlights the importance of contact materials at the solid-liquid interface and points out that the hydrodynamic forces can synergistically worsen the tendency of proteins to unfold or aggregate in presence of such interfaces. This is probably due to the ability of hydrodynamic forces to boost the protein adsorption and desorption process, thus accelerating the release of conformationally altered biomolecules in the bulk solution [180, 189, 190].
As matter of fact, the tendency of proteins to unfold or aggregate is affected by several variables, comprising type of hydrodynamic forces, their intensity, exposure time and nature of contact materials. Moreover, it must said that the propensity to destabilization is molecule- and formulation-dependent. For these reasons, generalization of the impact of hydrodynamic forces alone or in combination with diverse solid-liquid interfaces is difficult to be drawn.
Nevertheless, probing and characterizing the formulation stability against overmentioned sources remains a pivotal step that pharmaceutical industries need to take. The ability to predict formulation behavior in presence of challenging hydrodynamic forces in early stages of the development of biologics would be precious to bring ameliorated and more robust products to the manufacturing process. Along with the ability to screen formulation behavior with respect to HIHFs, there is an increasing need for novel probing technologies able to reliably recreate destabilizing conditions typical of manufacturing. In this context, the microfluidics represents a superb tool [156] as, along with the limitation of the sample consumption, microchannel walls can be readily used to recreate hydrodynamic contexts and solid-liquid interfaces typical of formulation manufacturing process.
In this chapter the design and the realization of an automated mechanical stress microfluidic platform to screen formulation stability under different shearing flow conditions is presented. Different polymer-based microfluidic chips were designed and fabricated to cover typical shear rate ranges of filtration, pumping and filling. Highly concentrated nAb-based formulations were processed through the mechanical stress platform and their behavior characterized through gold standard (SE-HPLC) and orthogonal techniques such as dynamic light scattering (DLS) and Fourier Transform Infrared Spectroscopy (FTIR). Additionally, the same formulations were subjected to conventional agitation protocols and their physical stability characterized through DLS and FTIR techniques.
Also, at the end of this chapter (section 4.5), the microfluidic mechanical stimulation is shown to be translatable to cell-based biologics. A proof of the concept is provided that the controlled microfluidic solicitation can influence the biogenesis of extracellular vesicles.

4.2 Materials and Methods

4.2.1 Materials

Trehalose dihydrate (product number T-104-4) was supplied by Ferro/Pfanstiehl in solid form; Poloxamer-188 (product number X0003307) was provided by Merck Serono S.p.A., L-Arginine (product number 1.01544) and Tris (product number 1.08386) were supplied by Sigma-Aldrich. The nAb (Mw 45 kDa) was provided by Merck Serono S.p.A.. The latter was given in liquid form at a concentration of 150 mg/ml in 10 mM Tris buffer, pH 7,5. NaOH (product number 1.58793) and HCl (product number 1.00317.1000) were provided by Sigma-Aldrich and used to adjust the pH of solutions. MilliQ water was used to prepare all the solutions. Polymethyl methacrylate (PMMA) sheets (product number ME30-SH-000110) were bought from GoodFellow Cambridge Ltd.

4.2.2 Preparation of buffer and formulations

A 10 mM of Buffer solution was obtained by solubilizing 1,21 g of Tris in 1 liter of milliQ water. HCl was used to bring the pH from ≈10 to 7,5.

Two distinct batches of formulations were prepared. Each of them consisted of the same three formulations. The latter were prepared in 10 mM tris buffer so as to have a final volume of 10 ml of each formulation for the first batch, and 20 ml for the second one. In all the prepared solutions, nAb concentration was 120 mg/ml, while excipients were solubilized at different concentrations. In particular, Trehalose concentration ranges from 53 to 106 mg/mL, L-Arginine spans from 0 to 14,7 mg/mL while Poloxamer-188 concentration is kept constant at 0,1 mg/mL. NaOH was used to adjust the final pH to 7,5. The composition of each formulation is detailed in *table 6*.

Formulation	Trehalose (mg/mL)	L-Arginine (mg/mL)	Poloxamer-188 (mg/mL)	nAb (mg/mL)
A	106	0	0,1	120
B	79,4	7,4	0,1	120
C	53	14,7	0,1	120

Table 6 – Composition of formulations in both batches

Solutions were gently stirred at 250 rpm and room temperature until the complete and homogeneous mixing was obtained. The final solutions were filtered through 0,22 µm PES syringe filters.

4.2.3 Design of the mechanical stress microfluidic platform

The mechanical stress platform is composed by two main sections: pumping and mechanical stress modules. The former consists of two syringe pumps (Model 11 Elite, Harvard Apparatus USA) and two two-position/three-port automated valves (part number AV201-T116, LabSmith, USA). The latter was designed to account for a main line (where the mechanical stimulation takes place – *figure 9a*, from element 7 to 9) and a recirculation one (intended to control the number of stimulation cycles (*i.e.,* stimulation time) – *figure 9a*, elements 11 and 12). In particular, the mechanical stress module is composed by a set of two-position/three-port automated valves (part number AV201-T116, LabSmith, USA), a shearing station and a peristaltic micropump (part number 3200243, Dolomite Microfluidics, UK). Particularly, the shearing station includes a custom-made microfluidic chip fabricated by using micromilling technology (Minitech CNC mini-mill/GX). All the microfluidic parts are interconnected through FEP tubes (ID 0,8 mm, OD 1,6 mm, Dolomite Microfluidics).

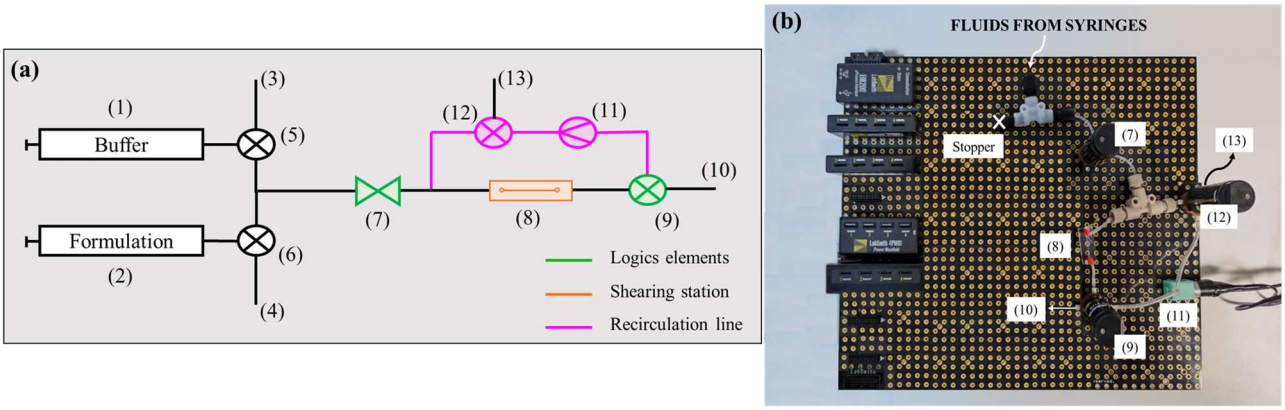

(1) Buffer pump; (2) Formulation pump; (3 - 4 - 10) Waste; (5 – 6 – 9 – 12) Automated switchers; (7) On/off automated valve; (8) Shearing station; (11) Micro-peristaltic pump; (13) Sample collection

Figure 9 – Microfluidic mechanical stress platform; (a) scheme of the microfluidic platform that includes pumping module (from element 1 to 6) and mechanical stress module (from element 7 to 13); (b) Elements of the mechanical stress module mounted on to Labsmith breadboard

4.2.4 Setup and programming of the microfluidic platform for mechanical stress

The setup of the mechanical stress microfluidic platform is outlined in *figure 9*. The two syringe pumps *(figure 9a, elements 1 and 2)* are connected in parallel by means of two automated valves *(figure 9a, elements 5 and 6)* that are used as switchers so as to enable selective injection of both buffer and formulation into the mechanical stress module. In the latter, the main line consists of a serial connection between two automated valves *(figure 9a, elements 7 and 9)* and the shearing station *(figure 9a, element 8)*. The recirculation line starts from *element 9* of *figure 9a* and ends up to the inlet of the shearing station (*figure 9a, element 8*). It includes a serial connection between the peristaltic micropump *(figure 9a, element 11)* and an automated valve *(figure 9a, element 12)*. In addition, both pumping and mechanical stress modules have some outlet lines *(figure 9a, elements 3, 4, 10, 13)*, realized through the FEP tubes. The mechanical stress module from element 8 to 12 exhibits a dead volume of ≈300 µl. All the presented parts were mounted on a single breadboard as reported in *figure 9b.* LabSmith proprietary software was used to program the microfluidic platform.

4.2.5 Microfluidic Chip design and Device Fabrication by micromilling technique

AutoCAD 2023 (didactic version T.72.0.0 AutoCAD 2023.0.1) was utilized to design different microfluidic chip geometries consisting in one-inlet-one-outlet straight channels with different cross-sectional dimensions (WxH - 250x300 µm, 250x240 µm, 250x150 µm) and a volume less than 2 µL. The three microfluidic devices correspond to diverse max shear rate thresholds (5500 s^{-1}, 8000 s^{-1}, 20000 s^{-1}) while being injected at 800 µl/min flow rate. DESKAM 2000 (version 5.1.5.11) was employed to realize computer aided manufacturing (CAM) files for the fabrication.

The microfluidic chip is made out of polymethyl methacrylate (PMMA) and obtained through a micromilling process. The polymer was processed through a Minitech CNC mini-mill/GX (Minitech Machinery Corporation, USA) to build up the customized microfluidic chip. The machining parameters were optimized according to the feasibility study conducted for the thermal stress chip realization reported in the previous chapter. The details of the study are reported in Appendix A, paragraph A2.

4.2.6 Ability of the microfluidic platform to process highly concentrated and viscous fluids

As said for the thermal stress platform (chapter 3), the ability of the platform to manage highly concentrated and viscous fluids was assessed by processing different Bovine Serum Albumin (BSA) and sucrose solutions at various concentrations. A *low* viscosity fluid (2 mPa*s) was achieved by solubilizing 50 mg/ml of BSA and 50 mg/ml of sucrose; a *moderate* viscosity level (7 mPa*s) was obtained by dissolving 175 mg/ml of BSA and 175 mg/ml of sucrose; finally, a *high* viscosity threshold (18 mPa*s) was reached by combining BSA and sucrose at 250 mg/ml each.

4.2.7 Fluid dynamic analysis

COMSOL Multiphysics® v. 5.6 was used to study the transport phenomena of designed chips in terms of fluid velocity profile, pressure drop and shear rate intensity.

4.2.8 Mechanical stimulation through conventional protocols (agitation)

The second batch of nAb-based formulations was stimulated according to conventional mechanical stress protocols. 2 ml glass vials were filled with 1 ml of each formulation and agitated (orbital shaker IKA® HS 260 basic) at room temperature and 300 rpm for 3 days. Checkpoint measurements were taken at 1,5 and 3 days.

4.2.9 Mechanical stimulation through mechanical stress microfluidic platform

Two different types of microfluidic mechanical stimulations were conducted for the three candidate formulations. A first batch of formulations was made pass one single time through each of the chips at room temperature and at different flow rates (50, 150, 500, 800 µl/min). Depending on chip geometry and flow rate, the three formulations were exposed for different time periods (from 14 to 450 ms) to various shear rate thresholds, ranging from 340 to 20000 s^{-1}. The experimented points and results are detailed in *table B1* (Appendix B, section B2).

A second batch of the three formulations was processed at 800 µl/min, room temperature and different shear rate thresholds (5500 s^{-1}, 8000 s^{-1}, 20000 s^{-1}) for different number of cycles (1, 6, 14, 28). The latter correspond to different time periods of recirculation (no recirculation, 2, 5 and 10 min) and different effective stress exposure time. In addition, the formulations were processed without the shearing station for 2, 5 and 10 min as control samples. The tested conditions are reported in *table 7*.

The stimulation through the microfluidic platform was carried out following platform programming. First, the platform was programmed so as to inject the buffer into the mechanical stress module. After a period for the complete filling of the latter, the formulation was injected in the microfluidic plant to start the stimulation. Particularly, the automated valves were programmed to switch to the syringe pump containing the formulation for the time needed to fill the mechanical stress module (including main and recirculation lines). Then, automated valves were programmed to allow fluid recirculation by means of the peristaltic micropump for the whole mechanical stimulation time. Finally, the stressed samples were collected in 0,5 ml safe lock tubes (Eppendorf S.r.l., Italy). Further details on the specific mechanical stress module configuration are reported in Appendix B, section B1.

Candidate formulation	Shear rate intensity (s^{-1})	Number of cycles	Recirculation time (min)	Effective stress exposure time (ms)
A,B,C	No shearing station	/	2	0
		/	5	0
		/	10	0
	5500	1	No recirculation	40
		6	2	240
		14	5	560
		28	10	1120
	8000	1	No recirculation	28
		6	2	168
		14	5	392
		28	10	784
	20000	1	No recirculation	13
		6	2	78
		14	5	182
		28	10	364

Table 7 – Mechanical stress conditions tested with the microfluidic platform

4.2.10 Assessment of aggregation through SE-HPLC

After being recollected, 50 µL of samples stimulated through the microfluidic mechanical stress were used to prepare samples to be analyzed by SE-HPLC in order to assess the amount of aggregates.

4.2.11 Size distribution through DLS

Sample stimulated through conventional protocols (orbital shaking) and microfluidic mechanical stress were analyzed through DLS (Zetasizer Nano, Malvern) soon after being processed in order to determine the size distribution. Particularly, 40 µL of each sample were diluted with 1960 µL of buffer, resulting in a 50-fold dilution. The dilution factor resulted from a feasibility study conducted on a model protein. Details are reported in Appendix B, section B3. 1 ml of diluted solution was analyzed by using a disposable polypropylene cuvette.

The measuring parameters were adjusted based on the solution and material characteristics. For each sample, three measurements of 15 runs of 10 seconds each were performed and averaged. “Protein analysis” model was adopted to fit the instrument raw data.

4.2.12 Secondary structure modification through FTIR

Sample stimulated through conventional protocols (orbital shaking) and microfluidic mechanical stress were analyzed with no dilution through FTIR (Mettler Toledo ReactIR equipped with a 50 µl microflow cell), soon after being mechanically stimulated through the microfluidic platform in order to acquire the absorbance spectrum. 128 scans were taken with a resolution of 4 cm^{-1} and then averaged to return the absorbance spectrum of each sample. Secondary structure modifications were detected by taking the second derivative of each spectrum and focusing on the amide I band [1680 – 1600] cm^{-1}.
In order to check whether secondary structure modifications were temporary or permanent, additional FTIR measurements were taken on same treated and untreated samples after 1 week from the stimulation. During this period, formulations were stored at 5 ± 3 °C.

4.2.13 Similarity score parameter for DLS size distributions and FTIR spectra

In order to identify a formulation ranking, the big data amount returned by the experimental campaign (size distributions and IR spectra) needs a proper rationalization strategy enabling efficient data comparison. In particular, the variations of size distributions and IR spectra of stimulated formulations with respect unstimulated ones were evaluated by computing the *coefficient of determination* (R^2) as *similarity score parameter*.

4.3 Results and Discussion

4.3.1 Design, fluid dynamic characterization and fabrication of the microfluidic chip for mechanical stress

Three microfluidic chips (*figure 10 a,b*) were designed in order to cover a wide range of shear rate intensities typical of manufacturing processes. The 0-5500 s^{-1} interval, referred to as *weak*, was achieved by designing a microfluidic channel with rectangular cross section of 250x300 µm (WxH). Similarly, the 0-8000 s^{-1} shear rate range, referred to as *medium*, was recreated by designing a 250x240 µm (WxH) rectangular cross section channel. Lastly, the highest shear rate intensity of 0-20000 s^{-1}, referred to as *strong*, was covered by designing a 250x150 µm (WxH) microfluidic channel. The microfluidic channels were design in order to offer the indicated shear rate interval while operating at a flow rate of 800 µl/min. The overall volume of each microfluidic device for mechanical shear stress is less than 2 µl. Numerical simulations were set and run to optimize microfluidic device geometries in relation to pressure drops, velocity and shear rate profiles. Specifically, the shear rate profiles computed in correspondence of the channel width (red line, *figure 10b*) are reported for all the microfluidic devices in *figure 10c*. Microfluidic devices were made from PMMA and fabricated through micromilling technique following geometry and fluid dynamic optimization. PMMA was selected due to its inexpensiveness and easy manufacturability, that make this polymer an excellent option for chip prototyping before stepping forward to more advanced materials (glass, quartz, etc.).
As reported in the previous chapter, both chip material and roughness can strongly impact the protein stability [170], promoting its adsorption to surface. For this reason, machining parameters were optimized through a feasibility study (Appendix A, paragraph A2) in order to minimize final product roughness. In particular, the best combination of parameters matching lower roughness, reliability to the CAD project and reasonable machining duration resulted to be:
Tip size: 100 µm;
X-Y step size: 12,5 µm (halved default value returned by CAM software);
Z step size: 50 µm (1/5 of the whole channel height);

Feed rate: 10%;
Spindle rate: 10000 rpm.

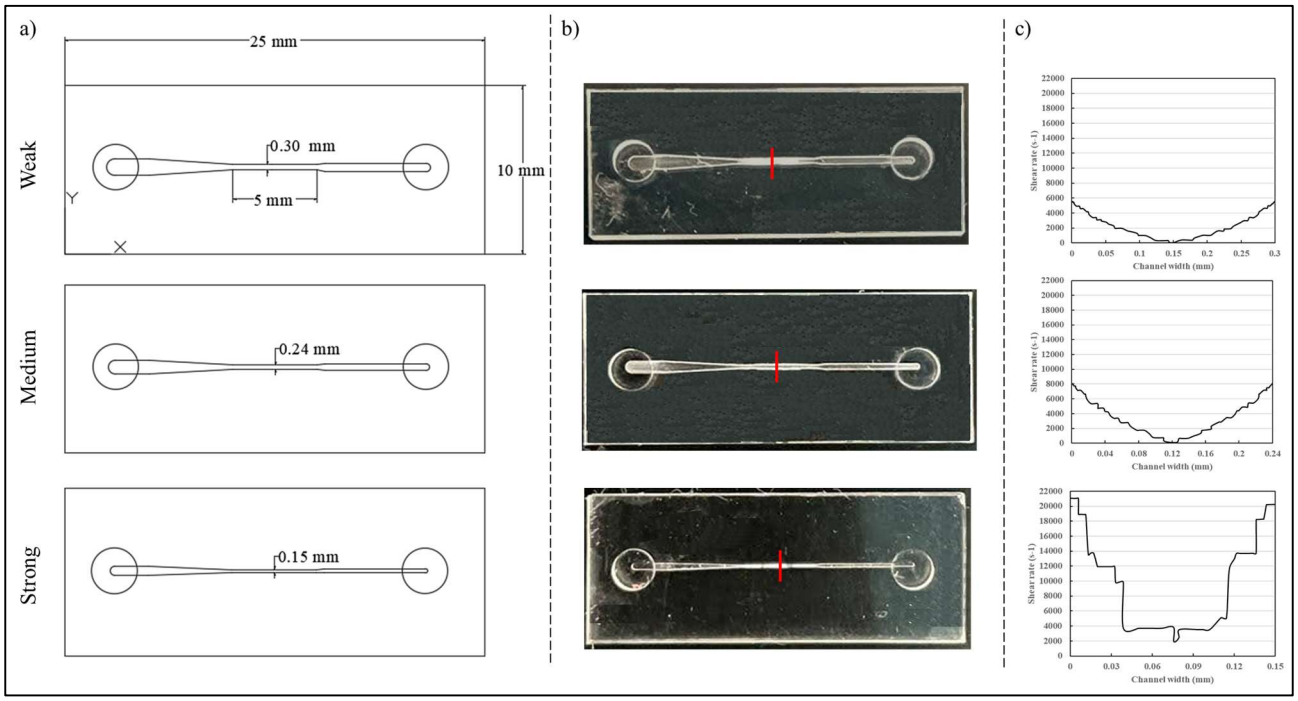

Figure 10 – Three different geometries for diverse shear rate thresholds. (a) CAD of the weak, medium and strong shear rate microfluidic chip; (b) Microfluidic chip constructed using PMMA; (c) shear rate profiles in each of the microfluidic device: 5500 s^{-1} for weak, 8000 s^{-1} for medium and 20000 s^{-1} for strong geometry.

4.3.2 Assessment of aggregation through SE-HPLC

The amount of aggregates in untreated and treated sample was determined by SE-HPLC. The first batch of formulations was stimulated with a single passage through each of the designed chip at different flow rates as described in material and methods (section 4.2.8) and detailed in Appendix B, section B2. Although the formulation C is the most inherently stable as it presents the lowest amount of aggregates than formulation A and B, none of the experimented shear rate thresholds determined an increase of protein aggregates.

The second batch of formulations was processed at 800 µl/min, room temperature and different shear rate thresholds (5500 s^{-1}, 8000 s^{-1}, 20000 s^{-1}) for different number of cycles (1, 6, 14, 28), that correspond to different recirculation time periods (no recirculation, 2, 5 and 10 min). The experimented points are reported in *table 7,* section 4.2.8. In all the formulations exposed to different shear rate thresholds for various stimulation times no aggregated species are detected by SE-HPLC analysis (*Figure 11*). Similarly to the first batch, formulation C is inherently more stable than the others, presenting the least amount of aggregates. The standard deviations for each point reported in *figure 11* fall in the 5% of the reported value.

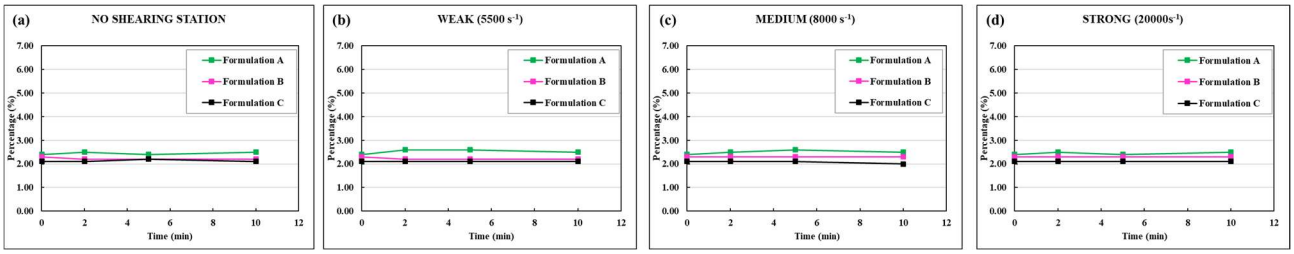

Figure 11 –aggregation percentage of untreated and mechanically treated samples. No aggregate increase is detected by SE-HPLC for none of the formulations exposed to different shear rate thresholds and exposure times. (a) no shearing station; (b) Weak shear rate range; (c) Medium shear rate range; (d) Strong shear rate range.

4.3.3 Analysis of the shear effects on colloidal and structural configuration of nAb

DLS analysis were run soon after the stimulation to obtain information about colloidal configuration (monomeric and oligomeric species) of nAb-based formulations in relation to the amount of stress duration, intensity and excipient composition. Because of the large amount of data obtained, catching relevant behaviors based on the visualization of size distribution plots may result inefficient. For this reason, the size distributions of stimulated and unstimulated formulations were compared by computing a *similarity score parameter* (coefficient of determination (R^2) – Materials and methods, section 4.2.13). This parameter measures the linearity between the size distributions of treated and untreated samples, providing an indication of their similarity. In fact, this parameter enables the extrapolation of information about configuration of monomeric and oligomeric species changes in stimulated formulations due to the mechanical shearing with respect to the unstimulated condition. The similarity score assigned to formulation A, B and C in weak, medium and strong shear rate ranges are reported in f*igure 12 a,b,c.* From the latter it can be said that longer stimulations do not necessarily implicate an increase or a decrease of similarity score. In other words, in none of the formulations it is possible to appreciate a clear correlation between the stimulation time and the similarity score magnitude. Rather, the latter seems to change without a defined trend while increasing the stimulation time. This observation might suggest that in all the tested formulations some random dynamic changes of monomeric and oligomeric configuration occur during shear exposure. This may indicate that, regardless of intensity and stimulation time, monomers and oligomers associate or dissociate while being sheared to give rise to larger or smaller transient species. In point of fact, higher formulation propensity to continuously modify its colloidal configuration over time (*i.e., R^2* ups and downs) can be itself considered an indication of greater formulation instability. Also, as it can be observed from *figure 12 a,b,c*, the microfluidic shear stress platform can highlight different colloidal behaviors of the formulations (higher or lower tendency to modify their colloidal configuration while being sheared) in relation to the stress intensity. As it can be seen, formulation A (*figure 12 a)* expresses higher R^2 variability at any stress level with respect to formulations B (*figure 12 b*) and C (*figure 12 c*). In fact, the latter are the ones expressing the lowest R^2 fluctuations and the highest R^2 magnitudes. This observation might give indication on the role of the arginine and trehalose combination on the colloidal stabilization of the nanobody. As it can be deducted, a mix of the two excipients better preserves the formulation colloidal configuration than the sugar alone.

Moreover, FTIR analysis were conducted, without sample dilution, immediately following stimulations to assess any change in the secondary structure of the nAb in each of the formulations at different shear rate intensities, time exposure to the stress and excipient combination. As for DLS analyses, a similarity score was computed to determine differences between spectra of stimulated and unstimulated formulations. Specifically, the evaluation was done in the range 1680-1600 cm^{-1} (amide I band), where intra- and intermolecular β-sheets can be identified. *Figure 12 d,e,f* reports the similarity score for each tested formulation at different shear rate intensities and stimulation times. As it can be deducted, secondary structure of all the formulations are sensitive to the stimulus intensity and practically insensitive to the solicitation time. In fact, longer stimulation do not determine any increase or decrease of similarity score, that keeps constant over time for every formulation. On the contrary, higher shear rate intensities induce greater modifications of the secondary structure with greater or unappreciable impact depending on the composition of the formulation. As individualized for the colloidal

configuration (*figure 12 a,b,c*), the combination of arginine and trehalose better mitigates the effects of HIHFs than the sugar alone.

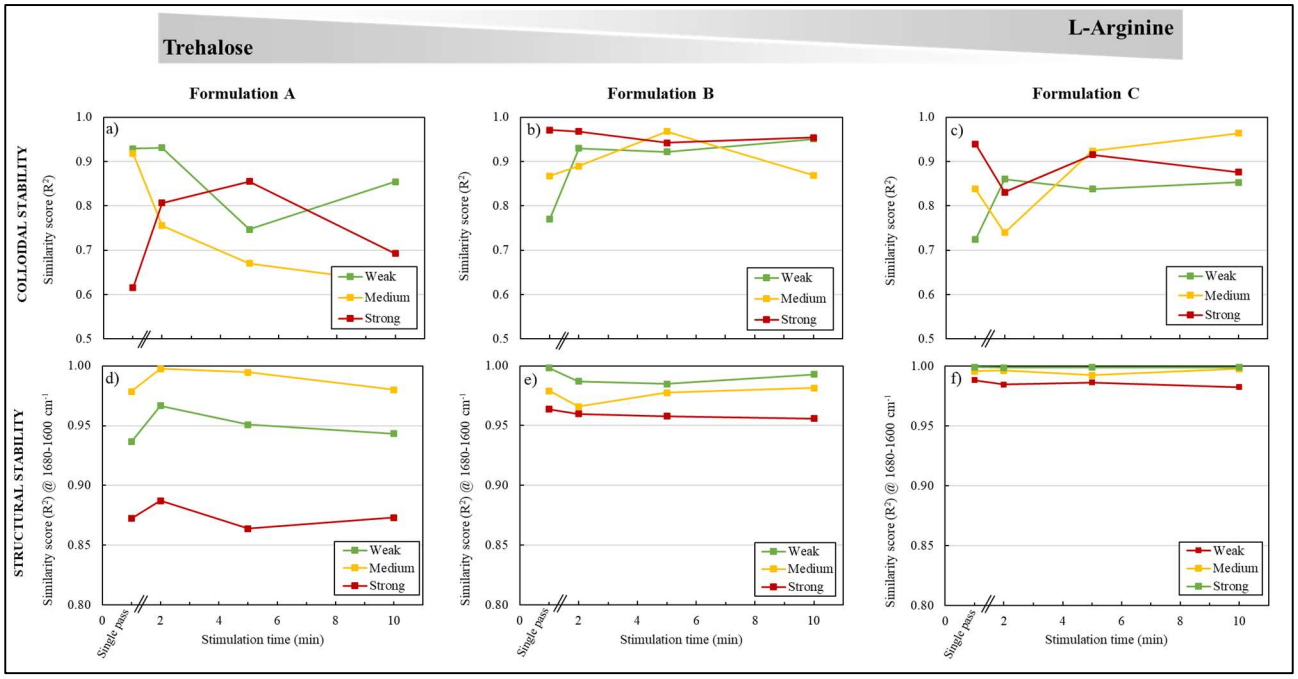

Figure 12 – Similarity score obtained from DLS (a,b,c) and FTIR (d,f,e) analyses. (a) Impact of the three shear rate intensities on the colloidal configuration of formulation A; (b) Impact of the three shear rate intervals on the colloidal configuration of formulation B; (c) Impact of the three shear rate ranges on the colloidal configuration of formulation C; (d) impact of shear rate intensity on the modification of secondary structure of formulation A; (e) impact of shear rate intensity on the modification of secondary structure of formulation B; (f) impact of shear rate intensity on the modification of secondary structure of formulation C.

Additionally, *figure 13* reports the effect of the same stress threshold on the three formulations, so as to define a ranking. R^2 values obtained from DLS data elaboration (*figure 13 a,b,c,d*) suggest that, from a colloidal point of view, the formulation B and formulation C are the least sensitive to any shear threshold.
Formulation A deserves a particular attention. Interestingly, *figure 13* points out that this formulation is extremely susceptible to dynamic modification of colloidal configuration even in absence of the shearing station. Surprisingly, the formulation A, when processed throughout the microfluidic platform with no shearing device, returns the worst R^2 values and the addition of the stressing microfluidic chip seems to have a stabilizing effect on the formulation. In fact, higher R^2 magnitude result from stimulations at weak, medium and strong shear rate intervals.
Similar considerations can be drawn by looking at the results coming from FTIR analysis (*figure 13 e,f,g,h*) at the various shear rate thresholds: secondary structure is better preserved in formulation B and C. Particularly, no significant differences can be noticed among formulations at lower shear rate intervals (weak and medium – *figure 13 f,g*), while instability behaviors are exalted when subjecting them to higher shear rate exposure (*figure 13 h*). Moreover, formulation A expresses the highest deviation from the unstimulated condition even when recirculated throughout the microfluidic platform with no shearing station. This phenomenon is in accordance with the observation made for the colloidal configuration of the same formulation. It could be speculated that the interaction between the protein and the excipients is ameliorated when higher mechanical energy is transmitted to the formulation. This event can be considered largely representative of the role that the microfluidic stimulation is supposed to have: although a mix of trehalose and arginine maximizes nAb colloidal and structural stability, the role of the sugar alone emerges when subjecting formulation A to higher mechanical stresses. In other words, the microfluidic stimulation makes it appreciable that the trehalose alone might be sufficient to stabilize the protein until certain shear thresholds (*i.e.,* weak), while for higher stress intensities (medium and strong) a cocktail of arginine and the overmentioned sugar returns better performances. This means that the platform is able to clarify the correlations among stress intensities,

colloidal/structural modifications and excipient types. Of course, to this information is also contributing the nature of stress source being applied (*i.e.,* HIHFs). In fact, as it will be demonstrated in next paragraph, conventional approaches might not be as exhaustive as the microfluidics. Furthermore, considering the kind of stressors recreated by the microfluidic mechanical stress platform, information coming from formulation screening can be exploited to preliminarily identify shear thresholds that could result in noteworthy colloidal and structural modifications that can potentially lead to instability undesired scenarios in later manufacturing steps.

Finally, to determine whether the effects of the microfluidic stimulation were transient or permanent, additional FTIR measurements were taken on the same treated and untreated samples one week after the stimulation. Results (reported in Appendix B *figure B4*) support the thesis of the transience of the secondary structure modifications detected soon after the stimulation, as the similarity score, one week following the stimulation, becomes much closer to 1.

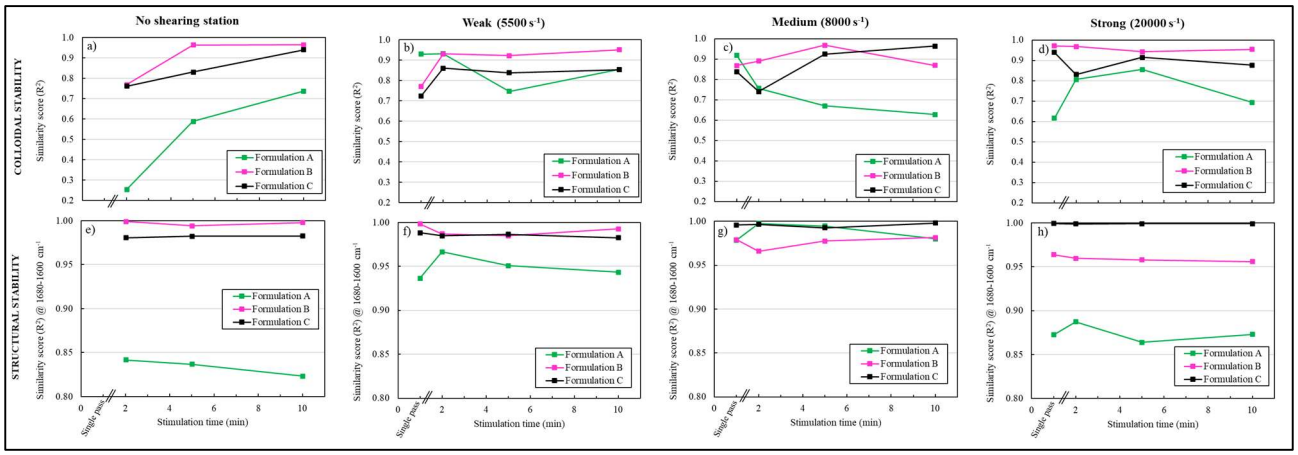

Figure 13 – Comparison of formulations based on the similarity score obtained by DLS (a,b,c,d) and FTIR (e,f,g,h) analyses. (a) Impact of the microfluidic platform on the colloidal configuration of the three formulations when processed without the shearing stimulation device; (b) Impact of the weak shear rate intensity on the colloidal configuration of formulations; (c) Impact of the medium shear rate interval on the colloidal configuration of formulations; (d) Impact of the strong shear rate range on the colloidal configuration of formulations; (e) Impact of the microfluidic platform on the secondary structure of the three formulations when processed without the shearing stimulation device; (f) impact of weak shear rate intensity on the modification of secondary structure of formulations; (g) impact of medium shear rate intensity on the modification of secondary structure of formulations; (h) impact of high shear rate intensity on the modification of secondary structure of formulations.

4.3.4 Inability of conventional mechanical stress protocols to mimic the effects of HIHFs

The three formulations were processed according to mechanical stress forced degradation protocols. In particular, 1 ml of each formulation were agitated (300 RPM, room temperature) for 3 days with an intermediate checkpoint at 1,5 days. Stimulated formulations were analyzed through DLS and FTIR protocols immediately after the stimulation. *Figure 14* reports the trends returned by computing the similarity score (R^2) from the overmentioned analysis. Differently to the microfluidic mechanical stress, the agitation do not highlight differences among the three formulations, that express the same stability performance. This result indicates that a conventional approach, typically used to study formulation stability with respect to manufacturing stress sources, might return irrelevant or non-representative picture of the actual phenomena triggered by HIHFs.

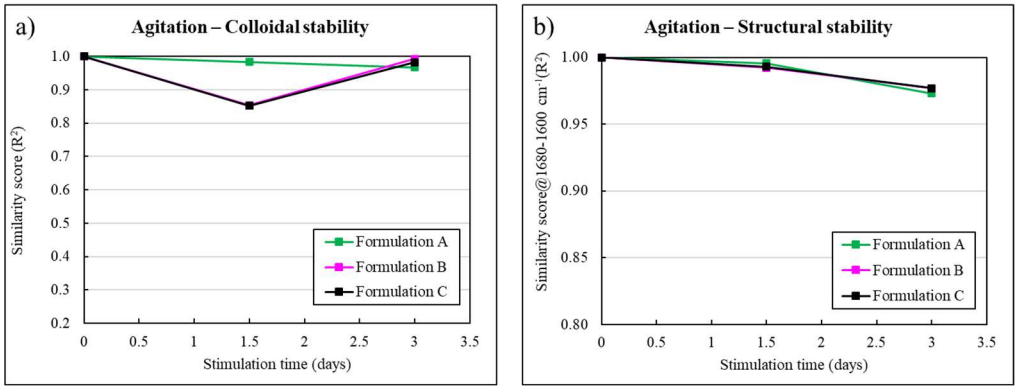

Figure 14 – colloidal and structural modifications induced by conventional mechanical stress agitation. (a) colloidal modifications detected through DLS analysis soon after the agitation; (b) secondary structure modification detected through FTIR soon after the agitation

4.4 Conclusions

The possibility to test formulations in a HIHF context is of outmost relevance as the conventional agitation is not able to mimic challenging hydrodynamic environment typical of a manufacturing process. In this chapter an automated mechanical stress microfluidic platform was designed, set up and proposed as a tool to screen the stability of biologics with respect to HIHFs. Particularly, the platform was designed according to a modular logic presenting a shearing station able to exert different levels of shear rate (weak, medium and strong) and a recirculation line for the control of the stimulation time. Three nAb-based DPs were tested through the microfluidic mechanical stress and the effect of the shear was characterized through conventional approaches (SE-HPLC) and orthogonal techniques (DLS and FTIR).

While SE-HPLC did not return any aggregation trend after shear exposure, orthogonal technique were capable to capture transient colloidal and structural modifications. Interestingly, the same orthogonal analytical technique approach does not express appreciable trends when combined to a conventional agitation protocol. This result emphasizes two main unmet needs: on a side there is the necessity to properly investigate the effect of the HIHFs during a DP development, on the other hand the limitations of an off-line analytical strategy are pointed out. In fact, the coupling of the microfluidic platform with a *quasi-real-time* analysis is a winning and indissoluble combination. While the microfluidic mechanical shear stress induces certain phenomena, only an analytical approach based on a short temporal distance from the stimulation and a minuscule or absent sample dilution could be suitable to grasp them. This suggests that the potentials of such a microfluidic tool can be further expanded with the employment of an *inline real-time analytical module*.

By properly intercepting destabilizations induced by the shearing, a broader spectrum of information can be generated. In fact, besides the possibility to establish a formulation ranking based on colloidal and structural modifications, one could extrapolate information of manufacturing operational parameters and stress thresholds that can positively or negatively impact the formulation condition. Additionally, the same information can be reversely used for the selection of the most suitable formulation in case manufacturing parameters are constrained to specific levels.

Furthermore, the effects exerted by shear were proven to be transient for this specific molecule and combination of excipients. However, it cannot be excluded that, for formulations other than the ones tested in this work (*i.e.*, different molecules and excipient combinations), such stressors might result in non-transient nature effects impacting on the aggregation status of the biomolecule.

Based on the results presented in this chapter, the proposed tool can pave the way for a significant step forward in the study of biologic stability, as such a technology may fill the intercommunication gap between formulation development and manufacturing process. In other words, the microfluidic platform is really opening the possibility to test candidate formulations against more representative process stressors in an early development phase. Plus, its modularity makes the exploration of hydrodynamic forces with alternative solid interfaces (glass, metals, silicone etc.) easily implementable. The information collected from the microfluidic

platform, integrated to others coming from more conventional approaches can really improve the clarity of the intricate landscape of biological drug stability.

4.5 Alternative application of the microfluidic mechanical stress to other types of biologics: manipulation of highly concentrated pool of cells to boost the release of extracellular vesicles (EVs)

Ongoing project in collaboration with Dr. Eng. Simona Silvestri (https://www.researchgate.net/profile/Simona-Silvestri-3) and Dr. Eng. Samuele Fiorenza (https://www.researchgate.net/profile/Samuele-Fiorenza)

4.5.1 Background

Intercellular communication is crucial for multicellular organisms and is facilitated by extracellular vesicles (EVs), which transport various biological materials, including proteins, lipids, DNA, and RNA between cells [191]. The specific types of biomolecules carried by these vesicles can vary from one cell to another [192]. The release of EVs takes place in various type of cells by fusion of Multivesicular bodies with the plasma membrane, but they can be also isolated by body fluids, including blood, semen, urine, cerebrospinal fluid, amniotic fluid or breast milk [193]. EV is a general term that involves a large spectrum of different vesicles that may vary in size, composition and biological role [192]. Among these, Small Extracellular Vesicles (SEVs), such as exosomes, have a size falling in the 30-150 nm range and, as natural carriers, they have proven to be relevant for diagnostic and therapeutic scopes in many pathological contexts, such as cancer, neurodegenerative diseases, cardiopulmonary issues etc. [194]. In spite of their promising role, the use of EVs encounters a series of biological and technical challenges that are hereafter summarized.

First, the isolation of EVs (and more specifically of SEVs) is highly challenging. The adopted method is functional to the success of the isolation and might offer different performances in terms of EVs homogeneity and amount [195]. Specially for research purposes, differential ultracentrifugation (dUC) represents a gold standard technique for pelleting biological entities as small as SEVs both from cell culture media and body fluids. Although it is widely employed, ultracentrifugation process is extremely lengthy and labor-requiring [196, 197]. In addition, due to EVs physico-chemical complexity, a multiple analytical approach is needed to fully characterize SEVs from size, morphological and biochemical point of view. Some techniques, such as Nanoparticle Tracking Analysis or Dynamic Light Scattering, can be adopted to have insights in the size range of EVs [198], while Transmission or Scanning Electron Microscopy can be selected to gather information about their morphology [198]. Importantly, characterizing the biochemical aspect, such as the presence of specific proteins, RNAs or lipids, results as challenging as crucial to define the biological function of the EVs. An exhaustive biochemical analysis necessitates the implementation of a range of methodologies or specialized assays, which may inherently pose technical challenges. Plus, the effectiveness of these methods relies heavily on the quality of the sample being examined [198].

Besides the mentioned challenges, a major concern is linked to the ability to produce a sufficient and clinically relevant amount of EVs. This task results even more complicated to achieve due to the concomitant need for sample high quality and purity, a pivotal requirement for clinical applications [199]. Some factors have been demonstrated to influence the biogenesis yield of EVs (and in particular SEVs). Among these factors the confluency condition of the cell culture is highly impacting on the secretion of SEVs [192]. Additionally, some chemical and biological stimulants, such as Ca^{2+} ionophores or hypoxia may impact on the production of EVs [192]. Along with them, some studies suggest that also physical stresses (thermal, light or mechanical) may intensify the secretion of SEVs on different cell types [200-204]. While this holds true, the employment of large scale or expensive setups to apply physical stresses to cells, remains not convenient. Plus, the ability to create stimulating environment in a high controllable and reproducible manner, might be beneficial to increase the biogenesis yield while ameliorating quality and homogeneity of secreted EVs. In this context, the microfluidics results to be an appropriate option, offering exceptional flow predictability and controllability [205]. Plus, its outperforming characteristics have made the microfluidics a rapid emerging technology for cell manipulation in a broad interval of applications [206]. In particular, its employment has been largely

investigated to apply mechanical (shear or elongational) stresses for different purposes (*e.g.*, cell deformability, breakage, remodeling etc.) on numerous classes of cells [207-210]. Anyway, the exploitation of the microfluidics for the enhancement of the EVs biogenesis through the application of mechanical stress has been investigated limitedly. Hao and colleagues [211] recently reported a successful microfluidic approach that boosts the secretion of SEVs by fourfold compared to conventional protocols. They propose a PDMS microfluidic chip fabricated through photolithography. The device has four straight channels, each integrating 10 fishbone-shaped squeezing ridges intended to compress individual cells as they pass through. The ten time repetition of single cell compression promotes the membrane permeabilization, that is considered responsible for an increased release of SEVs. The platform is intended to be operated for 30 minutes with a sample throughput of 10^5cells/min and a cellular concentration of 2 x 10^6 cells/ml.

In this brief paragraph, we prove the concept that the elevated control of the microfluidic mechanical stress can be extended to other kinds of biologics (based on cells) to potentially control biogenesis processes. Specifically, the realization of a microfluidic platform intended to speed up the release of EVs by applying high intensity mechanical (shear) stress on a pool of cells is here described. The proposed approach follows the rule "less is more". Particularly, an extremely simplified microfluidic device geometry is suggested as a tool to create stress thresholds that are relevant to induce a release boosting of EVs. Instead of recruiting single cells, here a much more straightforward approach based on the stimulation of cell groups is proposed. In particular, a highly concentrated pool of cells (>10^6 cells/ml) undergoes an instantaneous stimulation (in the order of milliseconds) by being injected in a straight microfluidic channel properly designed to offer high shear rate intensity. Preliminary analyses return promising indications that the microfluidics can have a role in the fine control of biogenesis processes, impacting on the concentration and size homogeneity of EVs.

4.5.2 Experimental approach

Pure shear was investigated as mechanical stress source. A straight squared cross-section microfluidic channel was designed by using AutoCAD and its fluid dynamics characterized through numerical analysis. In particular, the velocity profile and the shear rate intensity as function of fluid flow rates for a water-like fluid was computed through COMSOL Multiphysics. Following fluid dynamic characterization, the microfluidic chip was fabricated by engraving PMMA through micromilling process.

MDA-MB231 cells were cultured and then suspended into phosphate buffer saline (PBS) at a concentration of 10^6 cells/ml so as to be injected into the microfluidic device. The cell suspension was made flow at 1 ml/min, corresponding to a 10 ms stimulation at a shear rate as high as 10^5 s^{-1}. The collected samples were then purified through a differential ultracentrifugation procedure optimized by Romano and colleagues [212].

With the purpose to compare outcomes of microfluidic stimulation with conventional EV production and isolation protocols, an additional batch of MDA-MB231 cells was cultured according to procedures optimized by Romano and co-workers [212]. Briefly, the cells were cultured and brought to 70-80% confluence. Afterwards, the culture medium was replaced by a fetal bovine serum (FBS) depleted one and cells incubated for 48 hours. Subsequently, the FBS depleted medium was recollected and treated with differential ultracentrifugation for the isolation of EVs.

Preliminary size and concentration characterization was conducted through NTA analysis on both isolated EVs after microfluidic process and those obtained through conventional protocols.

4.5.3 Preliminary results and conclusions

The PMMA microfluidic chip presents a 0,12 x 0,12 x 10 mm (W x H x L) squared cross-section. *Figure 15 a,b* contains both the CAD and the real microfluidic device. *Figure 15c* reports the velocity profile returned by numerical simulations. Intuitively, the profile established in such a geometry at 1 ml/min is a paraboloid. In addition, the shear rate intensity at different flow rates – 0,5, 1 and 2 ml/min – is reported in *figure 15d*.

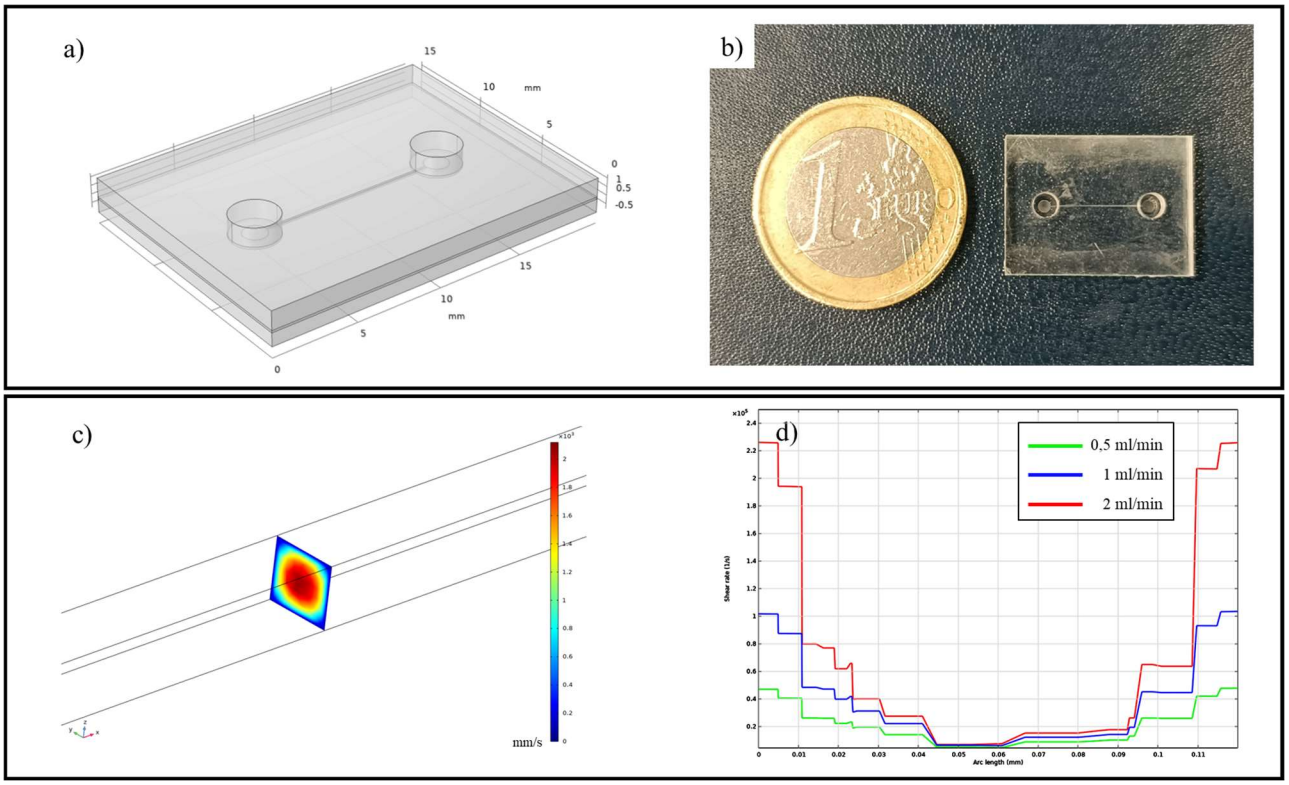

Figure 15 – mechanical stress microfluidic platform for the exploration of shear stress to boost the release of EVs.

Preliminary NTA characterization is reported in *figure 16.* By analyzing the plot, one could conclude that EVs obtained by the microfluidic process present an appreciably higher concentration and a more homogeneous size distribution than the EVs returned by conventional approaches. However, further investigations on the nature and quality of obtained EVs need to be carried out, including morphological and biological characterizations.

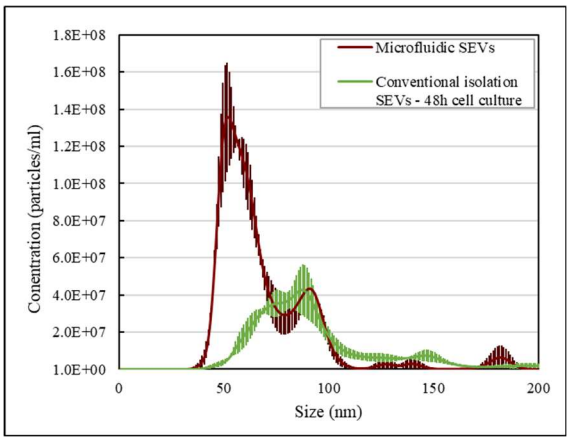

Figure 16 – Concentration of SEVs after sample stimulation and purification

5. Design and implementation of an automated microfluidic platform to screen therapeutic formulation stability under combined physical stresses

ABSTRACT

The protein-based therapeutics are highly promising for the care of challenging diseases. They are complex systems highly prone to destabilize and, during the development, their instability related to stressor exposure must be studied to find proper mitigation strategies. The current practice consists in subjecting formulations to isolated stresses (individual thermal or mechanical) and resultant information is then cross-correlated to return a formulation ranking. Reasonably, in a reality-related context, stresses might occur in various combined forms (*e.g.*, simulataneos thermal and mechanical stimulations) and degradation of drug products can follow pathways that might not be induced by single stress exposure. In this chapter, thermal and mechanical microfluidic platforms presented in chapters 3 and 4, respectively, are coupled according to a modular logic, in order to give rise to a versatile automated technology enabling stress combination. A nAb-based formulation is processed through the microfluidic platform to undergo a serial combination of thermal and mechanical stresses (thermal prior to mechanical and vice versa). The combination applied through the microfluidic platform points out some unobvious behaviors of the colloidal and structural configuration of the nAb in relation to the order of the stresses, thus proving that studying combined stimulation might result in meaningful information for a deeper knowledge of biomolecule-stressors and protein-excipient interactions.

GRAPHICAL ABSTRACT

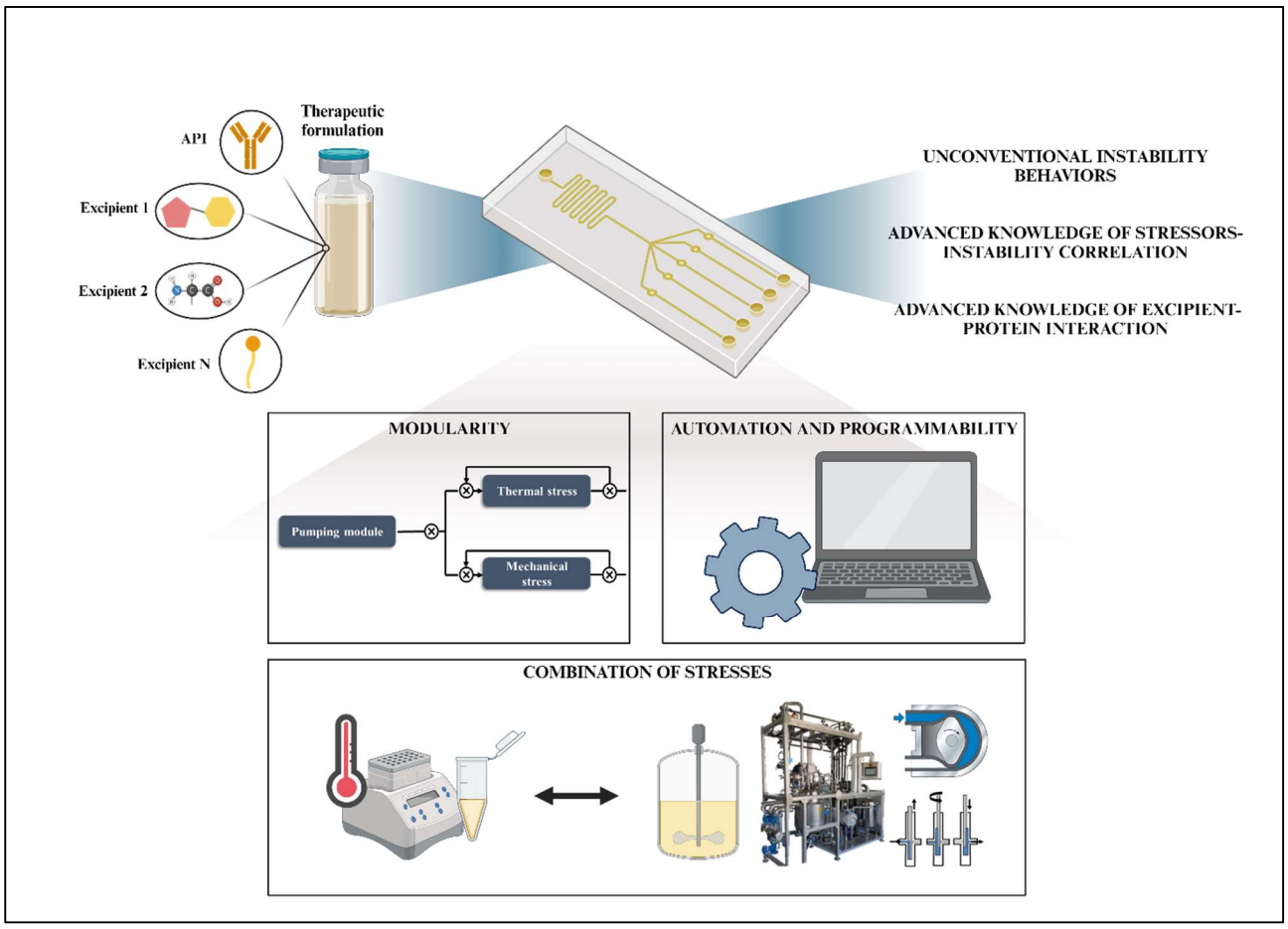

Image created with BioRender.com

5.1 Introduction

In previous chapters, some details about protein-based formulations and their exceptional potential to be used as therapeutic for challenging diseases have been outlined [21-23, 27-30]. Also, they have been defined as highly complex solutions possessing several chemical, rheological and thermodynamic complexities. The reason of their intricacy mainly lies in their multicomponent crowded composition (API plus several excipients). All the solutes in a formulation are typically solubilized at high concentration, thus determining a complex intermolecular network of interactions. As said, in order for the formulations to exert their therapeutic effect and not to show immunogenic behavior, the API stability must be preserved [35, 40, 51]. As discussed in chapter 1 (section 1.6), the stability of DPs is studied by exposing them to a number of physical and chemical stresses intended to quicken the protein degradation pathways and collect data on biomolecule stability in a reasonable short time period. This type of approach applied to biologics goes by the name of forced degradation studies [134, 135]. In accordance to regulations for the development of formulations and best practice reported in the literature about force degradation studies on liquid products, specific thresholds of physical/chemical stress have been identified in terms of intensity and exposure time.

As already pointed out, this type of solicitations are *individually* applied through batch-wise protocols on different lots of same formulation candidates. This means that same DPs experience one single type of stimulation at time (isolated thermal or isolated mechanical stress), expressing their degradation pathways with respect that specific destabilizing source. Actually, it could be argued that in the real therapeutic protein lifecycle, instability sources are very likely to occur in various combined forms, such as light plus agitation, high temperature overlapping to chemical exposure, or shearing and concomitant high temperature. In pharma industries, stability data from isolated stress tests are usually intercorrelated to determine a reliable ranking of DPs aimed to identify the most performing formulation. However, it is rather reasonable thinking that, catching unconventional, yet possible, degradation behaviors without subjecting biologics to more realistic instability sources, such as combined forms of stresses, becomes extremely challenging.

At early stages of formulation development (*pre-formulation*), the acquisition of information of alternative degradation pathways occurring in biologics when exposed to more realistic stimuli could potentially be of huge relevance for pharmaceutical companies to develop higher quality products. However, technologies able to accomplish such a combination are missing in the spectrum of industrial available tools. Their *in-batch* nature requires high volume amount and offers poor control of process parameters, thus resulting inconvenient and unsuitable to combine stresses.

In this chapter the design and the implementation of a *modular* microfluidic platform for the application of combined (sequential) physical stresses is presented. The thermal stress microfluidic platform described in chapter 4 and the mechanical stress microfluidic plant shown in chapter 5 are coupled, so as to enable the combination of thermal and mechanical (shear) stress. The ability of the modular microfluidic platform to combine different isothermal environments to various mechanical stress conditions in a versatile and automated manner is exploited to expose a nAb-based formulation to combined stresses. The DP is then analyzed through FTIR and DLS to prove the concept that different and unexpected behaviors can arise when more realistic instability sources are applied.

5.2 Materials and Methods

5.2.1 Materials

Trehalose dihydrate (product number T-104-4) was supplied by Ferro/Pfanstiehl in solid form; Poloxamer-188 (product number X0003307) was provided by Merck Serono S.p.A., L-Arginine (product number 1.01544) and Tris (product number 1.08386) were supplied by Sigma-Aldrich. The nAb (Mw 45 kDa) was provided by Merck Serono S.p.A.. The latter was given in liquid form at a concentration of 150 mg/ml in 10 mM Tris buffer, pH 7,5. NaOH (product number 1.58793) and HCl (product number 1.00317.1000) were provided by Sigma-Aldrich and used to adjust the pH of solutions. MilliQ water was used to prepare all the solutions. Polymethyl methacrylate (PMMA) sheets (product number ME30-SH-000110) were bought from GoodFellow Cambridge Ltd.

5.2.2 Preparation of buffer and nAb-based formulation

A 10 mM of Buffer solution was obtained by solubilizing 1,21 g of Tris in 1 liter of milliQ water. HCl was used to bring the pH from ≈10 to 7,5.

The nAb-based formulation (formulation C presented in previous chapters) was prepared in 10 mM Tris buffer with a final volume of 10 ml. The final formulation consisted of 120 mg/ml of nAb, 53 mg/ml of Trehalose, 14,7 mg/ml of L-Arginine and 0,1 mg/ml of Poloxamer.

5.2.3 Design, setup and programming of the microfluidic platform for combined stresses

The layout of the microfluidic platform for the stress combination is shown in *figure 17*. It presents three main sections: pumping, thermal stress and mechanical stress modules. Thermal and mechanical stress modules are detailed in chapter 4 and chapter 5. Briefly, the thermal stress modules consists of three parts: the main line, the thermal station and the recirculation line (*figure 4*, chapter 3). Similarly, the mechanical stress is composed by a main line, the mechanical (shearing) station and the recirculation line (*figure 9*, chapter 4). All the elements (valves, pumps, thermal and shearing stations) are linked through 0,8 mm inner diameter FEP tubes. In particular, the thermal-mechanical and mechanical-thermal combination is achieved through a FEP tube referred to as *stress bridge* (reported as a red line in *figure 17 a,b*). Specifically, the *stress bridge* for thermal-mechanical stress connects element 15 to element 16, while the stress bridge for the mechanical-thermal stress combination links element 22 to element 10. The setup of the platform including both thermal and mechanical stress modules is reported in *figure 17 c*.

The microfluidic combined stress was carried out following platform programming. Platform configurations reported for thermal (Appendix A, paragraph A1) and mechanical stress (Appendix B, paragraph B1) are sequentially run in order to accomplish the stimuli combination. Specifically, for the thermal-mechanical stress the DP was first made flow throughout the thermal stress module, automatically pumped via *stress bridge* to mechanical stress one and then stimulated through the latter. Conversely, for the mechanical-thermal combination, the formulation was first introduced into the mechanical module, then moved to the thermal stress one by using the *stress bridge* and, finally, treated thermally.

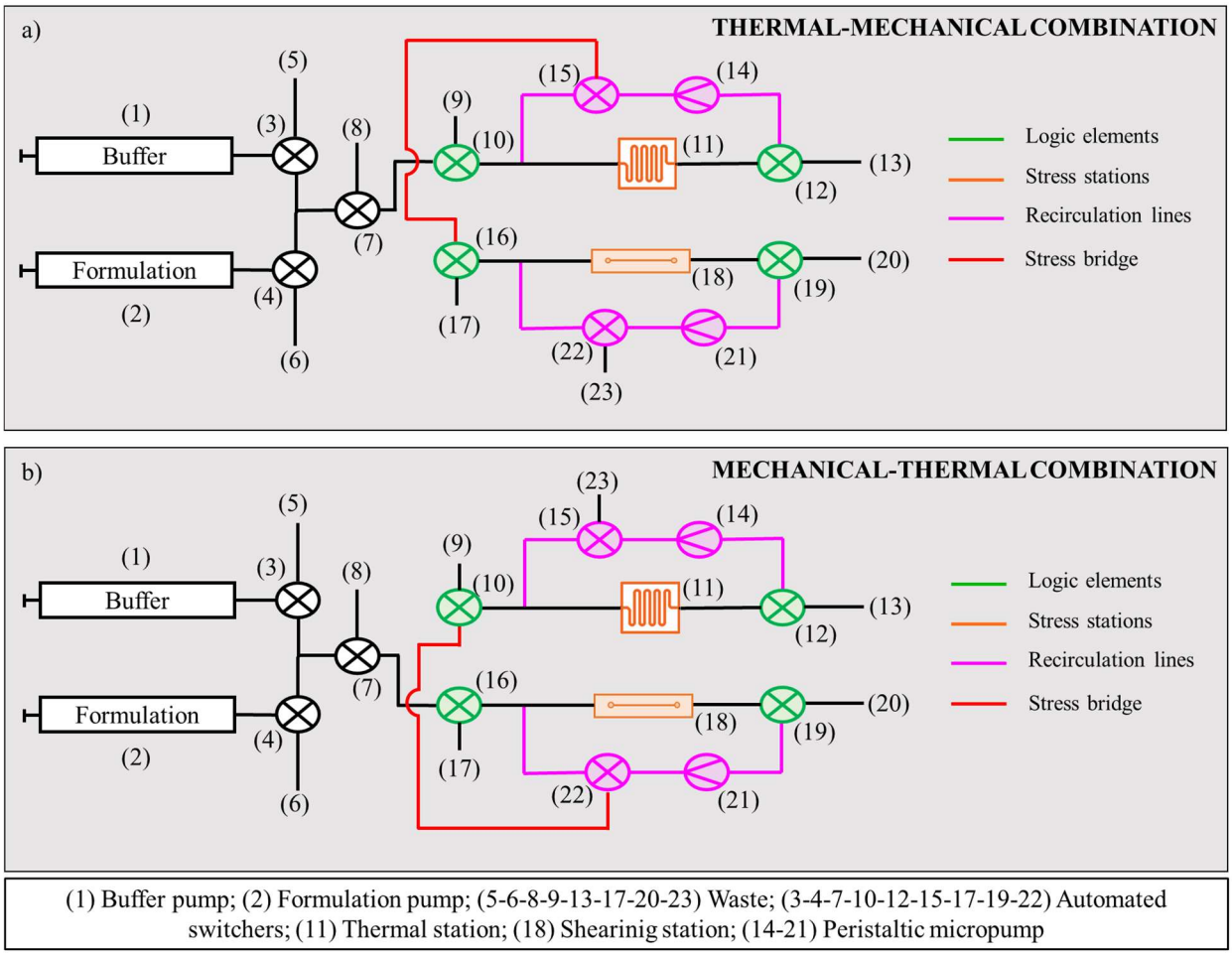

Figure 17 – Microfluidic platform layouts for the combination of stresses. (a) platform configuration for thermal-mechanical stress combination; (b) platform configuration for mechanical-thermal stress configuration; (c) setup of the microfluidic platform for thermal and mechanical stress combination -

5.2.4 Combined stress through the microfluidic platform

The nAb-based formulation C was selected due to its high stability with respect to both thermal and mechanical microfluidic stress (as demonstrated in chapter 3 and 4). The selection of the most stable formulation better challenges the capabilities of the microfluidic platform to highlight API behaviors other than the one recorded in previous chapters. Formulation C underwent thermal-mechanical and mechanical thermal stimulation. In the former, the formulation was first thermally treated at 52°C for 5 min and then sheared at 20000 s^{-1} (*strong* shear rate interval, *figure 10* chapter 4) for different number of cycles (1, 6, 14), that correspond to diverse recirculation times (no recirculation, 2, 5 min). Vice versa, in mechanical-thermal stimulations, the formulation

was first subjected to 20000 s^{-1} shear rate for different number of cycles (1, 6, 14), corresponding to diverse recirculation times (no recirculation, 2, 5 min), and subsequently treated with thermal module at 52°C for 5 min. Additionally, individual microfluidic thermal and mechanical stresses were conducted in order to compare nAb behavior under isolated stimuli to combined solicitations. The experimented points are reported in *table 8*.

Formulation	Thermal stress	Mechanical stress
Formulation C	/	0-20000 s^{-1} – single passage through microfluidic device
		0-20000 s^{-1} – 2 min
		0-20000 s^{-1} – 5 min
	52°C – 5 min	/
	52°C – 5 min	0-20000 s^{-1} – single passage through microfluidic device
		0-20000 s^{-1} – 2 min
		0-20000 s^{-1} – 5 min

Table 8 – Experimental points tested for the combination of stresses

5.2.5 Size distribution modifications through DLS

Stimulated samples were analyzed through DLS (Zetasizer Nano, Malvern) soon after being processed in order to determine the size distribution. Particularly, 40 µL of each sample were diluted with 1960 µL of buffer, resulting in a 50-fold dilution. As discussed in chapter 4, the dilution factor resulted from a feasibility study carried out on a model protein. Details are reported in Appendix B, section B3. 1 ml of diluted solution was analyzed by using a disposable polypropylene cuvette. The measuring parameters were adjusted based on the solution and material characteristics. For each sample, three measurements of 15 runs of 10 seconds each were performed and averaged. "Protein analysis" model was adopted to fit the instrument raw data.
Aiming to detect size distribution modifications between treated and untreated samples, the coefficient of determination (R^2) was computed as *similarity score parameter*. The latter enables an efficient comparison of stimulated and unstimulated formulation size distribution, returning a degree of similarity.

5.2.6 Secondary structure modifications through FTIR

Soon after being stimulated, samples were analyzed with no dilution through FTIR (Mettler Toledo ReactIR equipped with a 50 µl microflow cell). 128 scans were taken with a resolution of 4 cm^{-1} and then averaged to return the absorbance spectrum of each sample. Secondary structure modifications were detected by taking the second derivative of each spectrum and focusing on the amide I band [1680 – 1600] cm^{-1}. The latter contains major information of intra- and inter-molecular β-sheets, of which the nAb is rich.
The coefficient of determination (R^2) was computed as *similarity score parameter* of the second derivatives of treated and untreated samples. This parameter enables an efficient comparison of stimulated and unstimulated formulation secondary structure elements, returning a degree of similarity.

5.3 Results and discussion

5.3.1 Identification of colloidal and structural modifications of nAb-based formulation under stress combination

Unstimulated and stimulated samples were analyzed through DLS and FTIR to characterize size distributions and absorbance spectra. These analyses return information of the colloidal (monomeric and oligomeric species) and secondary structure configuration before and after the stimulations. As described in materials and methods (section 5.2.5 and 5.2.6), size distributions and second derivative of absorbance spectra in the amide I band of stimulated and unstimulated samples were compared through the coefficient of determination (R^2) used as

similarity score parameter. The higher the R^2, the more diverging the colloidal and structural configurations of stimulated formulation from unstimulated condition. *Figure 18* reports the colloidal (*figure 18 a*) and structural (*figure 18 b*) similarity score parameters of isolated and combined stresses. Focusing on the colloidal configuration (*figure 18 a*) it can be observed that the isolated thermal stimulation (red curve) has a more detrimental impact than the mechanical stress (green curve). Interestingly, *figure 18 a* reports that the combination of the stresses is not commutative: from a colloidal point of view, the application of thermal stress prior to mechanical and vice versa ends up in different outcomes. Specifically, thermal-mechanical (yellow curve) results more impactful on the colloidal configuration than mechanical-thermal stimulation (blue curve). It seems that mechanical stress applied before the thermal one, renders the latter completely ineffective. This is corroborated by the fact that isolated mechanical (green curve) and combined mechanical-thermal stress (blue curve) are essentially exhibiting the same trend. Interestingly, this observation goes along with what concluded for some points of the mechanical stimulation outcomes presented in chapter 4: from a colloidal point of view, the transmission of higher mechanical energy to the formulation makes the excipients better conduct their stabilizing role.
Figure 18 b reports the outcomes of FTIR analysis. First, it can be said that individual thermal and mechanical stresses have, from a structural configuration perspective, similar effects. Moreover, similarly to what observed for the colloidal configuration, it comes out that the application of combined thermal and mechanical stress is not commutative. The order in which they are provided to the formulation matters. However, unlike the colloidal configuration, the secondary structure seems to be more impacted by the mechanical-thermal combination rather than by the thermal-mechanical stimulation.

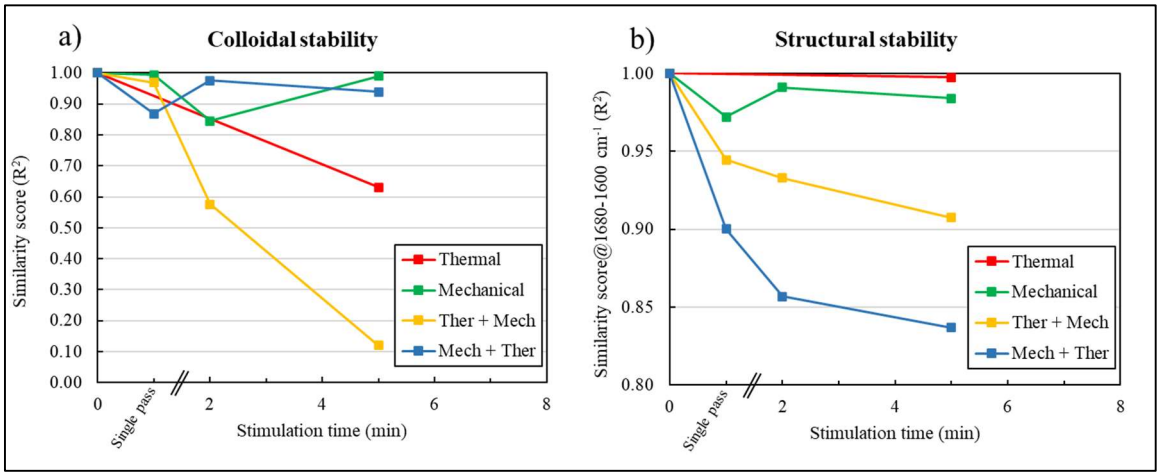

Figure 18 – Similarity score of isolated and combined stresses. (a) similarity score retuned by DLS analysis indicating colloidal configuration of treated samples with respect to the untreated ones; (b) similarity score retuned by FTIR analysis indicating structural configuration of treated samples with respect to the untreated ones.

5.4 Conclusions

Stability of biologics is essential in order to make protein therapeutics express their exceptional clinical potential. Besides the study of the effect of individual stressors (such as temperature changes or mechanical stimulation), the impact of stress combination might result in meaningful information to be cross-referenced with those coming from isolated stresses. Indeed, stressors are very likely to occur in combined forms during a biological therapeutic lifecycle. Thus, probing the response of formulations to combination of stimulations might shed light on instability behaviors that remain hidden when they are exposed to one single stress source at time. Although testing formulations against combined forms of stresses can clearly introduce advantages in the understanding of the biomolecule stability, there are neither standard protocols nor available technologies

that render this process easy to be performed. In fact, batchwise protocols make the combination of stresses impractical.
In this chapter an automated microfluidic approach is proposed as an eligible tool to combine stresses. It was demonstrated that the modular programmable platform can efficiently combine thermal and mechanical stresses and the concept that their combination can induce alternative instability behavior with respect to isolated ones was proved. Among the nAb-based formulations presented in the previous chapters 3 and 4, the most stable (formulation C) was selected, so as to challenge both the potentialities of the microfluidic platform and the validity of the approach. Additionally, it was considered a reasonable choice that reflected a possible function of the stress combination, to which only those formulations already expressing good robustness against isolated stressors could be exposed. As matter of fact, it was observed that the stress combination can induce instability that are not seen under isolated stresses. Interestingly, the commutation of stresses (*i.e.*, thermal prior to mechanical and vice versa) might not return same information about the formulation stability. In fact, the order of the type of energy (thermal-mechanical or mechanical-thermal) provided to the formulation can completely change the performances of the stabilizing co-solutes. Such an information can be beneficial to formulation scientists to make deeper evaluations for the selection of excipients, so as to better protect the biomolecules from both isolated and combined stresses.

6. Discussion and perspectives

Biological therapeutics, such as protein-based formulations, can improve clinical outcomes in treating challenging diseases. The exceptional features of protein biomolecules (*e.g.*, high specificity and complex chemical structure) contribute to the execution of biological functions that synthetic drugs cannot mimic. However, proteins are naturally prone to destabilization in the presence of physico-chemical factors (temperature, agitation, light etc.), representing the main roadblock to the clinics. In fact, there is scientific evidence that protein instability (e.g., protein aggregation) is the major cause of biomolecule immunogenicity, determining both therapeutic inefficacy and patients' dissatisfaction. The current era of patient centricity gives priority to individuals undergoing therapies, and their contentment is a great concern. Hence, bringing robust and non-immunogenic products to the clinics is of pivotal importance. To this purpose, the stability of injectables needs to be profoundly investigated during their development to assess their resistance to stressors that are encountered throughout biologics' lifecycle. Indeed, the formulation development aims to identify major threatening factors and define mitigation strategies to guarantee stable product to be administered to patients. Current protocols to study the stability of therapeutic formulations with respect to instability sources rely on batchwise approaches that are expensive, poorly controllable and, some times, non-representative of the real destabilizing factors. For example, previous chapters discussed the inefficiency of conventional mechanical stress protocols (agitation) to exhaustively recreate stressing conditions typical of manufacturing process or patient injection. Also, it was discussed that instability factors might occur in combined forms (*e.g.*, concomitant temperature change and mechanical stress) and *in-batch* standard protocols typically fall short of reproduce such a condition. Eventually, this limitation severely affects the scientific knowledge of protein instability and physico-chemical stimulus intercorrelation, consequently obfuscating the real stabilizing role of excipients. The need to test formulations with respect to more realistic instability sources, such as manufacturing high-intensity hydrodynamic forces or combination of stresses, is urgent in order to expand the understanding of therapeutic protein stability. Parallely, available technologies to conduct such investigations efficiently are scarce.

In this thesis, the development of a microfluidic platform for the application of physical stresses (high temperature, high shear and their combination) is described and proposed as a tool to study the stability of therapeutic biomolecules in complex formulations. The miniaturization, the high control and the possibility to integrate orthogonal technologies make the microfluidics an eligible means to address the limitations posed by current batchwise approaches (expensiveness, low control of process parameters and inferior representativeness of real stressors). The major findings of this study are hereafter summarized.

In chapter three, the microfluidic thermal stress platform was as valid as forced degradation in-batch procedures and equally capable of reflecting the formulation ranking of standard storage condition and accelerated stability protocols. However, the programmability of the automated platform and its miniaturization render the microfluidic process advantageous with respect to the other approaches in terms of cost-efficacy, control of transport phenomena (homogeneous transmission of thermal energy), experimental repeatability and minimization of human error.

In chapter four it was argued that the conventional agitation mechanical stress remains a good approach to test the resistance of formulations to air-liquid interface exposure, while they are inefficient to probe the stability of drug products under high intensity hydrodynamic forces typical of manufacturing process or patient injection. This observation dictated the driving force for the development of a microfluidic apparatus able to subject candidate formulations to hydrodynamic challenging conditions (high shear levels). Besides conventional analyses (SE-HPLC), the microfluidic shear stress was characterized through *quasi-real-time* analysis (immediately after the stimulation) to gather information about the colloidal and structural modifications of formulations exposed to high shear. While conventional analytical approaches were not able to catch any destabilization phenomena, orthogonal *quasi-real-time* analysis, with minimum or absent sample preparative phase (minimum or no sample dilution), intercepted interesting transient instability phenomena induced by the microfluidic platform. These results are useful to understand the behavior of formulation under high shear regime and the role of proteins-excipients interaction in a challenging hydrodynamic environment. The same analytical approach was coupled to a conventional agitation protocol and no meaningful trends emerged. Such a result opened two main points of discussion: on a side it highlights the need for more

appropriate analytical strategies, as the limitations of analytical conventional protocols, such as lengthy sample preparative phase and high sample dilution, drastically restrict the ability to grasp formulation destabilizing phenomena. On the other hand, outcomes of chapter four highlight the inadequacy of conventional agitation in providing substantial information, even when advanced analytical protocols are employed. Additional unobvious results showed that the amount of mechanical energy provided to the formulation might completely change the performances of the excipient-protein interaction. Surprisingly, in some cases it was observed that bigger amount of mechanical energy (*i.e.*, more intense mechanical stress) enhanced the protecting role of stabilizers.
In chapter 5, the versatility of the microfluidics was proven by coupling the thermal an mechanical stress modules, giving rise to an advanced modular microfluidic platform not only for the application of combined stresses. Thermal and mechanical shear were sequentially conducted and their effects on a therapeutic formulation were analyzed through the *quasi-real-time* analytical approach set in chapter four. It was discovered that the combination of stresses emphasizes unconventional formulation behaviors. Specifically, the order in which the stresses are provided can radically flip the outcomes. In fact, thermal and mechanical stresses are not commutative, meaning that when thermal energy is provided prior to the mechanical one and vice versa, the formulation might express different ability to preserve colloidal and structural configuration. As verified for a nAb-based formulation, the application of an initial physical stress can make the subsequent one completely ineffective. This was the case of the mechanical shear executed prior to the thermal stress: from the point of view of the colloidal configuration, the former made the latter not to induce appreciable modifications compared to the isolated mechanical shear. Phenomena captured and described in chapter 4 and 5 are rather illustrative of the unusual behaviors that the microfluidic platform can induce.

Often, microfluidics is reductively associated with the scaling-down, *i.e.*, the miniaturization of large-scale processes with the obvious advantage of reduced costs. Actually, in this specific case, one of benefits related to the developed technology is the cost-efficacy, thanks to the possibility to process small reagent volumes. However, in light of the outcomes detailed in previous chapters and summarized above, it can be said that this technology steps beyond a mere replication of processes at a smaller scale. Indeed, the advantage of cost reduction becomes marginal with respect to the other contributions that are brought by this platform. As demonstrated, the platform could generate data that turn into complex and peculiar information. This is made possible by the high controllability and versatility offered by the microfluidics. In fact, should a key word running throughout this work be identified, it would certainly be *"process control and versatility"*. Thanks to a sophisticated design, selection of proper circuit components and optimization of customized microfluidic chips, the platform has proven its ability to *control* the microenvironment, flexibly spanning a wide range of formulation viscosities, broad temperature interval and large mechanical stress window. This translate in *the platform versatility* to study diverse types of molecules and formulation conditions in an extensive set of physical stress nature, intensities and combinations. Moreover, the controlled flow regime typical of a microfluidic context enables the easy intercorrelation of transport phenomena (energy and momentum transfer) to instability behaviors. For example, the design of devices presenting specific shear rate thresholds permits the correlation of relevant instability phenomena to precise mechanical stress source characteristics. Plus, the predictability of the thermal energy transfer coupled to a laminar flow regime, makes the microfluidic thermal stress highly repeatable and controllable. On the contrary, batchwise applications are largely dominated by non-ordered transitional/turbulent flow regimes and high variability of the thermal energy transfer dynamics. In essential words, unlike *in-batch* processes, in a microfluidic environment the stimulation is transferred to the formulation in a more controlled and predictable manner. This helps clarify the relationship between biomolecule behavior and underlying causes. In addition, in a microfluidic context, the stimulation is more *homogeneously* transmitted to the whole microvolume, that can be easily and completely analyzed in order to have an information that is indicative of the entire formulation system. Conversely, in a batchwise approach, the stimulation is *heterogeneously* transferred to the liquid formulation, and typically, when analyses come into play, just a minimum aliquot of the whole large volume is processed. This might lead to imprecise outcomes that are not fully representative of the actual condition of the formulation.
All the strengths discussed so far - control, versatility, predictability and representativity - clearly impact the ability to generate *higher-quality data*, which eventually support the evidence that the microfluidic platform is

much more than large scale process replication and miniaturization. Indeed, while the potentials of the presented technology can be expanded by the implementation of a *programmable pumping module* for the automatic mixing of APIs and excipients, and by the integration of an *inline real-time analytical module*, this tool can already help answer some scientific open questions regarding the comprehension of protein-instability source correlation and biomolecule-excipient interaction.

The control of process parameters, the correlation of phenomena with root causes and the generation of advanced information align closely with a leading concept of the pharma industry: the *Quality by Design* (QbD) approach. In fact, "pharmaceutical QbD is a systematic approach to the development that begins with predefined objectives and emphasizes product and process understanding and control based on sound science and quality management" [213]. In a pharmaceutical QbD strategy, the main aim is achieving necessary product quality specifications (quality target product profile – QTPP) based on clinical performances, such as therapy efficacy and patients' satisfaction. The quality is achieved by carefully identifying the impact of *critical process parameters* (CPPs) to *critical quality attributes* (CQAs) of the product, that are those chemical or physical properties that need to fall in a specific tolerability interval so as to match the QTPP. This is feasible if only comprehensive studies and efficient monitoring and control strategies are set up during pharmaceutical processes. As redundantly recalled throughout the thesis, the current pharmaceutical landscape is dominated by non-continuous *in-batch*-driven processes that limit the applicability of the QbD approach. This is because of their inefficient controllability of process parameters and predictability of occurring physical phenomena. The identification of CPPs and their correlation to CQAs become reasonably tedious when the repeatability of the processes is not ensured. In such a context, the microfluidics, thanks to its control and predictability, could bring an improvement in the individualization of CPPs as well as in their connection to CQAs. In addition, as demonstrated in the present work, non-continuous approaches might not fully achieve their intended objectives. This is exemplified by the agitation protocol designed to test the mechanical resistance of liquid formulations, even in the face of manufacturing stresses (*i.e.*, intense hydrodynamic forces). This is somewhat emblematic of the *intercommunication gap* between early and late phases of a pharmaceutical process. In other words, agitation is not consistent with a QbD perspective. CPPs of a shaking process and their impact on CQAs are not adequately meaningful within the context of a manufacturing process. This is primarily because of the huge difference existing between the two types of process. Intuitively, this practice might determine, at later manufacturing steps, *downstream corrections* of the formulation composition, resulting in lengthy setbacks, laborious revisions and extra costs. The microfluidics could be integrated into this context to change the paradigm from a *downstream corrective* approach to an *upstream testing* strategy, thus bridging the communication gap between the earlier formulation development and the later formulation manufacturing phase. In fact, it was shown that the microfluidic platform can help identify peculiar behaviors of a therapeutic protein with different combination of excipients, highlighting their role under elevated shear. It was demonstrated the ability of the microfluidics in determining shear thresholds at which formulations exhibit noteworthy deviations from unstimulated condition. In the context of pre-formulation screening or in a study of molecule manufacturability, the platform could bring out the best, opening options to test candidate molecules and formulations in a wide spectrum of unconventional and more reliable conditions, thus gathering high-quality data laden with dense information.

In conclusion, in this thesis the development of a microfluidic platform to study the stability of biological therapeutics is presented. The main shortfalls of current batch-driven approaches were outlined and it was demonstrated that a microfluidic plant, if properly designed and programmed, can be an efficient means to address these limitations. Indeed, the results of this research activity suggest that such a platform can represent a *technological advancement* that goes beyond process replication and miniaturization. Rather, it might assist in elucidating intricate correlations among protein instability, destabilizing sources and complex role of stabilizers, thus introducing *scientific knowledge* that current technological approaches cannot generate. Finally, it was speculated how a pharmaceutical context can benefit from integrating this technology. The ability of the microfluidics to produce alternative advanced information can bridge the intercommunication gap between earlier and later stages of pharmaceutical processes. If this unconventional information is effectively integrated with that generated by current approaches, it could potentially steer the development of

biological therapeutics towards a more *quality-oriented* perspective, with the possibility to influence clinical outcomes.

Appendix A

A1. Thermal stimulation through microfluidics

Figure A1 depicts the configuration of automated valves and other circuit elements in order to complete the stimulation. In details, the buffer enters the platform to fill the thermal station (*figure A1*a), while the latter stabilizing at the target temperature. After the fluid reaches the element 5, the latter is switched to the left to allow the recirculation line filling (*figure A1*b). This configuration is kept until temperature stabilization is attained. Subsequently, the pumping module is set to switch to the pump containing the formulation, allowing the latter to be injected into the thermal stress module (*figure A1*c). For the latter to be fully filled with the formulation fluid, the dead volume of the tubing connecting circuit elements 7 and 3 must be expelled. To this purpose, valves were programmed to allow this fluid volume to be pumped (by the peristaltic micropump) to the thermal station (*figure A1*d) and then be washed out through the right outlet of the element 5 (*figure A1*e). After that, the thermal module is completely filled of candidate formulation and the stimulation can be conducted. The automated valves are programmed to allow the fluid recirculation through the peristaltic micropump for the required stimulation period (2 or 5 min), while the thermal station offering a stable isothermal environment (*figure A1*g). Following the thermal solicitation, the buffer is injected into the thermal module while the sample is collected from the left exit of the circuit element number 7 (*figure A1*h).

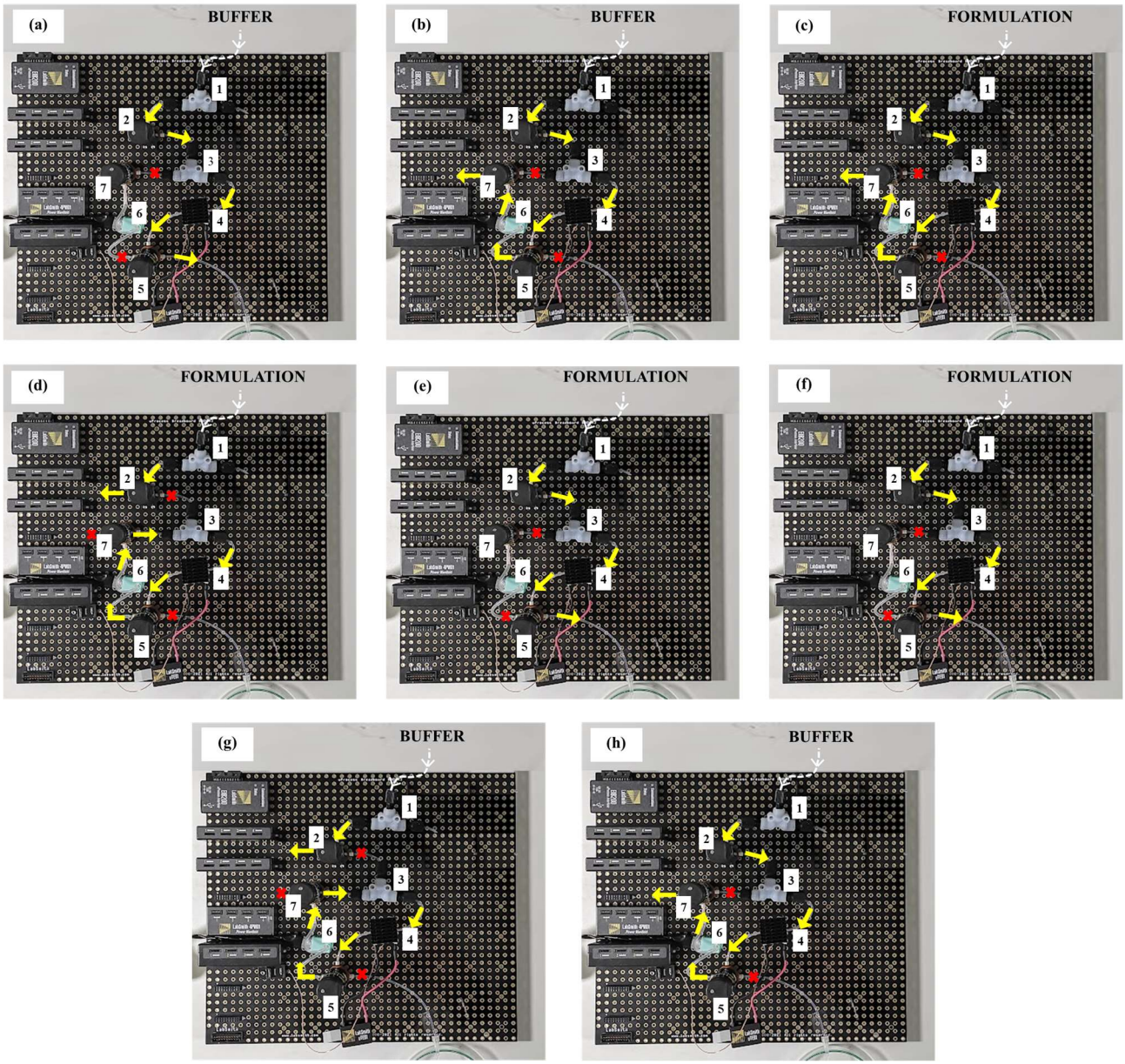

Figure A 1 - Platform management to conduct the thermal stimulation of formulation. (a) The buffer enters the main line of the platform and exit the right position of element 5 (automated valve). Meanwhile, the thermal station (element 4) is set to reach the target temperature. (b) The buffer fills the recirculation line by being injected through left position of element 5 (automated valve) by means of the peristaltic pump (element 6) and getting out of the platform through left position of the automated valve number 7. This position is kept until the thermal station (element 4) reaches the target temperature. (c) The formulation enters the thermal stress module after the thermal station is stabilized at the target temperature in order to fill the thermal module up to the element 7. (d) The dead volume in between element 7 and element 3 is transferred to the main line; (f) the valve are then configured to allow the volume ejection from the main line of the thermal module through the right exit of the valve number 5. (g) Configuration of elements to enable the fluid recirculation; (h) Valve configuration to enable stimulation fluid recollection through the left exit of the valve number 7.

A2. Fabrication through micromilling feasibility study

Investigated parameters intended to optimize machining fabrication are reported in table A1.

Sample	Tip (µm)	Z step	X-Y step
S1 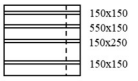	100	1/5, first 3 channels 1/10, last channel	Default
S3 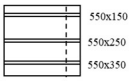	500	1/5	Default
S4 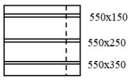	500	1/10	Default
S5 	500	1/5	Default
S6	500	1/5	Default/2

Table A 1 - Machining conditions tested in the feasibility study on different channel dimensions.

The best combination of parameters matching lower roughness, reliability to the CAD project and reasonable machining duration resulted to be the following:
Tip size: 500 µm;
X-Y step size: 62,5 µm (halved default value returned by CAM software);
Z step size: 125 µm (1/6 of the whole channel height);
Feed rate: 34,8%;
Spindle rate: 10000 rpm.
In addition, the machining setup is shown in *figure A2*a. *Figure A2*b,c,d,e report a channel of 550x250 µm (WxH). A same 500 µm tip was used and different Z-step sizes were applied. In particular, the channel in figures A2b,c was engraved with 50 µm Z-step (1/5 of the whole channel height) and the one reported in figures A2d,e with 25 µm Z-step (1/10 of the whole channel height). 1/5 of the total height Z-step returns an increased wall roughness compared to 1/10. While the former results in a channel height of 269 µm, the latter results in a less accurate channel height (320 µm) with respect to desired one (250 µm). In addition, different channel bed roughness are compared in *figure A2*f,g. In particular, *figure A2*f depicts a channel bed machined with default value of x-y step, while *figure A2*g shows a channel bed obtained with halved default value of x-y step.

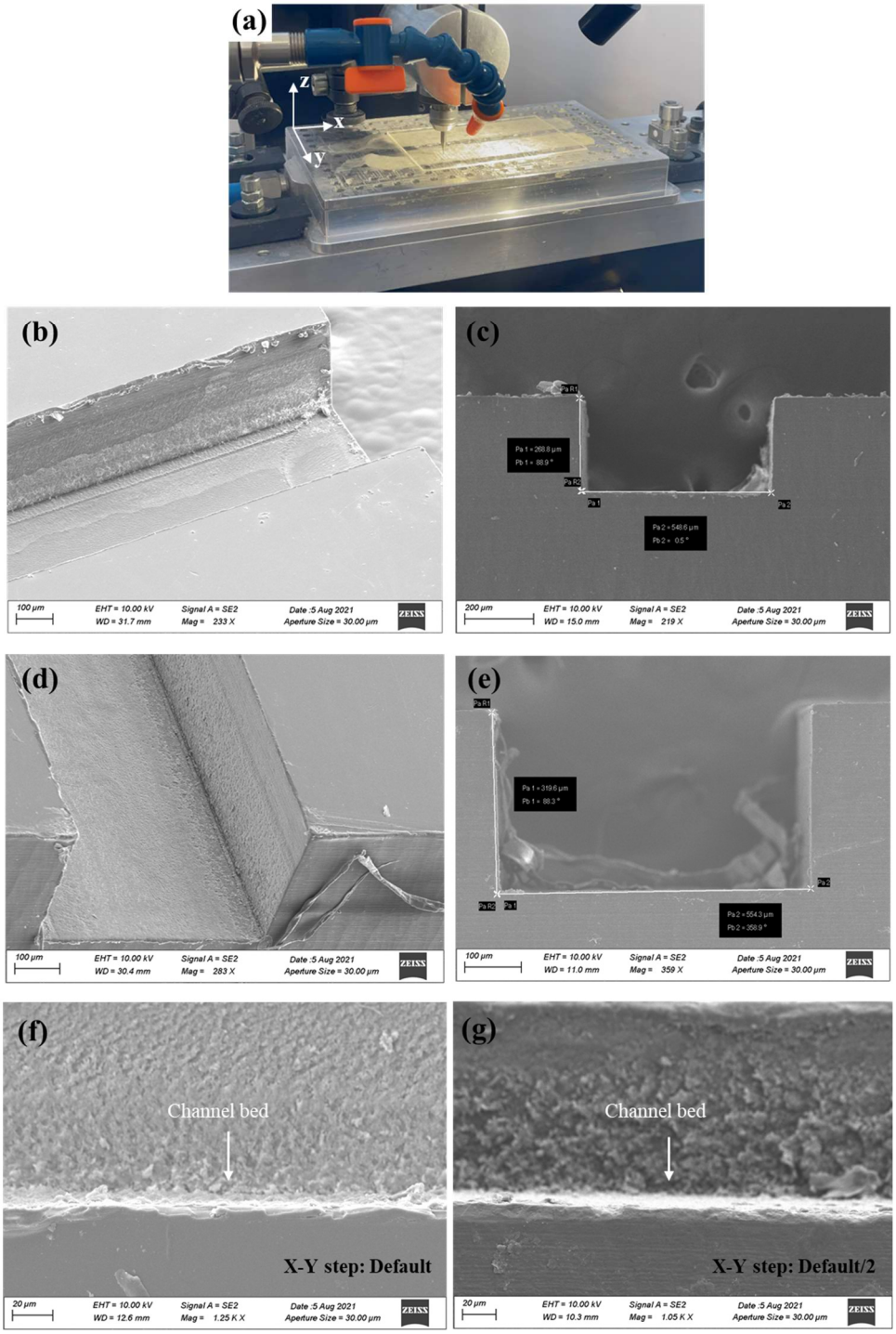

Figure A 2 - Comparison between different Z-step sizes for a 550x250 µm (WxH) channel engraved with a 500 µm tip. (a) Milling machine stage; (b-c) Channel obtained with a 1/5 Z-step size; (d-e) channel obtained with a 1/10 Z-step size; (f) channel bed roughness with default x-y step; (g) channel bed roughness with halved default x-y step.

A3. Feasibility study for the individualization of best parameters for fine temperature control

Combination of parameters tested under no flow and flow conditions are reported in the *table A2*.

ID	Flow rate (µl/min)	Peltier Cell operating voltage window (V)	Temperature Setpoint (°C)	Voltage ramp (mV/s)	Tolerance (±°C)
1	0	[-2.9; +2.9]	37	10	1,5
2				1	
3				0,2	
5			40	1	
6				0,2	
8			50	1	
9				0,2	
10	800	[-2.9; +2.9]	40	5	0,5
11					1,5
12			50		0,5
13					1,5
14			55		0,5
15					1,5
16			40	1	0,5
17					1,5
18			50		0,5
19					1,5
20			55		0,5
21					1,5

Table A 2 - Tested parameters and conditions for temperature control

A4. Fluid dynamic and energy transfer analysis

Figure A3 depicts the fluid dynamic outcomes and energy transfer kinetics. In particular, *figure A3*a reports the shear rate profile along the channel width at a fixed x-coordinate. *Figure A3*b indicates the pressure drop across the microfluidic channel according to the red cutlines. Finally, figureA3c reports the increase of fluid temperature at stimulation temperature (49°C and 52°C), while flowing at 800 µl/min. The initial temperature of the fluid is 25°C.

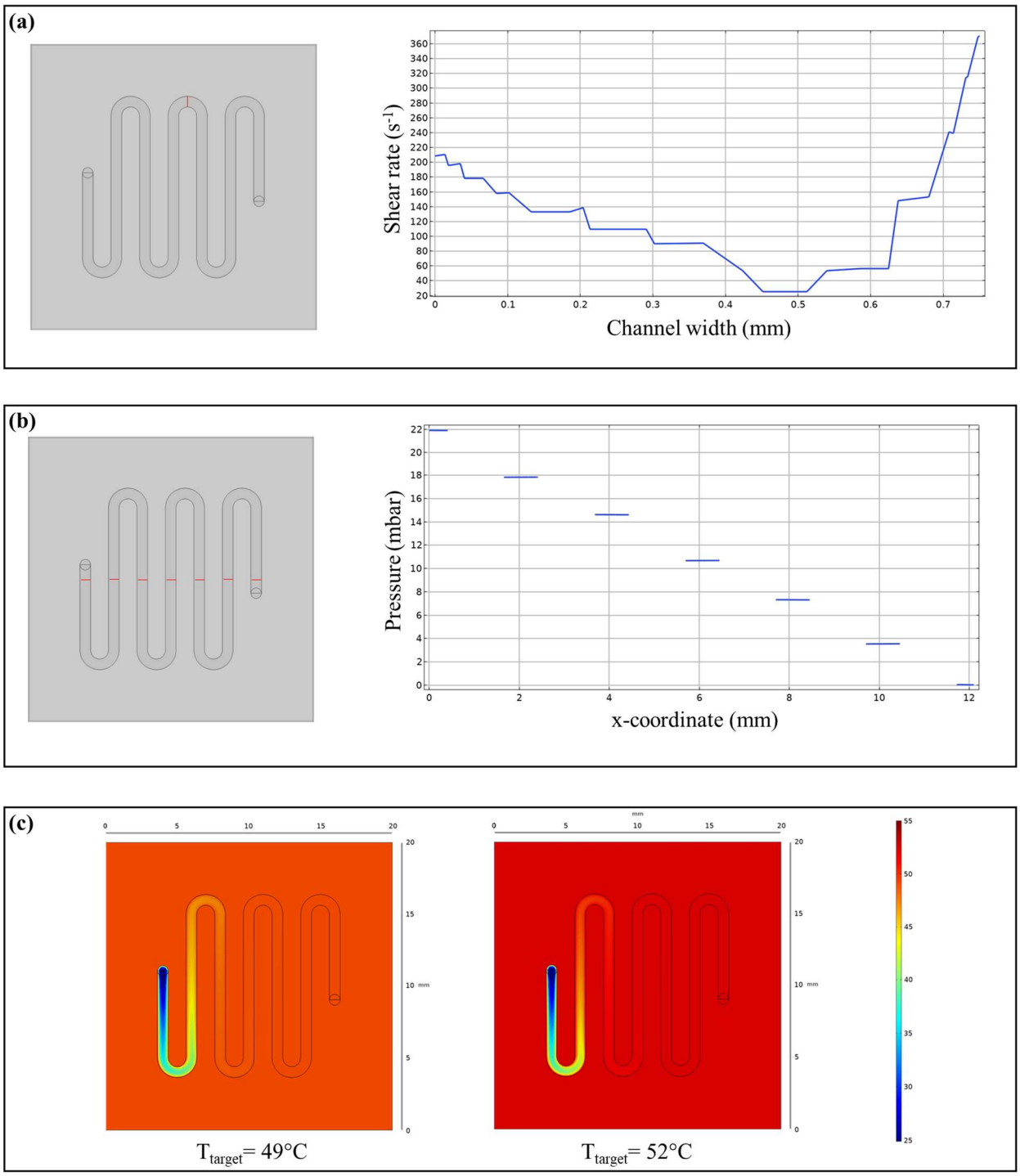

Figure A 3 - Numerical simulations for fluid dynamic and energy transfer analysis. (a) Shear rate profile across the channel section; (b) pressure drop across the channel; (c) flowing fluid heating at stimulation temperatures

Appendix B

B1. Mechanical stimulation through microfluidics

The microfluidic mechanical stimulation is carried out following platform programming in order to pump the fluid throughout proper pathways. *Figure B1* represents the circuit element configuration in order to inject the candidate formulations into the mechanical microfluidic platform, run the stimulations and collect the samples. In particular, the formulation is pumped from element 1 to 7 in order to fill the main line (from element 3 to element 5) and part of the recirculation line (from element 5 to 7) (*figure B1 a*). In this step, the formulation syringe pump (not represented in *figure B1*) and the peristaltic micropump (element 6) work together to transfer the fluid from element 1 to 7. Afterwards, the filling of the recirculation line is completed by configuring the valves in such a way that the dead volume of fluid between element 7 and 3 is moved to the main line (*figure B1 b*). In such a step, the fluid motion is accomplished through the peristaltic micropump (element 6). Once in the main line, this volume of fluid is expelled through the element 5 (*figure B1 c*). In this configuration step the formulation is pumped by the syringe pump. With the step reported in *figure B1 c* the mechanical stress module is completely filled and the stimulation can be initiated. To this purpose, the valves and the peristaltic micropump are configured so as to form a loop enabling fluid recirculation (*figure B1 f*). Meanwhile, the valves of the pumping module are set to switch to buffer syringe pump. After the completion of the stimulation, the sample recollection is accomplished by configuring the platform as reported in *figure B1 e*. In this step, the buffer syringe pump and the peristaltic micropump cooperate to move buffer solution into the mechanical stress module. At the same time, the stimulated formulation is recollected from the right exit of the element 7 in a safe lock tube.

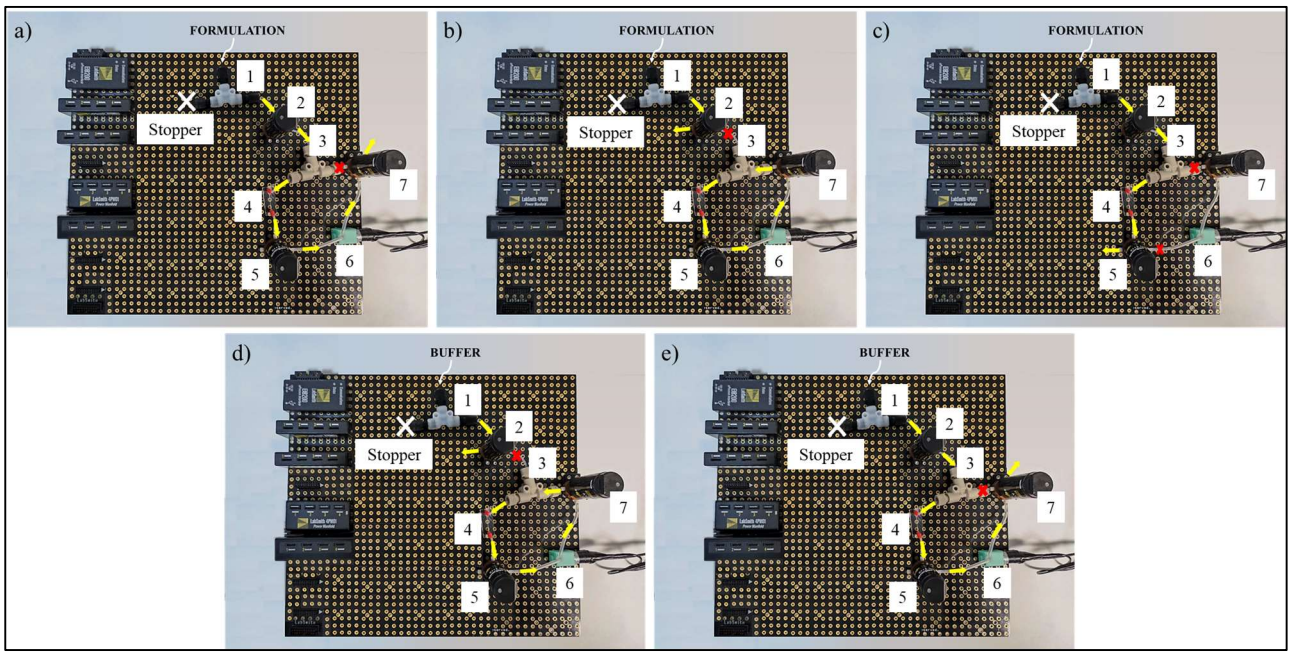

Figure B 1 – Platform configuration to complete the microfluidic mechanical stimulation. (a, b, c) injection of the formulation into the platform in order to fill the mechanical stress module; (d) configuration of circuit elements during the mechanical stimulation; (e) element configuration for the stimulated sample recollection.

B2. Single passage of formulations through the mechanical stress microfluidic device

A first batch of formulation was employed to explore the effect of a single passage through the microfluidic mechanical stress device. The formulations were processed through each chip geometry (weak, medium and strong) at different flow rates (50, 150, 500, 800 µl/min), corresponding to different residence times. The experimented points are reported in *table B1*.

Candidate formulation	Geometry	Flow rates (µl/min)	Shear rate intensity (s^{-1})	Effective stress exposure time (ms)
A, B, C	Weak	50	340	450
		150	1030	150
		500	3440	45
		800	5500	28
	Medium	50	500	360
		150	1500	120
		500	5000	36
		800	8000	23
	Strong	50	1250	225
		150	3750	75
		500	12500	23
		800	20000	14

Table B 1 – Experimental point tested for the formulation single passage through different mechanical stress microfluidic devices (weak, medium and strong)

As reported in plots in *figure B2*, SE-HPLC analysis did not detected any aggregation trend in tested formulations in none of the experimented conditions. The standard deviations of the reported points are in the 5% of the indicated values.

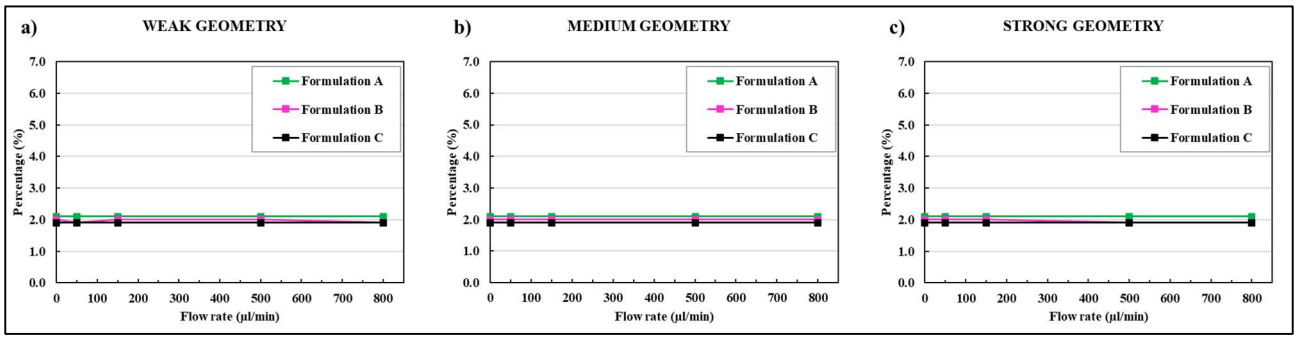

Figure B 2 – SE-HPLC analysis of formulations stimulated with a single passage through the mechanical stress microfluidic devices

B3. DLS measurement feasibility studies

Feasibility studies on the DLS measurements were conducted in order to identify optimal measurement conditions returning reliable measurement outcomes and ensuring the analytical instrument to operate in an appropriate concentration range. Different dilutions of 175 mg/ml of Bovine Serum Albumin (BSA) in PBS were prepared and analyzed according to the measurement protocol reported in chapter 4 (Material and methods, section 4.2.11). Tested conditions are reported in *table B2*.

Biomolecule	Initial concentration (mg/ml)	Dilution factor	Final concentration (mg/ml)
BSA	175	50	3,50
		250	0,70
		500	0,35
		1000	0,18

Table B 2 – Tested conditions for the feasibility study of DLS measurements

Size distributions obtained at different dilutions are reported in *figure B3*.

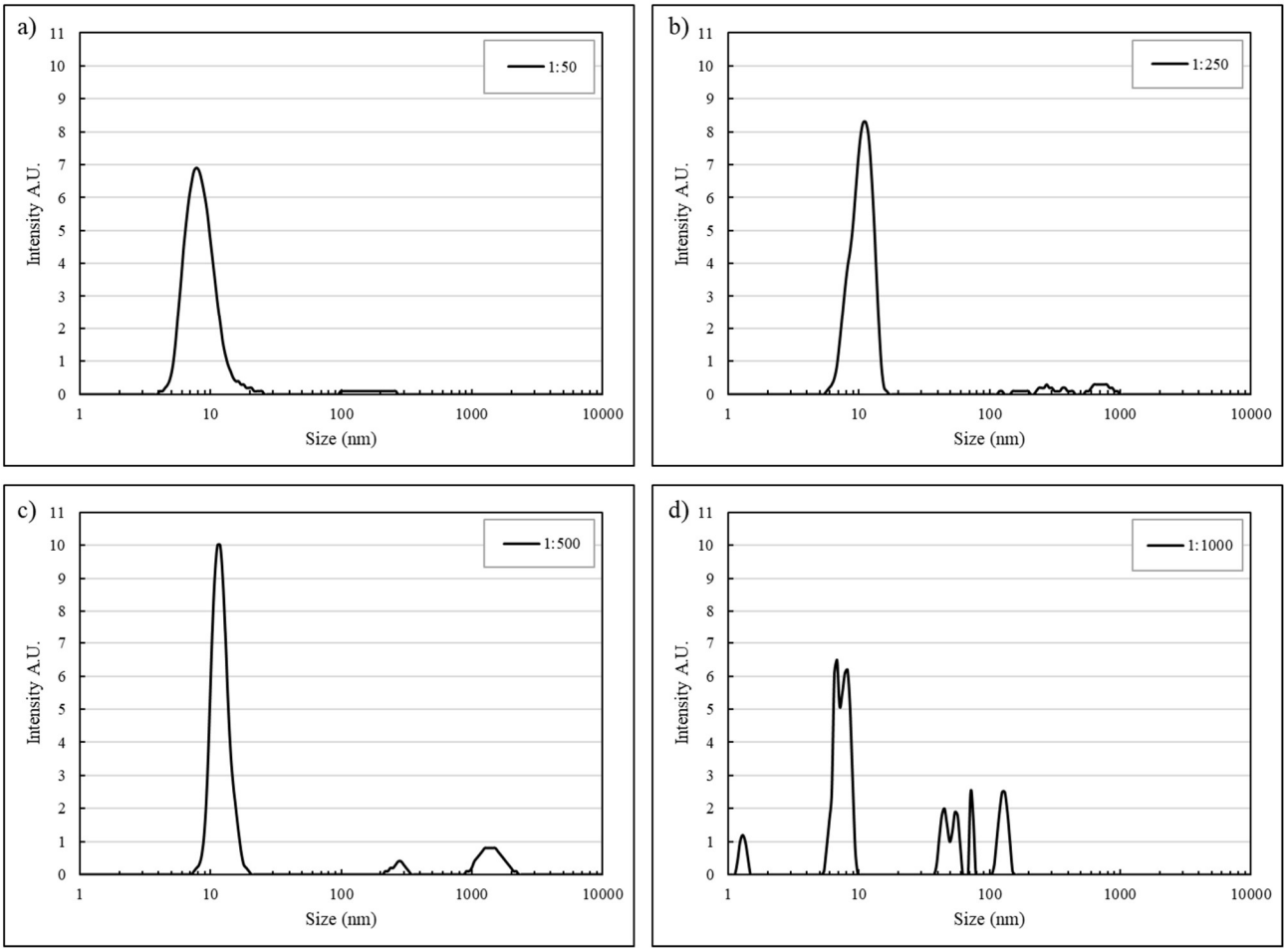

Figure B 3 – size distribution of BSA 175 mg/ml at different sample dilutions; (a) BSA 3,50 mg/ml – dilution factor 50; (b) BSA 0,70 mg/ml – dilution factor 250; (c) BSA 0,35 mg/ml – dilution factor 500; (d) BSA 0,18 mg/ml – dilution factor 1000

The need of analyzing a biomolecule under minuscule dilution is relevant not to induce modifications of the protein physical status due to changes in the solution conditions. In other words, a minimum dilution permits to avoid the occurrence of outcomes that might deviate from the real physical condition of the biomolecule. *Figure B3* demonstrates that changes in dilution factors can drastically affect the size distribution. Expected size distribution of an unstimulated stable protein would present a sharp monomeric peak centered at 5-10 nm and additional oligomeric peak(s) centered around 100-200 nm. Results reported in *figure B3* suggest that an optimal concentration range for the proteins to be analyzed can be [0,35; 3,5] mg/ml, that correspond to 50 to 500-fold dilution in the tested cases. Higher dilutions could potentially lead to unreliable distribution sizes.

B4. FTIR analysis conducted one week after the microfluidic stimulation

Treated and untreated samples were stored at 5 ± 3°C after the microfluidic stimulation in order to take an additional FTIR measurement after one week. Results, reported in *figure B4I*, confirm that the secondary structure modifications detected soon after the stimulation and described in chapter 4 (paragraph 4.3.3) are transitory phenomena.

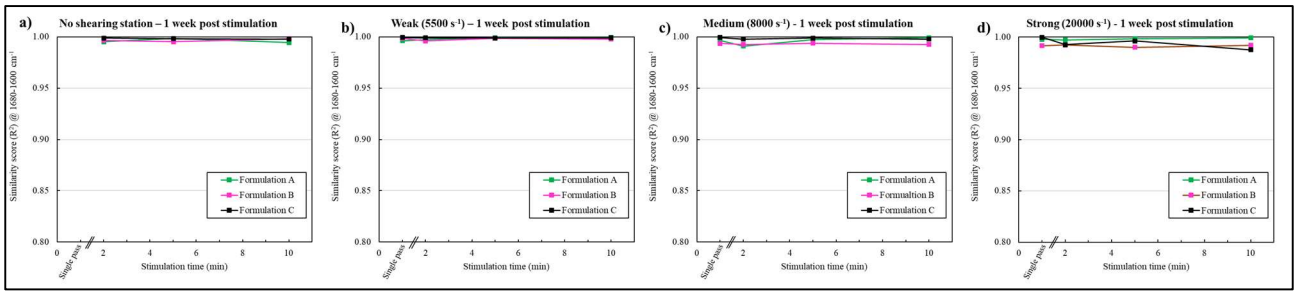

Figure B 4 – similarity score of FTIR spectra one week after the stimulation. (a) no shearing station; (b) Weak condition; (c) Medium condition; (d) Strong condition.

APPENDIX C

C1. Alternative droplet-based microfluidic approach to screen biomolecule stability in highly concentrated and viscous (HCV) systems

Ongoing project in collaboration with Dr. Eng. Samuele Fiorenza (https://www.researchgate.net/profile/Samuele-Fiorenza)

C1.1 Introduction

The microfluidics can be generally categorized into continuous and discontinuous. The former relies on monophasic fluidic context to perform different processes, such as controlled mixing [214] or particle manipulation [215]. The latter refers to the management at microscale of bubbles or droplets obtained by immiscible fluids. In particular, the discontinuous microfluidics has been largely employed for the production of highly controlled monodispersed emulsions (water in oil and vice versa) for different applications in biochemical [216], biomedical [217] and analytical fields [218]. Single droplets or bubbles generated by highly controlled microfluidic environment, can be considered as micro-batches where different physical, biological or chemical processes can be carried out. Moreover, such femto- to nano-volumetric batches can be passively or actively manipulated, stored and recovered for a wide range of applications. The scientific literature reports some examples of microfluidic platforms intended to store and, in some cases, retrieve arrays of droplets for the conduction of second-step actions or analyses [219-224]. In this framework, the droplet-based microfluidics can be employed to study biomolecules in highly concentrated and viscous (HCV) solutions (*e.g.*, biological therapeutics) exposed to external physico-chemical stimuli. Their behavior can be followed over time thanks to the possibility to store and recollect biomolecule-containing droplets. In this brief report, the feasibility study of a microfluidic process for the passive storage and recollection of droplets is described. The operational parameters (water and oil phase flow rates, composition and concentration of components etc.) are studied in order to characterize the process in terms of generated droplet size and optimal conditions for their storage and recollection. Additionally, preliminary results about the possibility to process biomolecule-loaded droplets are shown with a model protein.

C1.2 Experimental approach

A polycarbonate (PC) microfluidic chip was purchased by Microfluidic ChipShop (model Fluidic 488). The geometry, reported in *figure C1*, is intended to generate and store droplets in dedicated micro-wells. This chip was employed to generate W/O emulsions. Minera oil + Span80 1% v/v was used as continuous phase, while PBS 10 mM was employed as dispersed phase. Aiming to identify the operational window of the platform, different flow rates of continuous (from 0,6 to 32,5 µl/min - Q_{CP}) and discontinuous phase (from 0,6 to 10 µl/min – Q_{DP}) were tested and related to droplet size. These conditions returned a flow rate ratio ($FR^2 = Q_{DP}/Q_{CP}$) ranging from 0,033 to 1. Additional studies were conducted to set eligible flow rates and droplet size for the entrapment (storage) and retrieving process. Moreover, droplets were entrapped and stored at 5°C up to 1 week to study their stability over time. Bovine serum albumin (BSA) was used as model protein to preliminary test the platform with HCV solutions.

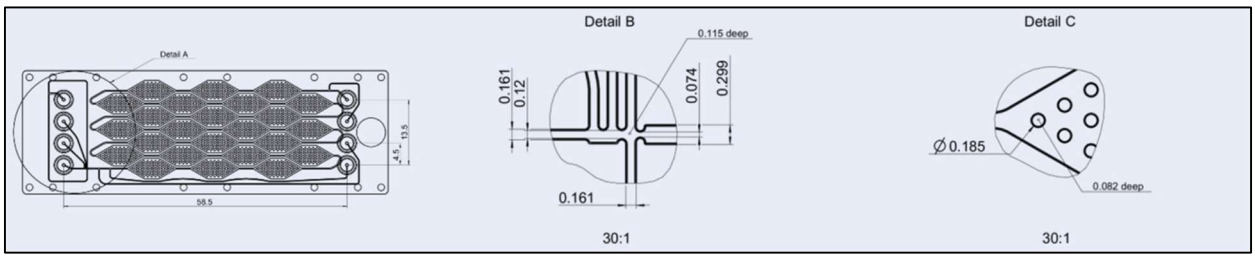

Figure C 1 – Microfluidic chip for the generation and storage of micro droplets

C1.3 Preliminary results and conclusions

Figure C2 reports the operational range of the microfluidic platform. By modulating the FR^2, the droplet size can be controlled.

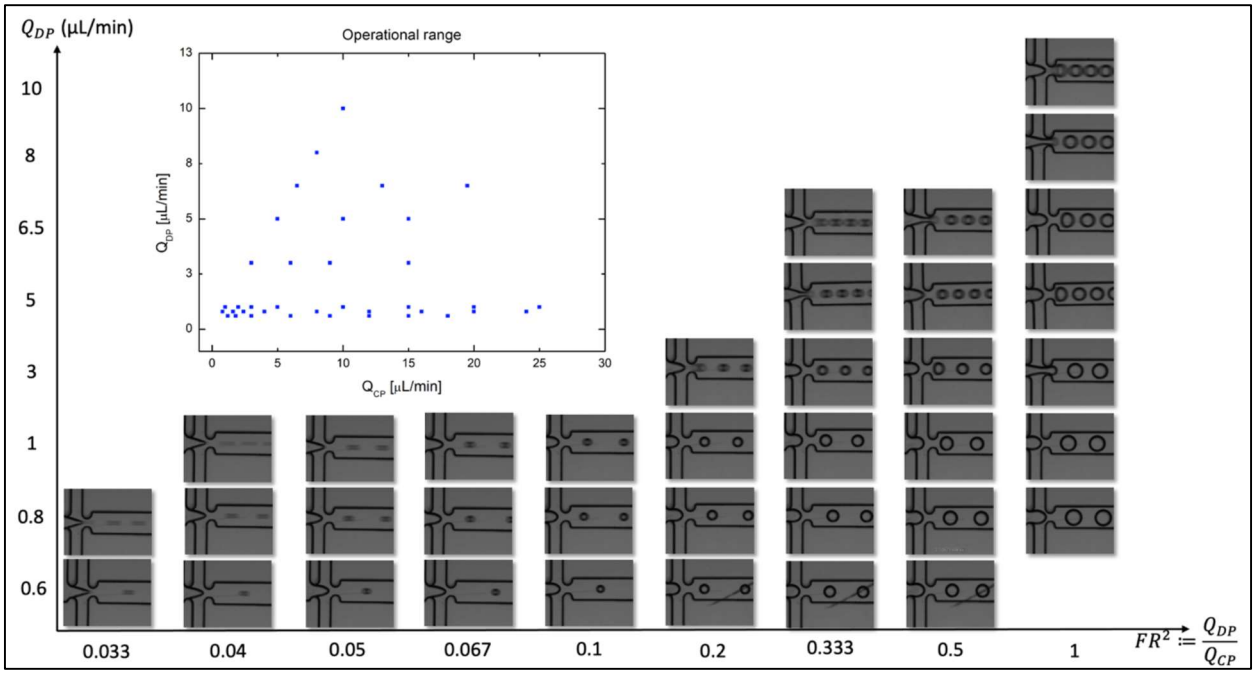

Figure C 2 – Droplet-based microfluidic platform operational window

As reported in *figure C3*, higher FR^2 corresponds to bigger droplet size. The identified operational range enables a controlled production of droplets whose mean diameter ranges from 30 to 240 µm.

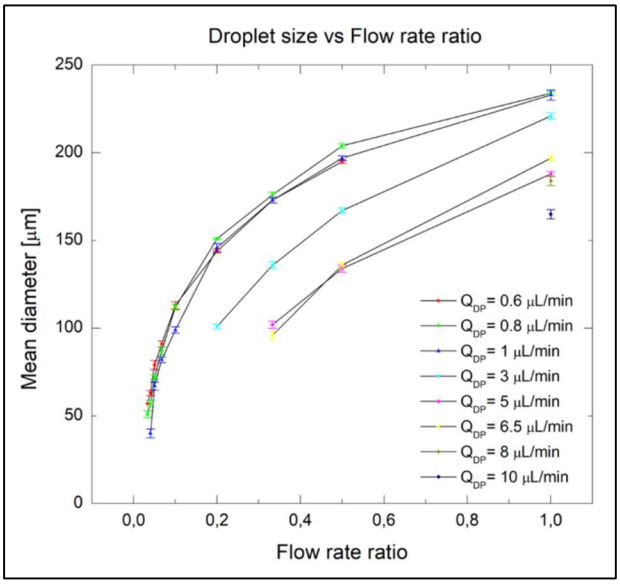

Figure C 3 – Droplet size vs flow rate ratio at different dispersed phase flow rates

The chip geometry is though to host up to 3000 droplets entrapped into cylindrical micro-wells. The entrapment efficiency (number of droplets successfully captured/number of droplets produced) is the result of a proper

combination of process flow rate and droplet size. In fact, after their production, the flow rate needs to be fine tuned in order to let the droplets engage with the micro-wells. The optimal oil phase flow rate for the droplet recruitment and the most suitable droplet size were identified to be 1,2 µl/min (Q_{CP}) and 230 µm, respectively (*figure C4a*). A close-up of a microfluidic chip section with successfully entrapped 230 µm droplets is reported in *figure C4b*.

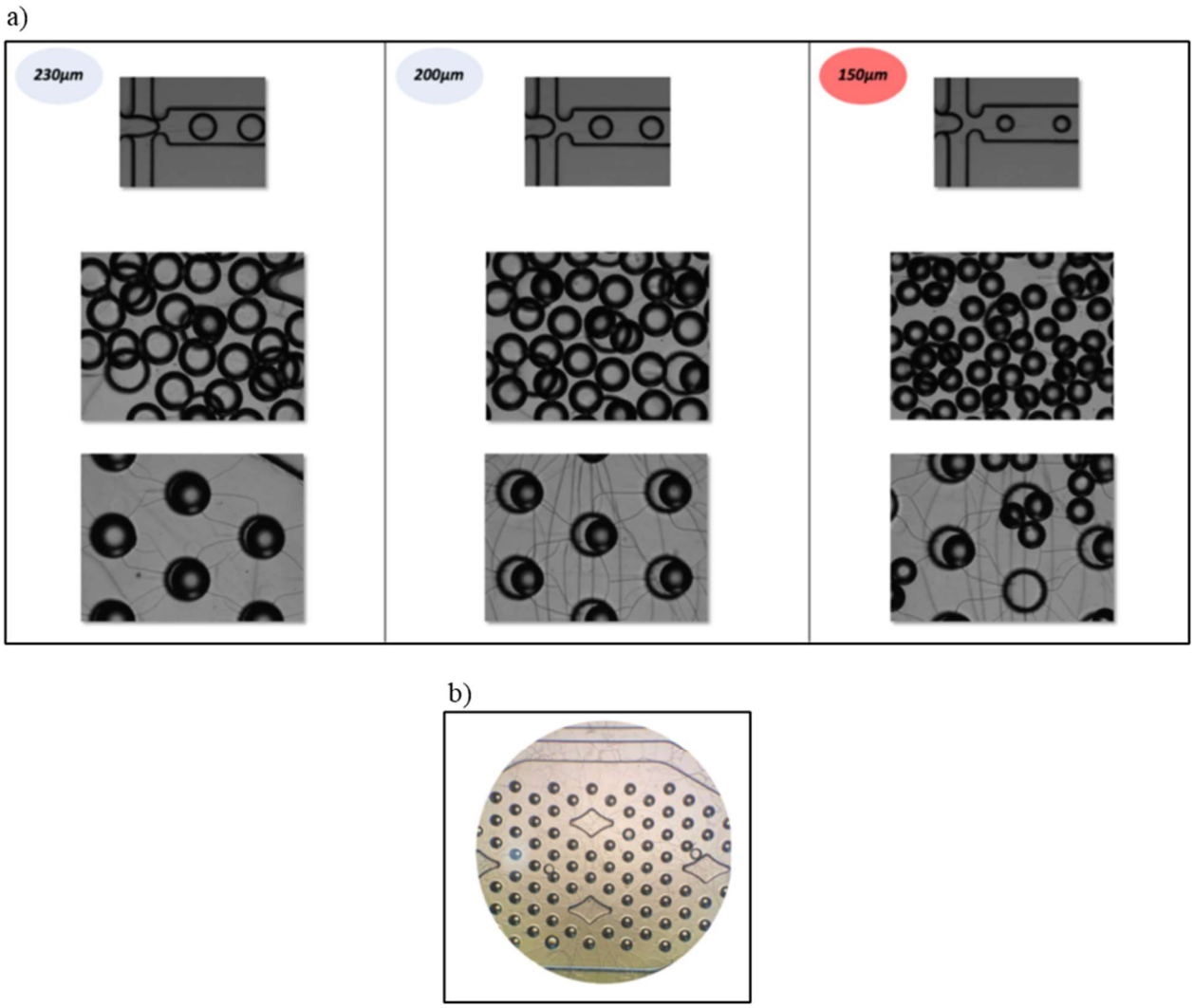

Figure C 4 – Droplet entrapment; (a) comparison among three different droplet sizes (230, 200, 150 µm). (b) closeup of a microfluidic chip section with entrapped drops

After being entrapped, the droplets were stored at 5°C up to 1 week (*figure C5*) . After 48 hours no particular instabilities could be observed. On the contrary, after 72 hours, and more prominently after 1 week of storage, an evident droplet shrinkage occurred. Additionally, *figure C5* reports that the most of the droplets exited the micro-wells after 72 hours. This might be due to the handling of the chip when moved from the fridge to the microscope for the observation. Plus, the shrinkage occurring over time can make it easier for the droplets to get out of the micro-traps.

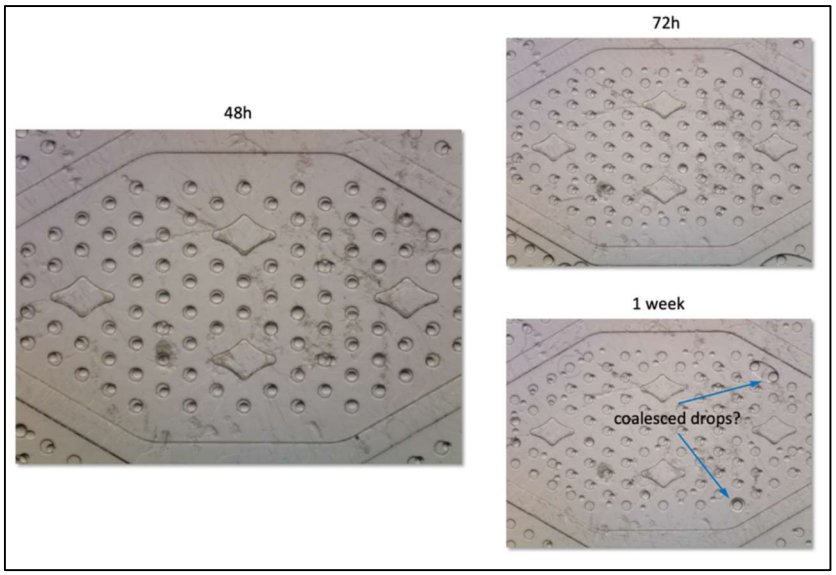

Figure C 5 – droplet stored at 5°C after 48, 72 hours and 1 week

Also, the recollection of droplet was studied by testing different flow rates in order to optimize the process. The best flow rate of the continuous phase being able to flush and orderly recollect the droplets resulted to be 30 µl/min.

Preliminary experiments were made with BSA as a model biomolecule to prove a successful droplet generation with HCV liquids. A solution of 300 mg/ml BSA in PBS was used as water phase. In this case, the droplet sizes resulted to be ≈10% smaller that those produced at same conditions with PBS for all the tested $Q_{CP} - Q_{DP}$ combinations. While the droplet generation can be finely controlled, the droplet storage with a viscous protein solution as dispersed phase was difficult to achieve due to an evident droplet tendency to coalesce (*figure C6*).

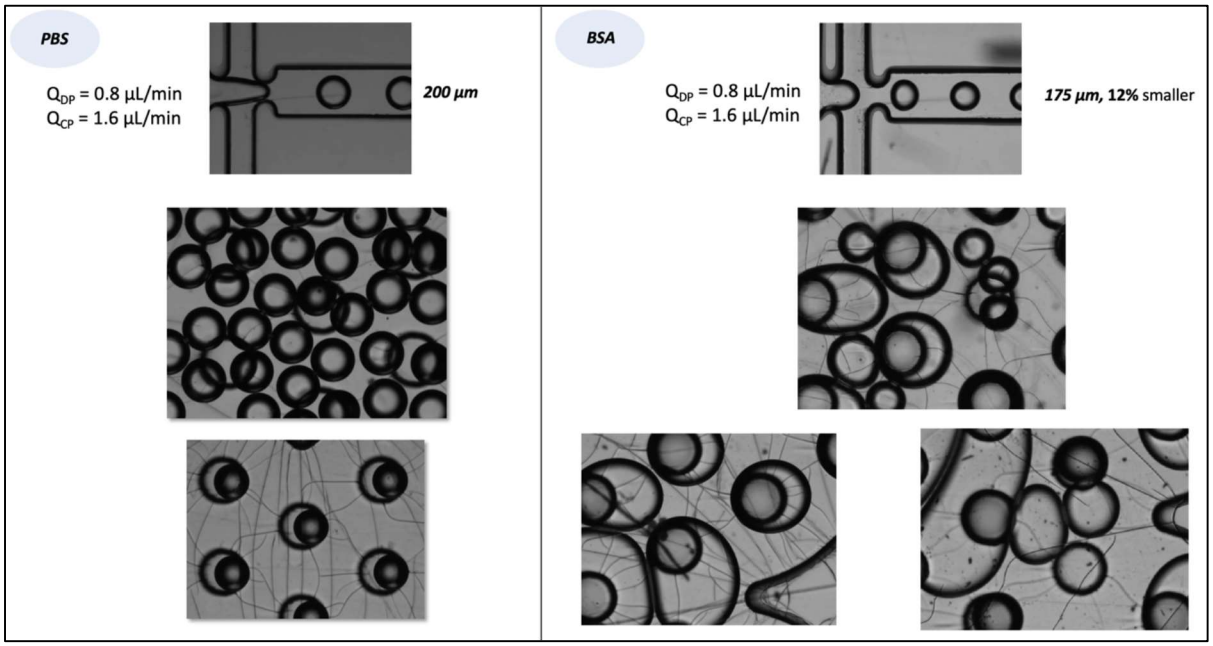

Figure C 6 – Comparison between droplet generation and storage carried out with PBS (left) and BSA 300 mg/ml (right)

Clearly, the introduction of the biomolecule determined an important impact on the thermodynamic equilibrium of the emulsion, thus requiring process fine tuning in terms of surfactant type and concentration.

Although this process poses an increased technical challenge related to the stability of the emulsion that is certainly threatened by the nature of the dispersed phase and, eventually, by the application of physical stimulation, it should be noted that the droplet-based approach could exponentially improve the throughput of the study of biomolecule stability under physico-chemical stimulations. Thousand droplets containing different solution conditions can be rapidly generated and exposed to external stimulations (*e.g.*, temperature or light). Besides ensuring a drastic saving of reagents, the possibility to store droplets for additional stimulations or analyses might further expand the potential of this approach.

References

[1] WHO, "World Healt Organization - Biologicals - https://www.who.int/health-topics/biologicals#tab=tab_1."

[2] A. Dabrowska, "Biologics and biosimilars: background and key issues," *Congressional Res Service*, pp. 27-66, 2019.

[3] P. C. a. R. P. a. D. L. a. B. N. a. J. K. a. E. M. R. a. V. N. U. a. M. N. K. a. R. Vivek, "Therapeutic monoclonal antibodies for COVID-19 management: an update," *Expert Opinion on Biological Therapy,* vol. 22, no. 6, pp. 763-780 , year = 2022.

[4] M. J. Hogan, and N. Pardi, "mRNA Vaccines in the COVID-19 Pandemic and Beyond," *Annual Review of Medicine,* vol. 73, no. 1, pp. 17-39, 2022.

[5] D. S. Dimitrov, "Therapeutic proteins," *Therapeutic Proteins: Methods and Protocols*, pp. 1-26, 2012.

[6] T. Reynolds *et al.*, "Overview of biopharmaceuticals and comparison with small-molecule drug development," *Nonclinical development of novel biologics, biosimilars, vaccines and specialty biologics*, pp. 3-33: Elsevier, 2013.

[7] C. Arturo, "Passive Antibody Therapies: Progress and Continuing Challenges," *Clinical Immunology,* vol. 93, no. 1, pp. 5-15, 1999.

[8] M. A. Keller, and E. R. Stiehm, "Passive immunity in prevention and treatment of infectious diseases," *Clinical microbiology reviews,* vol. 13, no. 4, pp. 602-614, 2000.

[9] F. G. Banting *et al.*, "Pancreatic extracts in the treatment of diabetes mellitus," *Canadian Medical Association Journal,* vol. 12, no. 3, pp. 141, 1922.

[10] B. Leader, Q. J. Baca, and D. E. Golan, "Protein therapeutics: a summary and pharmacological classification," *Nature reviews Drug discovery,* vol. 7, no. 1, pp. 21-39, 2008.

[11] A. Chakraborty *et al.*, "Protein therapeutics: an updated review," 2021.

[12] M. S. Castelli, P. McGonigle, and P. J. Hornby, "The pharmacology and therapeutic applications of monoclonal antibodies," *Pharmacology research & perspectives,* vol. 7, no. 6, pp. e00535, 2019.

[13] M. Durán-Lobato, Z. Niu, and M. J. Alonso, "Oral Delivery of Biologics for Precision Medicine," *Advanced Materials,* vol. 32, no. 13, pp. 1901935, 2020.

[14] A. Abramson *et al.*, "Oral delivery of systemic monoclonal antibodies, peptides and small molecules using gastric auto-injectors," *Nature Biotechnology,* vol. 40, no. 1, pp. 103-109, 2022/01/01, 2022.

[15] J. P. Manis. "Overview of therapeutic monoclonal antibodies," https://www.uptodate.com/contents/overview-of-therapeutic-monoclonal-antibodies/contributors.

[16] M. Joseph, H. M. Trinh, and A. K. Mitra, "Chapter 7 - Peptide and Protein-Based Therapeutic Agents∗," *Emerging Nanotechnologies for Diagnostics, Drug Delivery and Medical Devices*, A. K. Mitra, K. Cholkar and A. Mandal, eds., pp. 145-167, Boston: Elsevier, 2017.

[17] M. Ovacik, and K. Lin, "Tutorial on monoclonal antibody pharmacokinetics and its considerations in early development," *Clinical and translational science,* vol. 11, no. 6, pp. 540-552, 2018.

[18] H. H. Cai, and A. Pandit, "Therapeutic monoclonal antibodies approved by FDA in 2020," *Clin. Res. Immunol,* vol. 4, pp. 1-2, 2021.

[19] N. Chaffey, "Alberts, B., Johnson, A., Lewis, J., Raff, M., Roberts, K. and Walter, P. Molecular biology of the cell. 4th edn," Oxford University Press, 2003.

[20] A. Rosenberg, and B. Demeule, "Biobetters," 2015.

[21] M. Superson *et al.*, "Clinical application of monoclonal antibodies in targeted therapy," *European Journal of Clinical and Experimental Medicine*, no. 4, pp. 338-346, 2019.

[22] J. Ma *et al.*, "Bispecific antibodies: from research to clinical application," *Frontiers in Immunology,* vol. 12, pp. 1555, 2021.

[23] Y. Yao, Y. Hu, and F. Wang, "Trispecific antibodies for cancer immunotherapy," *Immunology*, 2023.

[24] U. Brinkmann, and R. E. Kontermann, "Bispecific antibodies," *Science,* vol. 372, no. 6545, pp. 916-917, 2021.

[25] M. Feng *et al.*, "Construction and next-generation sequencing analysis of a large phage-displayed VNAR single-domain antibody library from six naïve nurse sharks," *Antibody Therapeutics,* vol. 2, no. 1, pp. 1-11, 2018.

[26] H. Matz, and H. Dooley, "Shark IgNAR-derived binding domains as potential diagnostic and therapeutic agents," *Developmental & Comparative Immunology,* vol. 90, pp. 100-107, 2019/01/01/, 2019.
[27] J. P. Salvador, L. Vilaplana, and M. P. Marco, "Nanobody: outstanding features for diagnostic and therapeutic applications," *Analytical and Bioanalytical Chemistry,* vol. 411, no. 9, pp. 1703-1713, 2019/03/01, 2019.
[28] N. V. Bathula, H. Bommadevara, and J. M. Hayes, "Nanobodies: the future of antibody-based immune therapeutics," *Cancer biotherapy & radiopharmaceuticals,* vol. 36, no. 2, pp. 109-122, 2021.
[29] M. Liu *et al.*, "Nanobody—A versatile tool for cancer diagnosis and therapeutics," *Wiley Interdisciplinary Reviews: Nanomedicine and Nanobiotechnology,* vol. 13, no. 4, pp. e1697, 2021.
[30] E. Y. Yang, and K. Shah, "Nanobodies: next generation of cancer diagnostics and therapeutics," *Frontiers in Oncology,* vol. 10, pp. 1182, 2020.
[31] W. Jiskoot *et al.*, "Protein instability and immunogenicity: roadblocks to clinical application of injectable protein delivery systems for sustained release," *Journal of pharmaceutical sciences,* vol. 101, no. 3, pp. 946-954, 2012.
[32] D. Leipold, and S. Prabhu, "Pharmacokinetic and pharmacodynamic considerations in the design of therapeutic antibodies," *Clinical and Translational Science,* vol. 12, no. 2, pp. 130-139, 2019.
[33] R. Zaman *et al.*, "Current strategies in extending half-lives of therapeutic proteins," *Journal of Controlled Release,* vol. 301, pp. 176-189, 2019.
[34] J. Zarzar *et al.*, "High concentration formulation developability approaches and considerations." p. 2211185.
[35] N. B. Pham, and W. S. Meng, "Protein aggregation and immunogenicity of biotherapeutics," *International journal of pharmaceutics,* vol. 585, pp. 119523, 2020.
[36] F. D. Makurvet, "Biologics vs. small molecules: Drug costs and patient access," *Medicine in Drug Discovery,* vol. 9, pp. 100075, 2021/03/01/, 2021.
[37] B. Online. "Johnson & Johnson and Crucell reach agreement on intended public offer of Euro 24.75 per ordinary share of Crucell," https://www.bioprocessonline.com/doc/johnson-johnson-and-crucell-reach-agreement-0001.
[38] N. Y. Times. "How to decrease prices for an expensive class of drugs.," https://www.nytimes.com/2015/11/17/upshot/how-to-decrease-prices-for-an-expensive-class-ofdrugs.html.
[39] T. Laptoš, and J. Omersel, "The importance of handling high-value biologicals: Physico-chemical instability and immunogenicity of monoclonal antibodies," *Experimental and Therapeutic Medicine,* vol. 15, no. 4, pp. 3161-3168, 2018.
[40] R. Dingman, and S. V. Balu-Iyer, "Immunogenicity of protein pharmaceuticals," *Journal of pharmaceutical sciences,* vol. 108, no. 5, pp. 1637-1654, 2019.
[41] P. J. Brennan *et al.*, "Hypersensitivity reactions to mAbs: 105 desensitizations in 23 patients, from evaluation to treatment," *Journal of Allergy and Clinical Immunology,* vol. 124, no. 6, pp. 1259-1266, 2009/12/01/, 2009.
[42] G. A. C. Isabwe *et al.*, "Hypersensitivity reactions to therapeutic monoclonal antibodies: phenotypes and endotypes," *Journal of Allergy and Clinical Immunology,* vol. 142, no. 1, pp. 159-170. e2, 2018.
[43] B. Buelow, and J. Routes, "Immediate Hypersenstivity Reactions," *Retrieved. Disponível em http://emedicine. medscape. com/article/136217-overview# showall. Acedido em,* vol. 25, 2015.
[44] A. M. G. Cochrane *et al.*, "ANTIBODY-DEPENDENT CELL-MEDIATED (K CELL) CYTOTOXICITY AGAINST ISOLATED HEPATOCYTES IN CHRONIC ACTIVE HEPATITIS," *The Lancet,* vol. 307, no. 7957, pp. 441-444, 1976/02/28/, 1976.
[45] H. Z. Movat, "Inflammation, immunity, and hypersensitivity: cellular and molecular mechanisms," *(No Title)*, 1979.
[46] C. A. Janeway Jr *et al.*, "B-cell activation by armed helper T cells," *Immunobiology: The Immune System in Health and Disease. 5th edition*: Garland Science, 2001.
[47] M. Haniffa, M. Gunawan, and L. Jardine, "Human skin dendritic cells in health and disease," *Journal of Dermatological Science,* vol. 77, no. 2, pp. 85-92, 2015/02/01/, 2015.
[48] E. Segura *et al.*, "Characterization of resident and migratory dendritic cells in human lymph nodes," *Journal of Experimental Medicine,* vol. 209, no. 4, pp. 653-660, 2012.
[49] C. Ross *et al.*, "Immunogenicity of interferon-β in multiple sclerosis patients: Influence of preparation, dosage, dose frequency, and route of administration," *Annals of neurology,* vol. 48, no. 5, pp. 706-712, 2000.

[50] M. M. Van Beers, and M. Bardor, "Minimizing immunogenicity of biopharmaceuticals by controlling critical quality attributes of proteins," *Biotechnology journal,* vol. 7, no. 12, pp. 1473-1484, 2012.
[51] E. M. Moussa *et al.*, "Immunogenicity of therapeutic protein aggregates," *Journal of pharmaceutical sciences,* vol. 105, no. 2, pp. 417-430, 2016.
[52] C. Thorlaksen *et al.*, "In vitro and in vivo immunogenicity assessment of protein aggregate characteristics," *International Journal of Pharmaceutics,* vol. 631, pp. 122490, 2023/01/25/, 2023.
[53] E. Szomolanyi-Tsuda, and R. M. Welsh, "T-cell-independent antiviral antibody responses," *Current Opinion in Immunology,* vol. 10, no. 4, pp. 431-435, 1998/08/01/, 1998.
[54] J. S. Rudra *et al.*, "Immune responses to coiled coil supramolecular biomaterials," *Biomaterials,* vol. 31, no. 32, pp. 8475-8483, 2010/11/01/, 2010.
[55] B. J. Andrick *et al.*, "Predicting Hemagglutinin MHC-II Ligand Analogues in Anti-TNFα Biologics: Implications for Immunogenicity of Pharmaceutical Proteins," *PloS one,* vol. 10, no. 8, pp. e0135451, 2015.
[56] C. J. Roberts, "Therapeutic protein aggregation: mechanisms, design, and control," *Trends in biotechnology,* vol. 32, no. 7, pp. 372-380, 2014.
[57] J. C. Bischof, and X. He, "Thermal stability of proteins," *Annals of the New York Academy of Sciences,* vol. 1066, no. 1, pp. 12-33, 2006.
[58] A. Karshikoff, L. Nilsson, and R. Ladenstein, "Rigidity versus flexibility: the dilemma of understanding protein thermal stability," *The FEBS journal,* vol. 282, no. 20, pp. 3899-3917, 2015.
[59] P. L. Privalov, "Stability of proteins small globular proteins," *Advances in protein chemistry,* vol. 33, pp. 167-241, 1979.
[60] W. J. Becktel, and J. A. Schellman, "Protein stability curves," *Biopolymers: Original Research on Biomolecules,* vol. 26, no. 11, pp. 1859-1877, 1987.
[61] N. V. Prabhu, and K. A. Sharp, "Heat capacity in proteins," *Annu. Rev. Phys. Chem.,* vol. 56, pp. 521-548, 2005.
[62] F. Pucci, and M. Rooman, "Physical and molecular bases of protein thermal stability and cold adaptation," *Current opinion in structural biology,* vol. 42, pp. 117-128, 2017.
[63] P. L. Privalov, and S. J. Gill, "Stability of protein structure and hydrophobic interaction," *Advances in protein chemistry,* vol. 39, pp. 191-234, 1988.
[64] D. C. Rees, and A. D. Robertson, "Some thermodynamic implications for the thermostability of proteins," *Protein Science,* vol. 10, no. 6, pp. 1187-1194, 2001.
[65] A. W. Vermeer, and W. Norde, "The thermal stability of immunoglobulin: unfolding and aggregation of a multi-domain protein," *Biophysical journal,* vol. 78, no. 1, pp. 394-404, 2000.
[66] A. W. Vermeer, W. Norde, and A. van Amerongen, "The unfolding/denaturation of immunogammaglobulin of isotype 2b and its Fab and Fc fragments," *Biophysical journal,* vol. 79, no. 4, pp. 2150-2154, 2000.
[67] J. Seelig, and H.-J. Schönfeld, "Thermal protein unfolding by differential scanning calorimetry and circular dichroism spectroscopy Two-state model versus sequential unfolding," *Quarterly Reviews of Biophysics,* vol. 49, pp. e9, 2016.
[68] J. Seelig, and A. Seelig, "Molecular understanding of calorimetric protein unfolding experiments," *Biophysical Reports,* vol. 2, no. 1, pp. 100037, 2022/03/09/, 2022.
[69] A. Quigley, and D. R. Williams, "The second virial coefficient as a predictor of protein aggregation propensity: A self-interaction chromatography study," *European Journal of Pharmaceutics and Biopharmaceutics,* vol. 96, pp. 282-290, 2015/10/01/, 2015.
[70] D. Roberts *et al.*, "The Role of Electrostatics in Protein–Protein Interactions of a Monoclonal Antibody," *Molecular Pharmaceutics,* vol. 11, no. 7, pp. 2475-2489, 2014/07/07, 2014.
[71] J. Stetefeld, S. A. McKenna, and T. R. Patel, "Dynamic light scattering: a practical guide and applications in biomedical sciences," *Biophysical Reviews,* vol. 8, no. 4, pp. 409-427, 2016/12/01, 2016.
[72] A. Y. Xu *et al.*, "Studying Excipient Modulated Physical Stability and Viscosity of Monoclonal Antibody Formulations Using Small-Angle Scattering," *Molecular Pharmaceutics,* vol. 16, no. 10, pp. 4319-4338, 2019/10/07, 2019.
[73] A. Quigley *et al.*, "The accurate measurement of second virial coefficients using self-interaction chromatography: experimental considerations," *European Journal of Pharmaceutics and Biopharmaceutics,* vol. 85, no. 3, pp. 1103-1111, 2013.

[74] N. Sibanda, R. K. Shanmugam, and R. Curtis, "The Relationship between Protein–Protein Interactions and Liquid–Liquid Phase Separation for Monoclonal Antibodies," *Molecular Pharmaceutics,* vol. 20, no. 5, pp. 2662-2674, 2023/05/01, 2023.
[75] G. M. Ferreira *et al.*, "Identifying key residues that drive strong electrostatic attractions between therapeutic antibodies," *The Journal of Physical Chemistry B,* vol. 123, no. 50, pp. 10642-10653, 2019.
[76] P. D. Ross, and S. Subramanian, "Thermodynamics of protein association reactions: forces contributing to stability," *Biochemistry,* vol. 20, no. 11, pp. 3096-3102, 1981/05/01, 1981.
[77] W. Wang, S. Nema, and D. Teagarden, "Protein aggregation—pathways and influencing factors," *International journal of pharmaceutics,* vol. 390, no. 2, pp. 89-99, 2010.
[78] J. S. Philo, and T. Arakawa, "Mechanisms of protein aggregation," *Current pharmaceutical biotechnology,* vol. 10, no. 4, pp. 348-351, 2009.
[79] W. Wang, and C. J. Roberts, "Protein aggregation–mechanisms, detection, and control," *International journal of pharmaceutics,* vol. 550, no. 1-2, pp. 251-268, 2018.
[80] G. V. Barnett *et al.*, "Aggregate structure, morphology and the effect of aggregation mechanisms on viscosity at elevated protein concentrations," *Biophysical Chemistry,* vol. 207, pp. 21-29, 2015.
[81] A. M. Morris, M. A. Watzky, and R. G. Finke, "Protein aggregation kinetics, mechanism, and curve-fitting: A review of the literature," *Biochimica et Biophysica Acta (BBA) - Proteins and Proteomics,* vol. 1794, no. 3, pp. 375-397, 2009/03/01/, 2009.
[82] L. Nicoud *et al.*, "A multiscale view of therapeutic protein aggregation: a colloid science perspective," *Biotechnology journal,* vol. 10, no. 3, pp. 367-378, 2015.
[83] M. A. Watzky, and R. G. Finke, "Transition Metal Nanocluster Formation Kinetic and Mechanistic Studies. A New Mechanism When Hydrogen Is the Reductant: Slow, Continuous Nucleation and Fast Autocatalytic Surface Growth," *Journal of the American Chemical Society,* vol. 119, no. 43, pp. 10382-10400, 1997/10/01, 1997.
[84] J. Arora *et al.*, "Charge-mediated Fab-Fc interactions in an IgG1 antibody induce reversible self-association, cluster formation, and elevated viscosity." pp. 1561-1574.
[85] R. Esfandiary *et al.*, "Mechanism of reversible self-association of a monoclonal antibody: role of electrostatic and hydrophobic interactions," *Journal of pharmaceutical sciences,* vol. 104, no. 2, pp. 577-586, 2015.
[86] C. J. Roberts, "Protein aggregation and its impact on product quality," *Current opinion in biotechnology,* vol. 30, pp. 211-217, 2014.
[87] S. J. Shire *et al.*, *Current trends in monoclonal antibody development and manufacturing*: Springer Science & Business Media, 2009.
[88] D. Rodrigues *et al.*, "Product-specific impact of viscosity modulating formulation excipients during ultra-high concentration biotherapeutics drug product development," *Journal of Pharmaceutical Sciences,* vol. 110, no. 3, pp. 1077-1082, 2021.
[89] M. A. Blanco *et al.*, "Protein–Protein Interactions in Dilute to Concentrated Solutions: α-Chymotrypsinogen in Acidic Conditions," *The Journal of Physical Chemistry B,* vol. 118, no. 22, pp. 5817-5831, 2014/06/05, 2014.
[90] Lea L. Sorret *et al.*, "Challenges in Predicting Protein-Protein Interactions from Measurements of Molecular Diffusivity," *Biophysical Journal,* vol. 111, no. 9, pp. 1831-1842, 2016/11/01/, 2016.
[91] J. Liu *et al.*, "Reversible Self-Association Increases the Viscosity of a Concentrated Monoclonal Antibody in Aqueous Solution," *Journal of Pharmaceutical Sciences,* vol. 94, no. 9, pp. 1928-1940, 2005/09/01/, 2005.
[92] Eric J. Yearley *et al.*, "Observation of Small Cluster Formation in Concentrated Monoclonal Antibody Solutions and Its Implications to Solution Viscosity," *Biophysical Journal,* vol. 106, no. 8, pp. 1763-1770, 2014/04/15/, 2014.
[93] L. Li *et al.*, "Concentration Dependent Viscosity of Monoclonal Antibody Solutions: Explaining Experimental Behavior in Terms of Molecular Properties," *Pharmaceutical Research,* vol. 31, no. 11, pp. 3161-3178, 2014/11/01, 2014.
[94] J. J. Hung *et al.*, "Protein–Protein Interactions of Highly Concentrated Monoclonal Antibody Solutions via Static Light Scattering and Influence on the Viscosity," *The Journal of Physical Chemistry B,* vol. 123, no. 4, pp. 739-755, 2019/01/31, 2019.
[95] S. Hanslip *et al.*, "Syringe Filling of High-Concentration mAb Formulation: Slow Suck-Back Pump Speed Prevented Filling Needle Clogging," *Journal of Pharmaceutical Sciences,* vol. 106, no. 12, pp. 3651-3653, 2017/12/01/, 2017.

[96] M. A. Miller *et al.*, "Low Viscosity Highly Concentrated Injectable Nonaqueous Suspensions of Lysozyme Microparticles," *Langmuir,* vol. 26, no. 2, pp. 1067-1074, 2010/01/19, 2010.
[97] W. Wang, and S. Ohtake, "Science and art of protein formulation development," *International journal of pharmaceutics,* vol. 568, pp. 118505, 2019.
[98] B. Barz, and B. Urbanc, "Minimal Model of Self-Assembly: Emergence of Diversity and Complexity," *The Journal of Physical Chemistry B,* vol. 118, no. 14, pp. 3761-3770, 2014/04/10, 2014.
[99] G. Meric, A. S. Robinson, and C. J. Roberts, "Driving forces for nonnative protein aggregation and approaches to predict aggregation-prone regions," *Annual review of chemical and biomolecular engineering,* vol. 8, pp. 139-159, 2017.
[100] L. Galm, S. Amrhein, and J. Hubbuch, "Predictive approach for protein aggregation: Correlation of protein surface characteristics and conformational flexibility to protein aggregation propensity," *Biotechnology and bioengineering,* vol. 114, no. 6, pp. 1170-1183, 2017.
[101] E. Sahin *et al.*, "Aggregation and pH–Temperature Phase Behavior for Aggregates of an IgG2 Antibody," *Journal of Pharmaceutical Sciences,* vol. 101, no. 5, pp. 1678-1687, 2012/05/01/, 2012.
[102] L. Zhang *et al.*, "Phase Behavior of an Fc-Fusion Protein Reveals Generic Patterns of Ion-Specific Perturbation on Protein-Protein Interactions," *Journal of Pharmaceutical Sciences,* vol. 106, no. 11, pp. 3287-3292, 2017/11/01/, 2017.
[103] A. K. Buell *et al.*, "Electrostatic Effects in Filamentous Protein Aggregation," *Biophysical Journal,* vol. 104, no. 5, pp. 1116-1126, 2013/03/05/, 2013.
[104] P. Arosio *et al.*, "On the role of salt type and concentration on the stability behavior of a monoclonal antibody solution," *Biophysical Chemistry,* vol. 168-169, pp. 19-27, 2012/07/01/, 2012.
[105] G. Wu *et al.*, "Elucidating the weak protein-protein interaction mechanisms behind the liquid-liquid phase separation of a mAb solution by different types of additives," *European Journal of Pharmaceutics and Biopharmaceutics,* vol. 120, pp. 1-8, 2017/11/01/, 2017.
[106] J. Li *et al.*, "Interfacial stress in the development of biologics: fundamental understanding, current practice, and future perspective," *The AAPS journal,* vol. 21, no. 3, pp. 1-17, 2019.
[107] L. O. Narhi *et al.*, "Stress Factors in Primary Packaging, Transportation and Handling of Protein Drug Products and Their Impact on Product Quality," *Journal of Pharmaceutical Sciences,* vol. 111, no. 4, pp. 887-902, 2022/04/01/, 2022.
[108] T. K. Das *et al.*, "Stress factors in protein drug product manufacturing and their impact on product quality," *Journal of Pharmaceutical Sciences,* vol. 111, no. 4, pp. 868-886, 2022.
[109] H. Tim Dreckmann and Julien Boeuf and Imke-Sonja Ludwig and Jörg Lümkemann and Jörg, "Low volume aseptic filling: Impact of pump systems on shear stress," *European Journal of Pharmaceutics and Biopharmaceutics,* vol. 147, pp. 10-18, 2020.
[110] L. Brückl *et al.*, "The effect of shear on the structural conformation of rhGH and IgG1 in free solution," *Journal of Pharmaceutical Sciences,* vol. 105, no. 6, pp. 1810-1818, 2016.
[111] K. Uesugi *et al.*, "Mechanisms of ultrasonically induced fibrillation of amyloid β1–40 peptides," *Japanese Journal of Applied Physics,* vol. 52, no. 7S, pp. 07HE10, 2013.
[112] E. Koepf *et al.*, "Notorious but not understood: How liquid-air interfacial stress triggers protein aggregation," *International Journal of Pharmaceutics,* vol. 537, no. 1, pp. 202-212, 2018/02/15/, 2018.
[113] M. Duerkop *et al.*, "Impact of cavitation, high shear stress and air/liquid interfaces on protein aggregation," *Biotechnology journal,* vol. 13, no. 7, pp. 1800062, 2018.
[114] T. Maruno *et al.*, "Sweeping of Adsorbed Therapeutic Protein on Prefillable Syringes Promotes Micron Aggregate Generation," *Journal of Pharmaceutical Sciences,* vol. 107, no. 6, pp. 1521-1529, 2018/06/01/, 2018.
[115] S. J. Kapp *et al.*, "Competitive Adsorption of Monoclonal Antibodies and Nonionic Surfactants at Solid Hydrophobic Surfaces," *Journal of Pharmaceutical Sciences,* vol. 104, no. 2, pp. 593-601, 2015/02/01/, 2015.
[116] M. Hoehne *et al.*, "Adsorption of Monoclonal Antibodies to Glass Microparticles," *Journal of Pharmaceutical Sciences,* vol. 100, no. 1, pp. 123-132, 2011/01/01/, 2011.
[117] C. K. Kalonia *et al.*, "Protein Adsorption and Layer Formation at the Stainless Steel–Solution Interface Mediates Shear-Induced Particle Formation for an IgG1 Monoclonal Antibody," *Molecular Pharmaceutics,* vol. 15, no. 3, pp. 1319-1331, 2018/03/05, 2018.
[118] A. Allmendinger *et al.*, "Sterile filtration of highly concentrated protein formulations: impact of protein concentration, formulation composition, and filter material," *Journal of pharmaceutical sciences,* vol. 104, no. 10, pp. 3319-3329, 2015.

[119] S. Zheng *et al.*, "Particle characterization for a protein drug product stored in pre-filled syringes using micro-flow imaging, Archimedes, and quartz crystal microbalance with dissipation," *The AAPS journal,* vol. 19, pp. 110-116, 2017.
[120] I. Ahmad *et al.*, "Photostability and photostabilization of drugs and drug products," *International Journal of Photoenergy,* vol. 2016, 2016.
[121] C. Du *et al.*, "Protection of therapeutic antibodies from visible light induced degradation: Use safe light in manufacturing and storage," *European Journal of Pharmaceutics and Biopharmaceutics,* vol. 127, pp. 37-43, 2018/06/01/, 2018.
[122] A. Sreedhara *et al.*, "Effect of ambient light on IgG1 monoclonal antibodies during drug product processing and development," *European Journal of Pharmaceutics and Biopharmaceutics,* vol. 100, pp. 38-46, 2016/03/01/, 2016.
[123] S. Ohtake, Y. Kita, and T. Arakawa, "Interactions of formulation excipients with proteins in solution and in the dried state," *Advanced drug delivery reviews,* vol. 63, no. 13, pp. 1053-1073, 2011.
[124] J. L. Milner, D. J. McClellan, and J. M. Wood, "Factors reducing and promoting the effectiveness of proline as an osmoprotectant in Escherichia coli K12," *Journal of general microbiology,* vol. 133, no. 7, pp. 1851-1860, 1987.
[125] P. H. Yancey *et al.*, "Living with water stress: evolution of osmolyte systems," *Science,* vol. 217, no. 4566, pp. 1214-1222, 1982.
[126] A. C. Miklos *et al.*, "Volume exclusion and soft interaction effects on protein stability under crowded conditions," *Biochemistry,* vol. 49, no. 33, pp. 6984-6991, 2010.
[127] S. Jordan, J. S. Katz, and B. Yezer, "Excipients: Characterization, Purpose, and Selection," *Protein Instability at Interfaces During Drug Product Development: Fundamental Understanding, Evaluation, and Mitigation*, pp. 249-269, 2021.
[128] H. J. Lee *et al.*, "Molecular origins of surfactant-mediated stabilization of protein drugs," *Advanced drug delivery reviews,* vol. 63, no. 13, pp. 1160-1171, 2011.
[129] K. L. Zapadka *et al.*, "Factors affecting the physical stability (aggregation) of peptide therapeutics," *Interface focus,* vol. 7, no. 6, pp. 20170030, 2017.
[130] T. J. Kamerzell *et al.*, "Protein–excipient interactions: Mechanisms and biophysical characterization applied to protein formulation development," *Advanced Drug Delivery Reviews,* vol. 63, no. 13, pp. 1118-1159, 2011/10/01/, 2011.
[131] W. Wang, "Instability, stabilization, and formulation of liquid protein pharmaceuticals," *International Journal of Pharmaceutics,* vol. 185, no. 2, pp. 129-188, 1999/08/20/, 1999.
[132] ICH. " International Council for Harmonisation of Technical Requirements for Pharmaceuticals for Human Use," https://www.ich.org/page/ich-guidelines.
[133] ICH. "Quality Guidlines," https://www.ich.org/page/quality-guidelines.
[134] A. Hawe *et al.*, "Forced degradation of therapeutic proteins," *Journal of pharmaceutical sciences,* vol. 101, no. 3, pp. 895-913, 2012.
[135] C. Nowak *et al.*, "Forced degradation of recombinant monoclonal antibodies: A practical guide." pp. 1217-1230.
[136] ICH. "Q1B - Photostability testing of new active substances and medicinal products," https://www.ema.europa.eu/en/ich-q1b-photostability-testing-new-active-substances-medicinal-products-scientific-guideline.
[137] S. Venkataraman, and M. Manasa, "Forced degradation studies: Regulatory guidance, characterization of drugs, and their degradation products-a review," *Drug Invention Today,* vol. 10, no. 2, 2018.
[138] K. C. Waterman, and R. C. Adami, "Accelerated aging: prediction of chemical stability of pharmaceuticals," *International Journal of Pharmaceutics,* vol. 293, no. 1-2, pp. 101-125, 2005.
[139] D. Kuzman *et al.*, "Long-term stability predictions of therapeutic monoclonal antibodies in solution using Arrhenius-based kinetics," *Scientific reports,* vol. 11, no. 1, pp. 20534, 2021.
[140] W. Wang, and C. J. Roberts, "Non-Arrhenius protein aggregation," *The AAPS journal,* vol. 15, pp. 840-851, 2013.
[141] M. Mosharraf *et al.*, "Automated and Rapid Methods to Assess Quality & Stability of Biologics: Recent Developments and Practical Ways to Implement Them in Formulation Development, American," *American Pharmaceutical Review,* vol. 19, 09/30, 2016.
[142] D. S. Goldberg *et al.*, "Utility of high throughput screening techniques to predict stability of monoclonal antibody formulations during early stage development," *Journal of Pharmaceutical Sciences,* vol. 106, no. 8, pp. 1971-1977, 2017.

[143] J. S. Philo, “A critical review of methods for size characterization of non-particulate protein aggregates,” *Current pharmaceutical biotechnology,* vol. 10, no. 4, pp. 359-372, 2009.
[144] V. Filipe *et al.*, “Analytical approaches to assess the degradation of therapeutic proteins,” *TrAC Trends in Analytical Chemistry,* vol. 49, pp. 118-125, 2013.
[145] S. Zölls *et al.*, “Particles in therapeutic protein formulations, Part 1: overview of analytical methods,” *Journal of pharmaceutical sciences,* vol. 101, no. 3, pp. 914-935, 2012.
[146] J. Gross-Rother *et al.*, “Particle Detection and Characterization for Biopharmaceutical Applications: Current Principles of Established and Alternative Techniques,” *Pharmaceutics,* vol. 12, no. 11, pp. 1112, 2020.
[147] B. Bobály, E. Sipkó, and J. Fekete, “Challenges in liquid chromatographic characterization of proteins,” *Journal of Chromatography B,* vol. 1032, pp. 3-22, 2016.
[148] E. Menditto *et al.*, “Patient Centric Pharmaceutical Drug Product Design—The Impact on Medication Adherence,” *Pharmaceutics,* vol. 12, no. 1, pp. 44, 2020.
[149] W. Wang *et al.*, “Immunogenicity of protein aggregates—Concerns and realities,” *International Journal of Pharmaceutics,* vol. 431, no. 1, pp. 1-11, 2012/07/15/, 2012.
[150] V. I. Razinkov, M. J. Treuheit, and G. W. Becker, “Accelerated formulation development of monoclonal antibodies (mAbs) and mAb-based modalities: review of methods and tools,” *Journal of biomolecular screening,* vol. 20, no. 4, pp. 468-483, 2015.
[151] Q. Chai *et al.*, "Development of a high-throughput solubility screening assay for use in antibody discovery." pp. 747-756.
[152] Y. Wei *et al.*, “Chapter 7: An Empirical Phase Diagram: High-Throughput Screening Approach to the Characterization and Formulation of Biopharmaceuticals,” *Development of Biopharmaceutical Drug-Device Products*, pp. 139-185, 2020.
[153] P. M. Ihnat *et al.*, “Chapter 6: high-throughput conformational and colloidal stability screening of biologic molecules,” *Development of Biopharmaceutical Drug-Device Products*, pp. 117-138, 2020.
[154] R. Chaudhuri *et al.*, “High-throughput biophysical analysis of protein therapeutics to examine interrelationships between aggregate formation and conformational stability,” *The AAPS journal,* vol. 16, pp. 48-64, 2014.
[155] J. Charmet, P. Arosio, and T. P. Knowles, “Microfluidics for protein biophysics,” *Journal of molecular biology,* vol. 430, no. 5, pp. 565-580, 2018.
[156] M. R. Kopp, and P. Arosio, “Microfluidic approaches for the characterization of therapeutic proteins,” *Journal of pharmaceutical sciences,* vol. 107, no. 5, pp. 1228-1236, 2018.
[157] S. Gupta, W. S. Wang, and S. A. Vanapalli, “Microfluidic viscometers for shear rheology of complex fluids and biofluids,” *Biomicrofluidics,* vol. 10, no. 4, 2016.
[158] S. D. Hudson *et al.*, “A Microliter Capillary Rheometer for Characterization of Protein Solutions,” *Journal of Pharmaceutical Sciences,* vol. 104, no. 2, pp. 678-685, 2015/02/01/, 2015.
[159] M. Zidar *et al.*, “Control of viscosity in biopharmaceutical protein formulations,” *Journal of Colloid and Interface Science,* vol. 580, pp. 308-317, 2020/11/15/, 2020.
[160] D. Yang *et al.*, “Droplet-Based Microfluidic Tool to Quantify Viscosity of Concentrating Protein Solutions,” *Pharmaceutical Research,* vol. 38, no. 10, pp. 1765-1775, 2021/10/01, 2021.
[161] N. A. Erkamp *et al.*, “Multidimensional Protein Solubility Optimization with an Ultrahigh-Throughput Microfluidic Platform,” *Analytical Chemistry,* vol. 95, no. 12, pp. 5362-5368, 2023/03/28, 2023.
[162] M. R. G. Kopp *et al.*, “Microfluidic Shrinking Droplet Concentrator for Analyte Detection and Phase Separation of Protein Solutions,” *Analytical Chemistry,* vol. 92, no. 8, pp. 5803-5812, 2020/04/21, 2020.
[163] N. Pham *et al.*, “Coupling High Throughput Microfluidics and Small-Angle X-ray Scattering to Study Protein Crystallization from Solution,” *Analytical Chemistry,* vol. 89, no. 4, pp. 2282-2287, 2017/02/21, 2017.
[164] P. Arosio *et al.*, “Microfluidic Diffusion Analysis of the Sizes and Interactions of Proteins under Native Solution Conditions,” *ACS Nano,* vol. 10, no. 1, pp. 333-341, 2016/01/26, 2016.
[165] F. A. Vicente *et al.*, “Separation and purification of biomacromolecules based on microfluidics,” *Green chemistry,* vol. 22, no. 14, pp. 4391-4410, 2020.
[166] J. Q. Xia, and L. Zhang, *Capillary electrophoresis-mass spectrometry: therapeutic protein characterization*: Springer, 2016.
[167] X. Yang *et al.*, “A novel microfluidic system for the rapid analysis of protein thermal stability,” *Analyst,* vol. 139, no. 11, pp. 2683-2686, 2014.

[168] C. G. Alexander *et al.*, "Novel microscale approaches for easy, rapid determination of protein stability in academic and commercial settings," *Biochimica et Biophysica Acta (BBA)-Proteins and Proteomics,* vol. 1844, no. 12, pp. 2241-2250, 2014.
[169] EMA. "ICH Q1 A (R2) - Stability Testing of new Drug Substances and Products," http://www.ich.org/products/guidelines/quality/article/quality-guidelines.html.
[170] D. H. Cho, and J.-i. Hahm, "Protein–polymer interaction characteristics unique to nanoscale interfaces: A perspective on recent insights," *The Journal of Physical Chemistry B,* vol. 125, no. 23, pp. 6040-6057, 2021.
[171] A. Liga, J. A. S. Morton, and M. Kersaudy-Kerhoas, "Safe and cost-effective rapid-prototyping of multilayer PMMA microfluidic devices," *Microfluidics and Nanofluidics,* vol. 20, no. 12, pp. 164, 2016/11/25, 2016.
[172] C. Matellan, and A. E. del Río Hernández, "Cost-effective rapid prototyping and assembly of poly(methyl methacrylate) microfluidic devices," *Scientific Reports,* vol. 8, no. 1, pp. 6971, 2018/05/03, 2018.
[173] W. Zhang *et al.*, "PMMA/PDMS valves and pumps for disposable microfluidics," *Lab on a Chip,* vol. 9, no. 21, pp. 3088-3094, 2009.
[174] J. B. Nielsen *et al.*, "Microfluidics: Innovations in Materials and Their Fabrication and Functionalization," *Anal Chem,* vol. 92, no. 1, pp. 150-168, Jan 7, 2020.
[175] Y. F. Maa, and C. C. Hsu, "Effect of high shear on proteins," *Biotechnology and bioengineering,* vol. 51, no. 4, pp. 458-465, 1996.
[176] C. Thomas, and D. Geer, "Effects of shear on proteins in solution," *Biotechnology letters,* vol. 33, pp. 443-456, 2011.
[177] S. Salatin *et al.*, "Biological Stability of Peptides/Proteins Therapeutic Agents," *International Journal of Peptide Research and Therapeutics,* vol. 29, no. 5, pp. 77, 2023/07/17, 2023.
[178] H.-C. Mahler *et al.*, "Protein aggregation: pathways, induction factors and analysis," *Journal of pharmaceutical sciences,* vol. 98, no. 9, pp. 2909-2934, 2009.
[179] G. Bai *et al.*, "Computational fluid dynamics (CFD) insights into agitation stress methods in biopharmaceutical development," *International journal of pharmaceutics,* vol. 423, no. 2, pp. 264-280, 2012.
[180] D. Nesta *et al.*, "Aggregation from shear stress and surface interaction: Moleculespecific or universal phenomenon?," *BioProcess International,* vol. 15, 04/01, 2017.
[181] J. S. Bee *et al.*, "Response of a concentrated monoclonal antibody formulation to high shear," *Biotechnology and bioengineering,* vol. 103, no. 5, pp. 936-943, 2009.
[182] C. Berry. "Syringeability and Injectability - https://merrowscientific.com/syringeability-and-injectability/."
[183] F. Johann *et al.*, "Miniaturized forced degradation of therapeutic proteins and ADCs by agitation-induced aggregation using orbital shaking of microplates," *Journal of Pharmaceutical Sciences,* vol. 111, no. 5, pp. 1401-1413, 2022.
[184] J. Jaspe, and S. J. Hagen, "Do protein molecules unfold in a simple shear flow?," *Biophysical journal,* vol. 91, no. 9, pp. 3415-3424, 2006.
[185] S. Schneider *et al.*, "Shear-induced unfolding triggers adhesion of von Willebrand factor fibers," *Proceedings of the National Academy of Sciences,* vol. 104, no. 19, pp. 7899-7903, 2007.
[186] G. L. Lin *et al.*, "Interfacial dilatational deformation accelerates particle formation in monoclonal antibody solutions," *Soft Matter,* vol. 12, no. 14, pp. 3293-3302, 2016.
[187] L. F. Willis *et al.*, "Using extensional flow to reveal diverse aggregation landscapes for three IgG1 molecules," *Biotechnology and bioengineering,* vol. 115, no. 5, pp. 1216-1225, 2018.
[188] J. Dobson *et al.*, "Inducing protein aggregation by extensional flow," *Proceedings of the National Academy of Sciences,* vol. 114, no. 18, pp. 4673-4678, 2017.
[189] F. Grigolato, and P. Arosio, "Synergistic effects of flow and interfaces on antibody aggregation," *Biotechnology and bioengineering,* vol. 117, no. 2, pp. 417-428, 2020.
[190] M. R. Kopp *et al.*, "Surface-induced protein aggregation and particle formation in biologics: current understanding of mechanisms, detection and mitigation strategies," *Journal of Pharmaceutical Sciences*, 2022.
[191] G. Raposo, and W. Stoorvogel, "Extracellular vesicles: exosomes, microvesicles, and friends," *Journal of Cell Biology,* vol. 200, no. 4, pp. 373-383, 2013.

[192] S. Gurunathan *et al.*, "Review of the isolation, characterization, biological function, and multifarious therapeutic approaches of exosomes," *Cells,* vol. 8, no. 4, pp. 307, 2019.
[193] E. Romano, P. A. Netti, and E. Torino, "Exosomes in Gliomas: Biogenesis, Isolation, and Preliminary Applications in Nanomedicine," *Pharmaceuticals,* vol. 13, no. 10, pp. 319, 2020.
[194] G. R. Willis, S. Kourembanas, and S. A. Mitsialis, "Toward exosome-based therapeutics: isolation, heterogeneity, and fit-for-purpose potency," *Frontiers in Cardiovascular Medicine,* vol. 4, pp. 63, 2017.
[195] C. Théry, M. Ostrowski, and E. Segura, "Membrane vesicles as conveyors of immune responses," *Nature reviews immunology,* vol. 9, no. 8, pp. 581-593, 2009.
[196] E. Zeringer *et al.*, "Strategies for isolation of exosomes," *Cold Spring Harbor Protocols,* vol. 2015, no. 4, pp. pdb. top074476, 2015.
[197] K. W. Witwer *et al.*, "Standardization of sample collection, isolation and analysis methods in extracellular vesicle research," *Journal of extracellular vesicles,* vol. 2, no. 1, pp. 20360, 2013.
[198] K. P. De Sousa *et al.*, "Isolation and characterization of extracellular vesicles and future directions in diagnosis and therapy," *Wiley Interdisciplinary Reviews: Nanomedicine and Nanobiotechnology,* vol. 15, no. 1, pp. e1835, 2023.
[199] T. Yamashita, Y. Takahashi, and Y. Takakura, "Possibility of Exosome-Based Therapeutics and Challenges in Production of Exosomes Eligible for Therapeutic Application," *Biological and Pharmaceutical Bulletin,* vol. 41, no. 6, pp. 835-842, 2018.
[200] H. S. Bagheri *et al.*, "Low-level laser irradiation at a high power intensity increased human endothelial cell exosome secretion via Wnt signaling," *Lasers in Medical Science,* vol. 33, pp. 1131-1145, 2018.
[201] M. Hedlund *et al.*, "Thermal-and oxidative stress causes enhanced release of NKG2D ligand-bearing immunosuppressive exosomes in leukemia/lymphoma T and B cells," *PloS one,* vol. 6, no. 2, pp. e16899, 2011.
[202] Z. Zhao *et al.*, "Low-intensity ultrasound radiation increases exosome yield for efficient drug delivery," *Journal of Drug Delivery Science and Technology,* vol. 57, pp. 101713, 2020/06/01/, 2020.
[203] S. Guo *et al.*, "Stimulating Extracellular Vesicles Production from Engineered Tissues by Mechanical Forces," *Nano Letters,* vol. 21, no. 6, pp. 2497-2504, 2021/03/24, 2021.
[204] H. Kang *et al.*, "Extracellular vesicles generated using bioreactors and their therapeutic effect on the acute kidney injury model," *Advanced Healthcare Materials,* vol. 11, no. 4, pp. 2101606, 2022.
[205] P. Tabeling, *Introduction to microfluidics*: Oxford university press, 2023.
[206] H. Cha *et al.*, "Multiphysics microfluidics for cell manipulation and separation: a review," *Lab on a Chip,* vol. 22, no. 3, pp. 423-444, 2022.
[207] P. Becquart *et al.*, "Human mesenchymal stem cell responses to hydrostatic pressure and shear stress," *Eur Cell Mater,* vol. 31, pp. 160-173, 2016.
[208] A. Sabine, C. Saygili Demir, and T. V. Petrova, "Endothelial cell responses to biomechanical forces in lymphatic vessels," *Antioxidants & redox signaling,* vol. 25, no. 7, pp. 451-465, 2016.
[209] K. M. Foster, D. V. Papavassiliou, and E. A. O'Rear, "Elongational Stresses and Cells," *Cells,* vol. 10, no. 9, pp. 2352, 2021.
[210] M. Piergiovanni *et al.*, "Deformation of leukaemia cell lines in hyperbolic microchannels: investigating the role of shear and extensional components," *Lab on a Chip,* vol. 20, no. 14, pp. 2539-2548, 2020.
[211] R. Hao *et al.*, "Mechanical stimulation on a microfluidic device to highly enhance small extracellular vesicle secretion of mesenchymal stem cells," *Materials Today Bio,* vol. 18, pp. 100527, 2023/02/01/, 2023.
[212] E. Romano, P. A. Netti, and E. Torino, "A High Throughput Approach Based on Dynamic High Pressure for the Encapsulation of Active Compounds in Exosomes for Precision Medicine," *International Journal of Molecular Sciences,* vol. 22, no. 18, pp. 9896, 2021.
[213] FDA. "FDA guidance for industry: Pharmaceutical Development (Revision 2)," https://www.gmp-compliance.org/guidelines/gmp-guideline/fda-guidance-for-industry-q8r2-pharmaceutical-development-revision-2.
[214] L. Capretto *et al.*, "Micromixing within microfluidic devices," *Microfluidics: technologies and applications*, pp. 27-68, 2011.
[215] S. Zhang *et al.*, "A concise review of microfluidic particle manipulation methods," *Microfluidics and Nanofluidics,* vol. 24, no. 4, pp. 24, 2020/03/19, 2020.

[216] J. Sánchez Barea, J. Lee, and D.-K. Kang, "Recent Advances in Droplet-based Microfluidic Technologies for Biochemistry and Molecular Biology," *Micromachines,* vol. 10, no. 6, pp. 412, 2019.
[217] L. Amirifar *et al.*, "Droplet-based microfluidics in biomedical applications," *Biofabrication,* vol. 14, no. 2, pp. 022001, 2022.
[218] W.-w. Liu, and Y. Zhu, ""Development and application of analytical detection techniques for droplet-based microfluidics"-A review," *Analytica Chimica Acta,* vol. 1113, pp. 66-84, 2020/05/29/, 2020.
[219] P. Laval *et al.*, "A microfluidic device based on droplet storage for screening solubility diagrams," *Lab on a Chip,* vol. 7, no. 7, pp. 829-834, 2007.
[220] S. H. Jin *et al.*, "A programmable microfluidic static droplet array for droplet generation, transportation, fusion, storage, and retrieval," *Lab on a Chip,* vol. 15, no. 18, pp. 3677-3686, 2015.
[221] A. Huebner *et al.*, "Static microdroplet arrays: a microfluidic device for droplet trapping, incubation and release for enzymatic and cell-based assays," *Lab on a Chip,* vol. 9, no. 5, pp. 692-698, 2009.
[222] S. Ota, H. Kitagawa, and S. Takeuchi, "Generation of femtoliter reactor arrays within a microfluidic channel for biochemical analysis," *Analytical chemistry,* vol. 84, no. 15, pp. 6346-6350, 2012.
[223] H. S. Rho, and H. Gardeniers, "Microfluidic droplet-storage array," *Micromachines,* vol. 11, no. 6, pp. 608, 2020.
[224] H.-H. Jeong *et al.*, "Microfluidic static droplet array for analyzing microbial communication on a population gradient," *Lab on a Chip,* vol. 15, no. 3, pp. 889-899, 2015.